TITLE PAGE

Report Title: Identification and Experimental Database for Binary and Multicomponent Mixtures with Potential for Increasing Overall Cycle Efficiency

Type of Report: Final

Reporting Period Start Date: June, 1999

Reporting Period End Date: August, 2001

Principal Authors: Stephen M. Bajorek, J. Schnelle

Date Report was Issued: May, 2002

DOE Award Number: DE-FG26-99FT40589

Name and Address of Submitting Organization:

Department of Mechanical and Nuclear Engineering
302 Rathbone Hall
Kansas State University
Manhattan, KS 66506

DISCLAIMER

ABSTRACT

This report describes an experimental investigation designed to identify binary and multicomponent mixture systems that may be for increasing the overall efficiency of a coal fired unit by extracting heat from flue gases. While ammonia-water mixtures have shown promise for increasing cycle efficiencies in a Kalina cycle, the costs and associated range of thermal conditions involved in a heat recovery system may prohibit its use in a relatively low temperature heat recovery system. This investigation considered commercially available non-azeotropic binary mixtures with a boiling range applicable to a flue gas initially at 477.6 K (400 ^{o}F) and developed an experimental database of boiling heat transfer coefficients for those mixtures. In addition to their potential as working fluids for increasing cycle efficiency, cost, ease of handling, toxicity, and environmental concerns were considered in selection of the mixture systems to be examined experimentally. Based on this review, water-glycol systems were identified as good candidates.

However, previous investigations of mixture boiling have focused on aqueous hydrocarbon mixtures, where water is the heaviest component. There have been few studies of water-glycol systems, and those that do exist have investigated boiling on plain surfaces only. In water-glycol systems, water is the light component, which makes these systems unique compared to those that have been previously examined. This report examines several water-glycol systems, and documents a database of experimental heat transfer coefficients for these systems. In addition, this investigation also examines the effect of an enhanced surface on pool boiling in water-glycol mixtures, by comparing boiling on a smooth surface to boiling on a Turbo IIIB.

The experimental apparatus, test sections, and the experimental procedures are described. The mixture systems tested included water-propylene glycol, water-ethylene glycol, and water-diethylene glycol. All experimental data were obtained at atmospheric pressure with the test section oriented horizontally.

The effect of subcooling in pool boiling of mixtures is another area that has received limited attention. Therefore, experimental data were obtained for the water-propylene glycol and water-ethylene glycol systems for subcoolings ranging from 0° to 30°C.

The experimental data showed that boiling heat transfer coefficients were found to have significant degradation due to the mixture effect for each of the water-glycol systems examined. This result is consistent with previous studies which examined water-hydrocarbon mixtures with large boiling ranges. The Turbo BIII surface was found to significantly increase heat transfer in each mixture and pure component in comparison to that for the smooth surface.

TABLE OF CONTENTS

LIST OF GRAPHICAL MATERIALS

LIST OF TABLES

NOMENCLATURE

Symbol	Description
T_{sat}	Temperature at saturation
X_{local}	Liquid mole fraction local to boiling site
Y_{local}	Vapor mole fraction local to boiling site
X_b	Liquid mole fraction of the bulk fluid
Y_b	Vapor mole fraction of the bulk fluid
X_1	Component 1 liquid mole fraction
Y_1	Component 1 vapor mole fraction
X_w	Liquid mole fraction of water
X_{eg}	Liquid mole fraction of ethylene glycol
X_{pg}	Liquid mole fraction of propylene glycol
T_w	Temperature of the wall
T_b	Temperature of the bulk fluid
a	Boiling heat transfer coefficient
a_{id}	Ideal boiling heat transfer coefficient
q’	Heat flux
$? T_{bp}$	Boiling range

1.0 INTRODUCTION

One of the methods that has been considered for an improvement of power plant efficiency, is to use a binary mixture as the working fluid in a thermodynamic cycle. The Kalina cycle (1984), has been suggested as a replacement for the Rankine cycle, with nearly all development and evaluations focusing on the use of ammonia and water as the binary fluid. As shown by El-Sayed and Tribus (1985), the Kalina cycle can indeed provide a higher overall cycle efficiency than a simple Rankine cycle mainly by increasing the amount of energy captured from a hot gas stream.

The higher efficiency that can be obtained by a Kalina cycle is due to the variable boiling temperature of a (non-azeotropic) mixture. In a mixture, the light component evaporates preferentially, and as the liquid becomes depleted of the light component, its saturation temperature decreases. The Kalina cycle exploits this mixture effect by using the decreasing bubble point curve (saturation curve) to maintain a temperature difference sufficient to continue boiling in the working fluid as the gas side temperature decreases. Ammonia-water binary mixtures have been the working fluid in Kalina cycles such as the Pioneer power plant in Livingston, California and in DOE's pilot plant in Canoga Park, CA. Properties of the ammonia-water system have been established, and the system is well suited to the high temperatures and pressures associated with a power plant. Little effort however, has gone into investigating the suitability of other mixture systems that may be work in a Kalina cycle. It may be possible to improve the efficiency of a coal or gas fired power plant by using a Kalina bottoming cycle to recover heat from flue gas, if a suitable working fluid is identified.

The following sections of this report discuss the fluid systems investigated, and describes the experiments to determine pool boiling heat transfer coefficients for both plain and enhanced surfaces. The results are presented, and the effects of composition, surface and subcooling are identified.

1.1 EXECUTIVE SUMMARY

An experimental investigation with the objective to identify and obtain heat transfer coefficients for binary and multicomponent mixtures with the potential for increasing the overall efficiency of a coal fired unit by extracting heat from flue gases was completed. While ammonia-water mixtures have shown promise for increasing cycle efficiencies in a Kalina cycle, the costs and associated range of thermal conditions involved in a heat recovery system may prohibit its use in a relatively low temperature heat recovery system. This investigation considered commercially available non-azeotropic binary mixtures with a boiling range appropriate for a flue gas initially at 477.6 K (400 ^{o}F) and developed an experimental database of boiling heat transfer coefficients for those mixtures. In addition to their potential as working fluids for increasing cycle efficiency, cost, ease of handling, toxicity, and environmental concerns were considered in selection of the mixture systems to be examined experimentally. Based on these factors, water-glycol systems were identified as good candidates.

There have been few studies of water-glycol systems, howevr, and those that do exist have investigated boiling on plain surfaces only. In water-glycol systems, water is the light component, which makes these systems unique compared to those that have been previously examined.

This investigation generated a database of empirical information for aqueous glycol mixtures on smooth and Turbo BIII surfaces at saturation and various subcoolings. The mixture systems tested included water-propylene glycol, water-ethylene glycol, and water-diethylene glycol. All experimental data were obtained at atmospheric pressure with the heating surface oriented horizontally.

The experimental apparatus was previously used in investigations by Bajorek (1988), Shakir (1986), Hui (1985), and Thome (1984). The data generated by this investigation complements the data previously taken using this apparatus. The experimental apparatus, test sections, and the experimental procedures are described.

The effect of subcooling in pool boiling of mixtures is another area that has received limited attention. Therefore, experimental data were obtained for the water-propylene glycol and water-ethylene glycol systems for subcoolings ranging from 0° to 30°C. . The water-diethylene glycol mixture system was only tested at saturation on the smooth tube due to its high saturation temperature.

The experimental data showed that boiling heat transfer coefficients were found to have significant degradation due to the mixture effect for each of the water-glycol systems examined. This result is consistent with previous studies which examined water-hydrocarbon mixtures with large boiling ranges. The Turbo BIII surface was found to significantly increase heat transfer in each mixture and pure component in comparison to that for the smooth surface.

A review of the experimental results clearly shows that mixture composition has a large effect on the boiling heat transfer coefficient. Ideal heat transfer coefficients are calculated for a mixture by a linear mixing law from pure component data. When the observed heat transfer coefficients are compared to the calculated ideal heat transfer coefficients, it is seen that the heat transfer coefficients for the mixtures are severely degraded. For the water-ethylene glycol mixture system reductions of approximately

65% are observed on the smooth and the Turbo BIII tubes at $X_w = 0.5$. For the water-propylene glycol mixture system at $X_w = 0.5$ reductions on the order of 60% and 65% are observed for the smooth and Turbo BIII tubes, respectively. The water-diethylene glycol mixture system has reductions in the heat transfer coefficient of nearly 75% on the smooth tube at $X_w = 0.5$. These reductions are rather large, but are consistent with results previously observed for mixture systems with large boiling ranges.

The experimental results also clearly show that the surface had a large effect on the heat transfer coefficient. Throughout all the tests conducted in which the smooth surface was compared to the Turbo BIII surface, the Turbo BIII surface consistently had much higher heat transfer coefficients.

1.2 BOILING HEAT TRANSFER IN MIXTURES

The Kalina cycle takes advantage of several unique features of mixture boiling, which plays and important role in many industrial processes. In general, chemical processes and separations involve binary or multi-component mixtures rather than pure components. Mixture boiling, however, involves several processes that do not occur in the boiling of pure components, which can be detrimental to a system. The rate of evaporation in a mixture is determined by the rate of mass diffusion as opposed to heat transfer. Because mass diffusion is slower than heat diffusion in the liquid, mass transfer of the more volatile component becomes the limiting process in bubble growth. As a result, heat transfer coefficients in a mixture can be significantly lower than those expected based on heat transfer coefficients of their pure components and the total surface area of a heat exchanger may need to be increased in order to transfer the same amount of heat.

Numerous investigations have shown that mixture boiling heat transfer coefficients can be significantly lower than those based on a linear interpolation of pure component heat transfer coefficients. In Figure 1.1, for example, it can be seen that the boiling curves for methanol and water mixtures lie below those for the pure components.

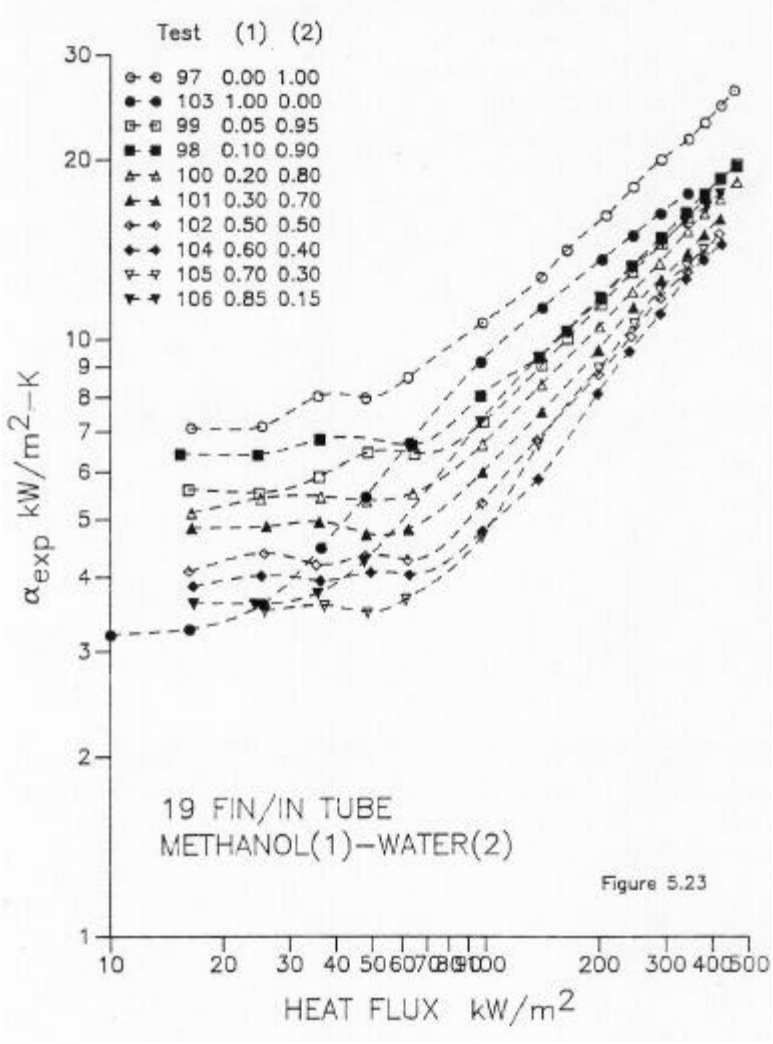

Figure 1.1- α vs. heat flux data for methanol/water mixtures at 1.0 bar on a finned tube from Bajorek (1988). Legend shows bulk liquid mole fractions for methanol (1) and water (2).

This degradation in the boiling heat transfer coefficient has been attributed to several processes. The key to understanding mixture boiling lies in the vapor-liquid equilibrium. Figure 1.2 is an example of a phase equilibrium diagram for an ideal binary mixture.

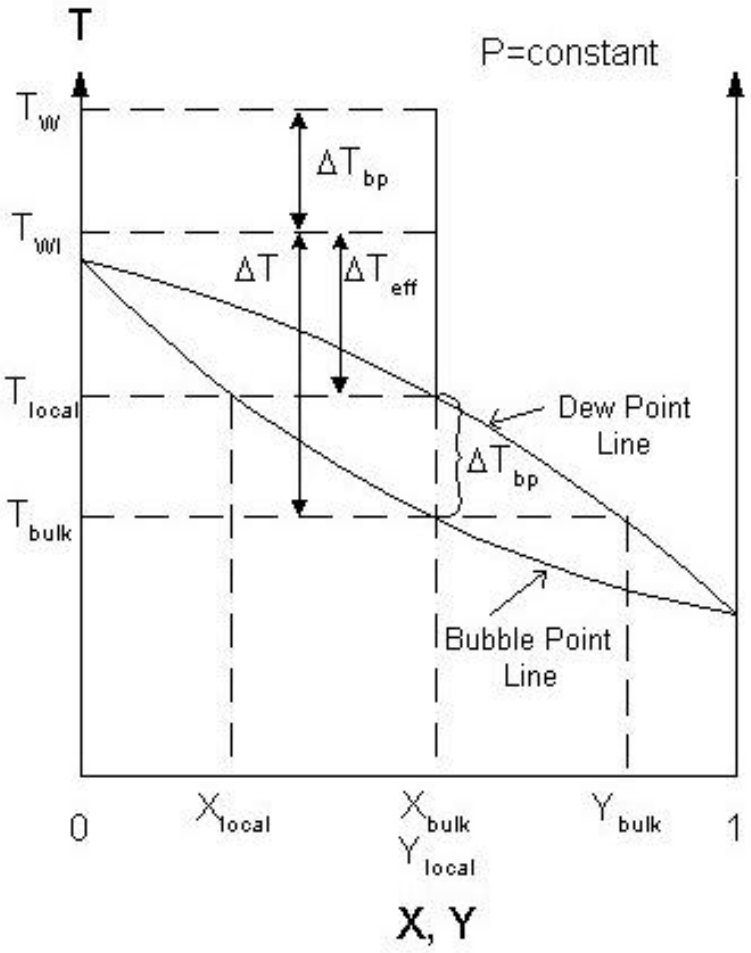

Figure 1.2-Phase equilibrium diagram for an ideal binary mixture system.

The temperature at which two phases can coexist in a binary mixture is uniquely determined by the pressure and the mole fraction of the components in each of the phases. A phase equilibrium diagram is used to show this relationship between temperature and the liquid phase mole fraction in a binary mixture at a given pressure. In Figure 1.2 the saturation temperature is plotted on the vertical axis, and the liquid (X) and vapor (Y) mole fractions of the more volatile component are plotted on the horizontal axis. The dew point curve represents the variation of equilibrium vapor mole fraction with saturation temperature, and the bubble point curve shows the dependence of the saturation temperature with liquid mole fraction. Figure 1.2 also shows the boiling range,

? T_{bp}, which is the difference in bubble and dew point temperatures at a given liquid mole fraction.

Van Wijk, Vos, and Van Stralen (1956) offered the first explanation for the mixture boiling phenomena. Their observation was that because the equilibrium vapor contained a higher mole fraction of the more volatile component, more of this component must be evaporated at the bubble interface to maintain phase equilibrium. This increased evaporation depletes the boundary layer of the more volatile component. This depletion at the boundary layer results in a rise of the local bubble point temperature at the interface.

Figure 1.2 shows this depletion clearly as the liquid mole fraction moves from X_{bulk} to X_{local} resulting in a rise of the local bubble point from T_{bulk} to T_{local}. In turn, the temperature driving the evaporation process is reduced from ΔT to ΔT_{eff} by an amount of ΔT_{bp}. Therefore, to maintain the same heat flux, the temperature of the heated surface must be raised by an amount equivalent to the increase in the local bubble point temperature, shown as T_{wI} moves to T_w. This effect can also be seen in Figure 1.3, which shows the bubble growth model in homogeneous superheated binary mixtures by Van Stralen. However, Thome (1983) pointed out that this effect was limited by the size of the mixture's boiling range.

Another theory was proposed by Sternling and Tichacek (1961), Grigor'ev (1962), and Stephan and Korner (1969), which states that the lower heat transfer coefficients were the result of the adverse effect of mass diffusion on the boiling nucleation. Thus, as the more volatile component is preferentially evaporated at the bubble interface, mass diffusion of the more volatile component would be necessary to maintain equilibrium. This could dramatically reduce the evaporation rate since the rate of mass diffusion is usually much slower than that of heat diffusion in the liquid phase. This mass diffusion effect would lower the boiling site density and thus reduce the boiling heat transfer coefficient. Hui and Thome (1985) validated this theory with a photographic study on boiling site densities in mixtures.

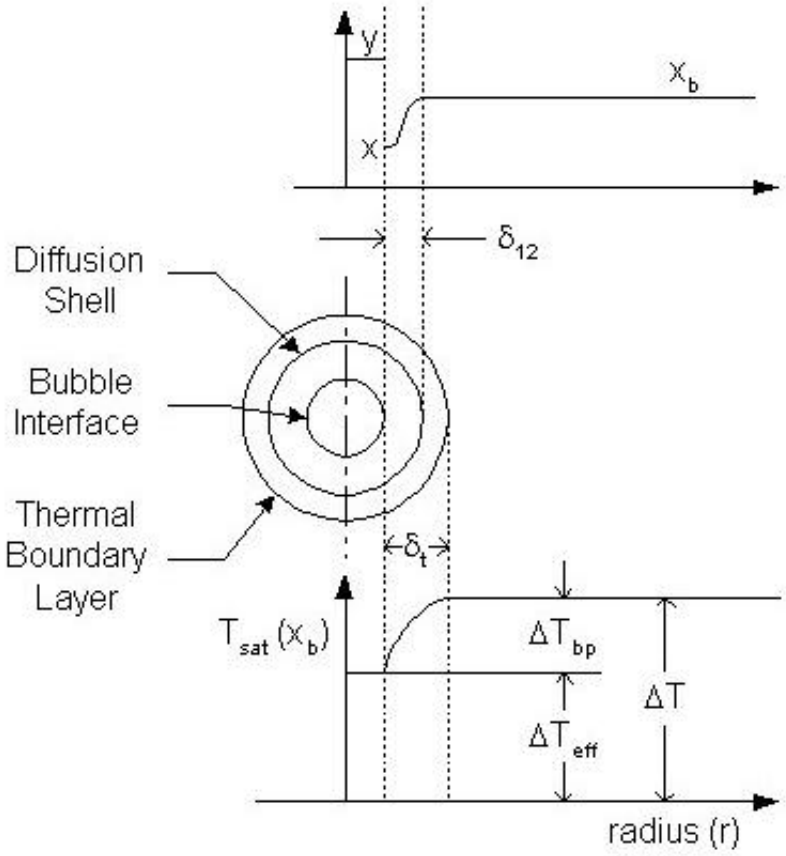

Figure 1.3-Bubble growth model in homogeneous superheated binary mixture by Van Stralen.

Stephan and Preusser (1979) demonstrated that part of the reduction in the mixture boiling heat transfer coefficient is simply due to the non-linear variations in the physical properties of the mixture with composition. Thome (1981) showed that the mass diffusion process also affected bubble departure diameters and frequencies which reduces the mixture boiling heat transfer coefficient. Bubble departure diameters were greatly reduced in mixtures from the pure components, however the frequency was slightly increased. Thome (1982) also showed that the heat transfer mechanisms of evaporation and cyclic thermal boundary layer stripping are diminished by the mass diffusion process; which, hence, are partially responsible for the decrease in the mixture boiling heat transfer coefficient.

1.3 SUBCOOLED BOILING IN MIXTURES

The processes of subcooled boiling are significantly different than those in saturated boiling. Subcooled boiling occurs when the wall temperature exceeds saturation but the bulk temperature is less than the saturation temperature. However, the wall temperature is sufficiently high to heat the fluid at the surface to the saturation temperature. The fluid near the wall begins to boil, but as the bubbles grow outward into the colder fluid the bubble condenses and collapses. These bubbles continue to nucleate, grow, and collapse on the heated surface. Subcooled boiling is an efficient form of heat transfer which relies on both convection and boiling heat transfer regimes.

There have been relatively few studies of the subcooling effect on the boiling of mixtures. Sternman *et al*. (1966) presented the first experimental results for the effect of subcooling on nucleate pool boiling of binary mixtures. The mixture system they examined was benzene-diphenyl at 3.5 and 8.0 bars with subcoolings of 0, 10, 30, and 80° C. Figure 1.4 shows their results at 8.0 bars. Their heater was a thin-walled stainless steel tube of 5 mm diameter. As in pure component boiling, they observed that the heat transfer coefficient based on (T_W-T_b) decreased as subcooling increased. They also observed that heat transfer coefficients saw a more significant decrease in the pure components than in any of the mixtures. They presented no explanation for this behavior.

Hui (1983) also studied the effect of subcooling on the heat transfer coefficient in the ethanol-water and ethanol-benzene mixture systems. In this study the heat transfer coefficients decreased approximately the same magnitude for the pure components and the mixtures. Hui also observed an inexplicable maximum in the mixture heat transfer coefficient curve at $X_{ethanol} = 0.7$.

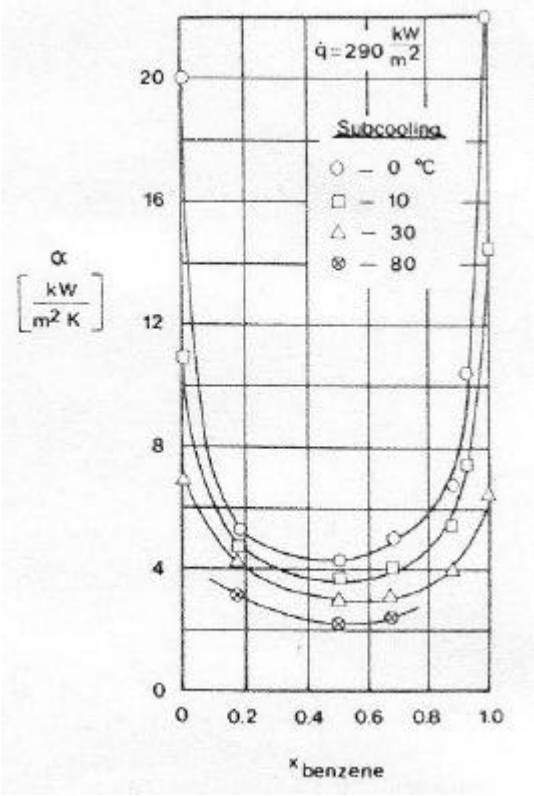

Figure 1.4-Sternman's experimental results for the effect of subcooling on nucleate pool boiling in a benzene-diphenyl mixture system from Thome (1984).

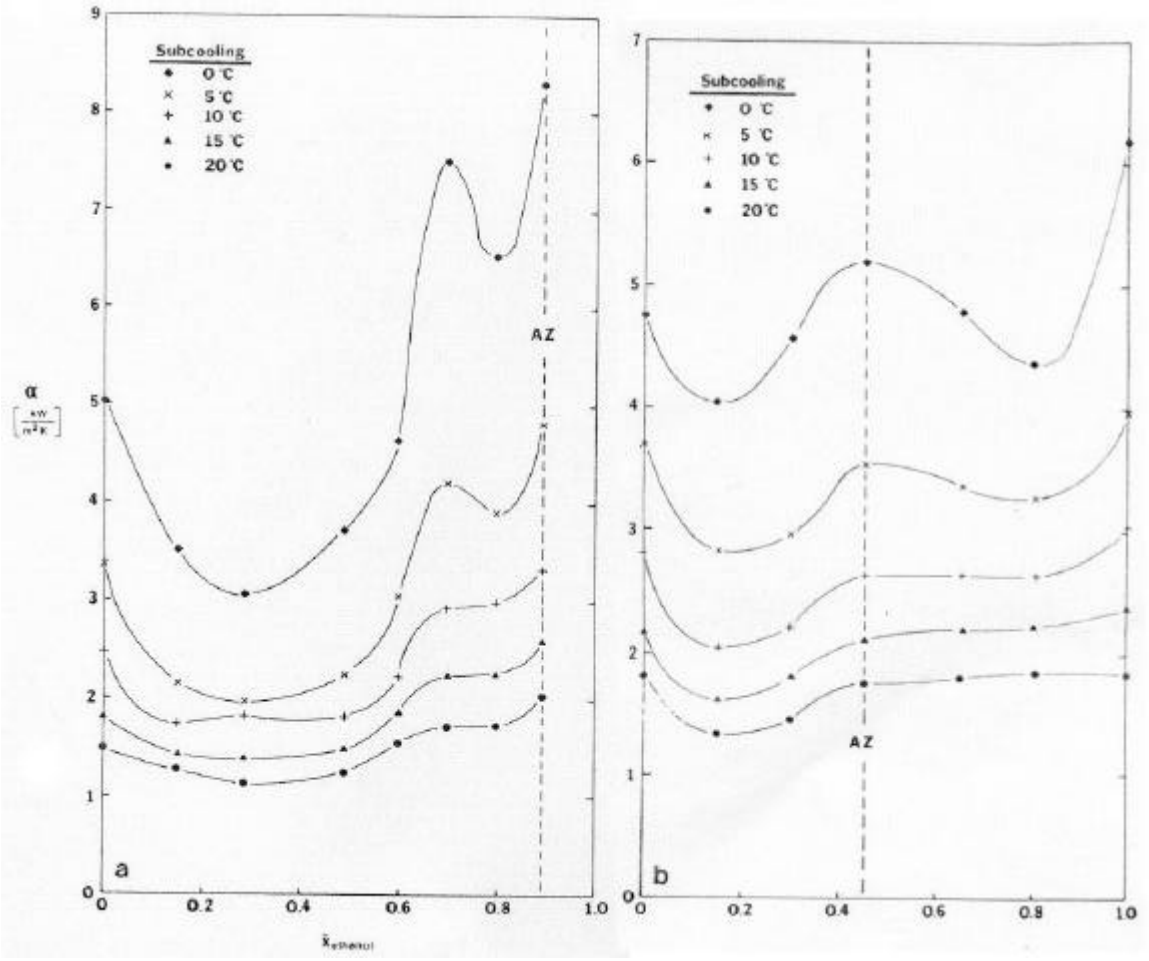

Figure 1.5-Hui's experimental results for the effect of subcooling on boiling heat transfer coefficient at 75 kW/m^2 in (a) ethanol-water and (b) ethanol-benzene from Thome (1984).

1.4 ENHANCED SURFACES

Enhanced boiling surfaces are surfaces which are intended to provide a significant increase in the boiling heat transfer coefficient for a given wall superheat compared to a smooth surface. The principle benefit from enhanced surface boiling is an economic one. Using enhanced boiling surfaces in heat exchangers allow for a reduction in size and cost on new units and a decrease in energy-related operating costs when retubing existing units with enhanced boiling tubes.

There are many different types of commercially available enhanced boiling tubes. The boiling enhancements are classified into the following six categories: externally finned tubes, modified externally finned tubes, porous layer or coated tubes, internally

finned tubes, doubly enhanced tubes, and tube inserts. This study examines shell-side boiling so we will focus on external modifications in this discussion.

Although externally finned tubes are manufactured with various fin densities, profiles, and heights, only low-finned versions are used for boiling applications due to the low fin efficiency of high- and medium-finned tubes. Typically longitudinally finned tubes are not used in boiling services. Bajorek *et al*. (1991) extensively studied externally finned tubing and its effect on boiling heat transfer coefficients in mixtures.

The next category of external tube enhancement is porous layer or coated tubes. The most effective way to achieve a porous coated surface was developed by Union Carbide. Their High Flux tube was the first enhanced boiling tube to be widely used in industry after the low-finned tubes. The High Flux tube is produced by spraying a thin coating made up of a binder, a metallic powder, and a brazing powder on to the exterior surface of the tube. The tube is then heated in an oven to melt the brazing powder and to burn off the binding material, leaving behind a thin, porous metallic matrix that is several layers of particles thick and has many random, interconnected passageways throughout. The particle size range, thickness, and material can all be varied to match different tubing applications.

The last category of external tube enhancements is the modified externally finned tubes. Standard finned tubes are modified by cutting, knurling, notching, or rolling in order to form complex fin geometries with higher boiling performance ratings. This modified surface then has what are called re-entrant cavities. These cavities allow the bulk liquid to return to the surface more rapidly while boiling is occurring.

The modified tube used in this investigation is the Wolverine Tube Turbo BIII shown in Figure 1.6. The enhancement on this surface is created by raising integral low fins on the surface, cutting diagonally across these fins, and then rolling the fins to compress them to form mushroom-like pedestals. Re-entrant cavities are thus formed in a rectangular crosshatch pattern. Figure 1.7 shows a cross-section of the tube surface. For more information on enhanced surfaces see Thome (1990) or Webb (1981).

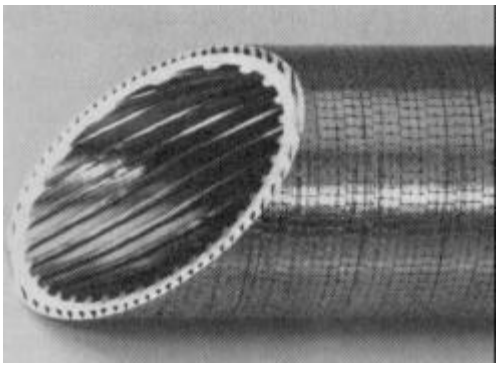

Figure 1.6-Photograph of a section of Wolverine Tube Turbo BIII from Thome (1990)

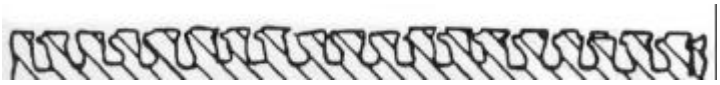

Figure 1.7-Cross section of the Turbo BIII surface from Thome (1990)

1.5 MIXTURE SYSTEMS CONSIDERED

The goal of this proposed investigation is to identify one or more mixture systems that may be well suited to heat recovery from flue gases, where it is assumed, that the flue gas temperature is initially 300 to 400 ^{o}F. As heat is recovered from the flue gas, its temperature decreases as well, so the working fluid must have a variable boiling curve so that as the light component(s) are evaporated, a ΔT sufficient to maintain boiling over the entire length of a heat exchanger tube exists. Thus, a suitable working fluid is one that has a boiling range that decreases sufficiently with mixture composition to maximize the energy recovery from the flue gas. Although the working fluid for a Kalina cycle is assumed to be a binary mixture, a ternary or multicomponent fluid may actually be superior by providing a better match to the flue gas temperature decrease.

Therefore, the following criteria can be applied to identify a mixture system suitable as a potential Kalina cycle working fluid:

(a) The system must have a wide boiling range.

(b) The fluid must have saturation temperatures less than the flue gas initial temperature.
(c) The fluid system should be relatively safe, not posing undue occupational or environmental hazards.
(d) Working properties of the system, such as thermal properties and vapor-liquid equilibrium information should be known and well-established.

A review of numerous mixture systems identified three that met these criteria. These were:

(a) Water – ethylene glycol
(b) Water- propylene glycol, and
(c) Water - diethylene glycol.

An interesting feature of each of these mixture systems, is that water is the light component, which makes them unique compared to most that have been previously examined. It may also have the attractive feature of making water the condensing fluid in a thermodynamic system.

1.6 PREVIOUS WATER-GLYCOL INVESTIGATIONS

Previous mixture boiling studies have focused primarily on aqueous hydrocarbon mixtures. Relatively few studies have included glycol mixtures. Bhowmick *et al*. (1996) performed tests comparing heat transfer performance of engine coolants under subcooled and saturated flow boiling conditions at a pressure of 205 kPa. This test was primarily a comparison between a 50/50 by volume ethylene glycol-water mixture and a 50/50 by volume propylene glycol-water mixture. The variables in the test were mixture type and flow rates ranging from 1.89×10^{-3} m^3/min to 11.4×10^{-3} m^3/min, which are typical engine operating conditions. These data were then compared to analytical calculations presented by McAssey, Stinson, and Gollin (1995) based on the Chen correlation for saturated boiling and the modified Chen correlation for subcooled boiling. The Chen

correlation under-predicted the wall temperature at the higher flux levels. However, below 0.5 MW/m^2 agreement between the predictions and experimental results were good. These tests were then expanded to include 30/70 by volume mixtures of ethylene glycol-water and propylene glycol-water. These results were presented in Branchi *et al*. (1997). An example of these results is shown in Figure 1.8.

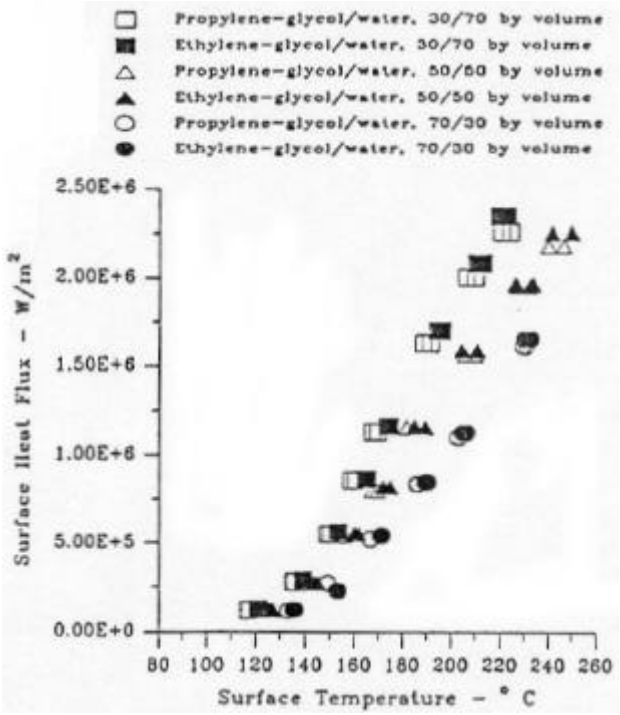

Figure 1.8-Concentration comparisons for ethylene-glycol/water and propylene-glycol/water at an inlet velocity of 0.445 m/s, inlet temperature of 85°C and system pressure of 205 kPa from Branchi (1997).

Fujita *et al*. (1996) next examined ethylene glycol-water mixtures. This test was performed on a horizontal platinum wire 0.5 mm in diameter. The mixture system was examined at water mole fractions of 0.0, 0.1, 0.3, 0.4, 0.5, 0.6, 0.7, 0.8, 0.9, and 1.0. The measured data was then compared to six existing empirical correlations. The Stephan-Korner correlation (1969) was found to be the best correlation among the six, but it appreciably under-predicted the heat transfer coefficient for the system. A new correlation was then developed which predicted the heat transfer coefficients within ±20% accuracy when measured heat transfer coefficients of pure components were used as the anchoring data. However, boiling heat transfer coefficients are dependent on

system pressure, so the proposed correlation remains to be verified at various pressures. Some of their test results can be seen in Figure 1.9. Further information on the Stephan-Korner correlation can be found in Stephan *et al.* (1969).

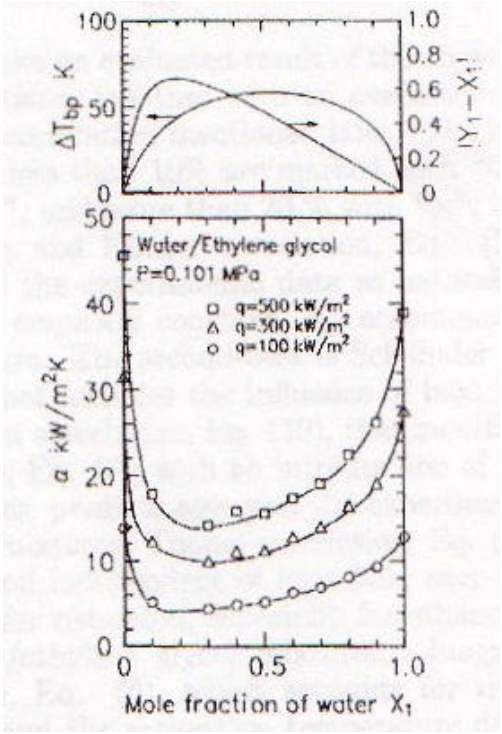

Figure 1.9-Variations of measured heat transfer coefficients with mixture composition and heat flux along with variations of ?T_{bp} and $|Y_1-X_1|$ from Fujita (1996).

2.0 EXPERIMENTAL

The pool boiling facility in the Thermal Hydraulics Lab at Kansas State University was used to obtain the measurements reported in this study. This facility was previously located at Michigan State University. It has been used to obtain nucleate boiling incipient superheats and nucleate boiling pool boiling heat transfer coefficients in several previous investigations including those by Shakir (1986), Hui (1983), and Bajorek (1988). This section describes the pool boiling facility, peripheral equipment, and the procedures followed in obtaining the experimental values of nucleate boiling heat transfer coefficients.

2.1 POOL BOILING FACILITY

The pool boiling facility consists of a pressure vessel, its supporting structure, the peripheral equipment, and the measuring instruments. The pressure vessel, shown in Fig. 2.1, is a stainless steel cross with four 101.6 mm (4.0 inch) ID flanged openings. Stainless steel cover plates were bolted to each flange to enclose the vessel. Teflon O-rings were used as a seal between the cover plates and the vessel. Openings were made in the cover plates to provide entry for the test section, condenser, thermocouples, pressure transducer, bulk fluid heaters, and fluid inlet and outlet lines. Attachments to the pressure vessel were made through and sealed by stainless steel Swagelok fittings. One of the cover plates was designed with no attachments so that it could be removed and replaced with a window in order to view the boiling process. The supporting structure was manufactured from Unistrut.

The vessel was filled with liquid through an inlet line in the bottom plate. Approximately 4.0 liters (1.06 gallons) were required to fill the vessel to a level at least 70 mm (2.75 inches) above the top of the test section. Two Watlow 750 W Firerod heaters were used to heat the bulk liquid up to test conditions. The bulk liquid temperature was measured by two stainless steel clad 30 gauge copper-constantan thermocouples inserted through the bottom plate to the level of the test section. A water cooled condenser, made from several coils of stainless steel tubing was mounted inside the top cover plate. Tap water was used as the coolant, and could be chilled by routing it

through an ice bath before entry into the condenser. The flow rate of the condenser was controlled manually by use of a needle valve. Vapor leaving the vessel through the degassing line in the top plate was condensed by passing it through copper tubing submerged in a tank of room temperature water. A pressure relief valve was mounted to the top plate set at 0.6895 Mpa (100 psig) in order to prevent accidental over pressurization of the vessel above its maximum rating of 1.03 MPa (150 psig).

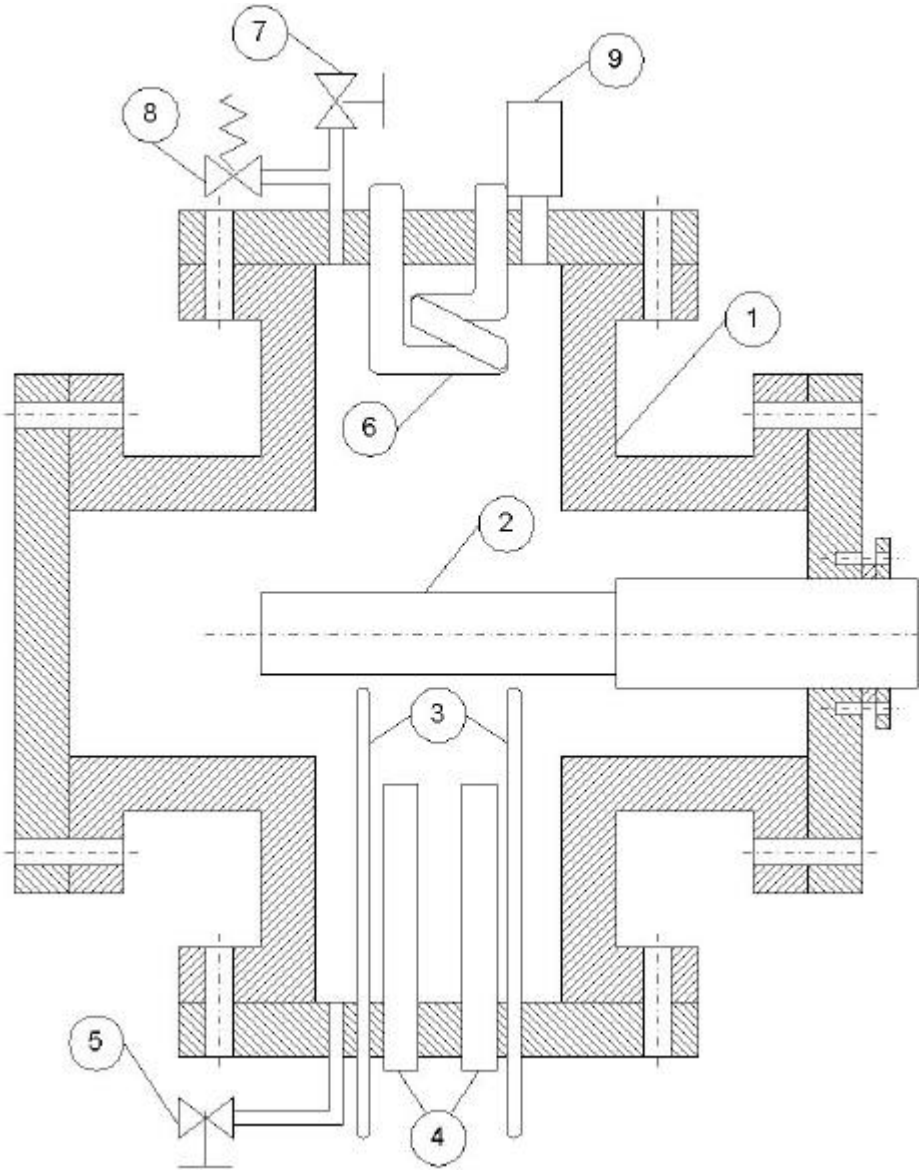

Figure 2.1-Schematic of pool boiling facility. Legend: 1-boiling vessel, 2-test section, 3-bulk liquid thermocouples, 4-immersion heaters, 5-liquid feed line, 6-water cooled condenser, 7-degassing vent, 8-pressure relief valve, 9-pressure transducer. (not to scale)

2.2 EQUIPMENT AND INSTRUMENTATION

Power to the test section was supplied by a variable AC power supply. The power delivered to the test section was determined by measuring the current in the electrical circuit and the voltage drop across the heating element in the test section. The current was determined by measuring the voltage drop across a 1.0 ±1.0% ohm resistance element placed in the circuit. A Fluke 8000A digital multi-meter accurate to 1% of full scale was used to measure the voltages. Figure 2.2 shows the electrical circuit used to supply and measure power to the test section.

The temperatures were measured with an Omega Trendicator model 400A digital indicator, accurate to within ±0.1 K. A convenient check of the calibration was to observe the measured temperatures and compare them to the known saturation temperature of the fluid.

Pressure was measured using an Omega Engineering pressure transducer with a digital output accurate to 0.0069 bar (±0.1 psi). The pressure transducer was calibrated against a dead weight pressure source, and corrected for local conditions obtained from a mercury barometer.

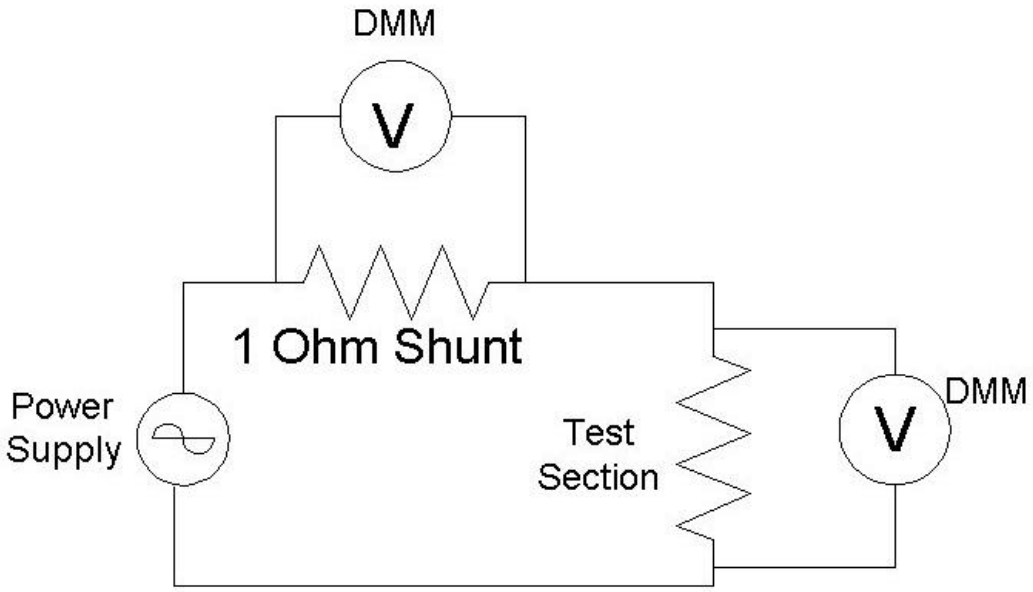

Figure 2.2-Electrical circuit used for measurement of power to test section.

2.3 TEST SECTIONS

The experimental measurements reported in this study were obtained using three different test sections. Two of the test sections were smooth tubes and the third had a Turbo BIII™ surface manufactured by Wolverine Tube, Inc. All of the tests were conducted with the tubes supported horizontally inside the pressure vessel.

Figures 2.3 and 2.4 show cross sectional diagrams of the two smooth tube test sections. The first test section, shown in Figure 2.3 has a diameter of 19.05 mm (0.75 inches) and a heated length of 50.8 mm (2.0 inches). The heating element was a Chromalox CIR 3030 electrical resistance heater. Copper-constantan thermocouples were inserted axially in the wall of the copper tube. Three thermocouples were located at the center of the heated length, and two additional thermocouples were positioned 22.23 mm (0.875 inches) outside the heated length closest to the stainless steel support tube. The surface of the tube was prepared by rubbing it with 400 grade emery paper.

The second smooth tube test section, shown in Figure 2.4, had a diameter of 19.05 mm (0.75 inches) and a heated length of 50.8 mm (2.0 inches). The heating element was a Watlow 500 W Firerod resistance heater, model G2J109. Copper-constantan thermocouples were again inserted axially in the wall of the copper tube. Four thermocouples were located at the center of the heated length. Two thermocouples were located 22.23 mm(0.875 inches) outside the heated length closest to the stainless steel support tube, and two more thermocouples were located 9.525 mm (0.375 inches) inside the heated length closest to the stainless steel support tube. The tube surface was also prepared using 400 grade emery paper.

The third test section, shown in Figure 2.5, used a Turbo BIII surface. The base diameter of this surface was 17.12 mm (0.674 inches) and the outer diameter was 19.05 mm (0.75 inches). The heating element was a Watlow 500 W Firerod® resistance heater, model G2J109. Four copper-constantan thermocouples were located at the center of the heated length, and two additional thermocouples were placed 6.35 mm (0.25 inches) outside the heated length closest to the stainless steel support tube. Due to the fact that

most of the surface area is recessed, the surface of this test section was left unfinished to achieve a uniform surface treatment.

The test sections were cleaned thoroughly before use by rinsing the surface with acetone. After the surfaces had been prepared, care was taken to ensure that the surfaces were not marred or scratched.

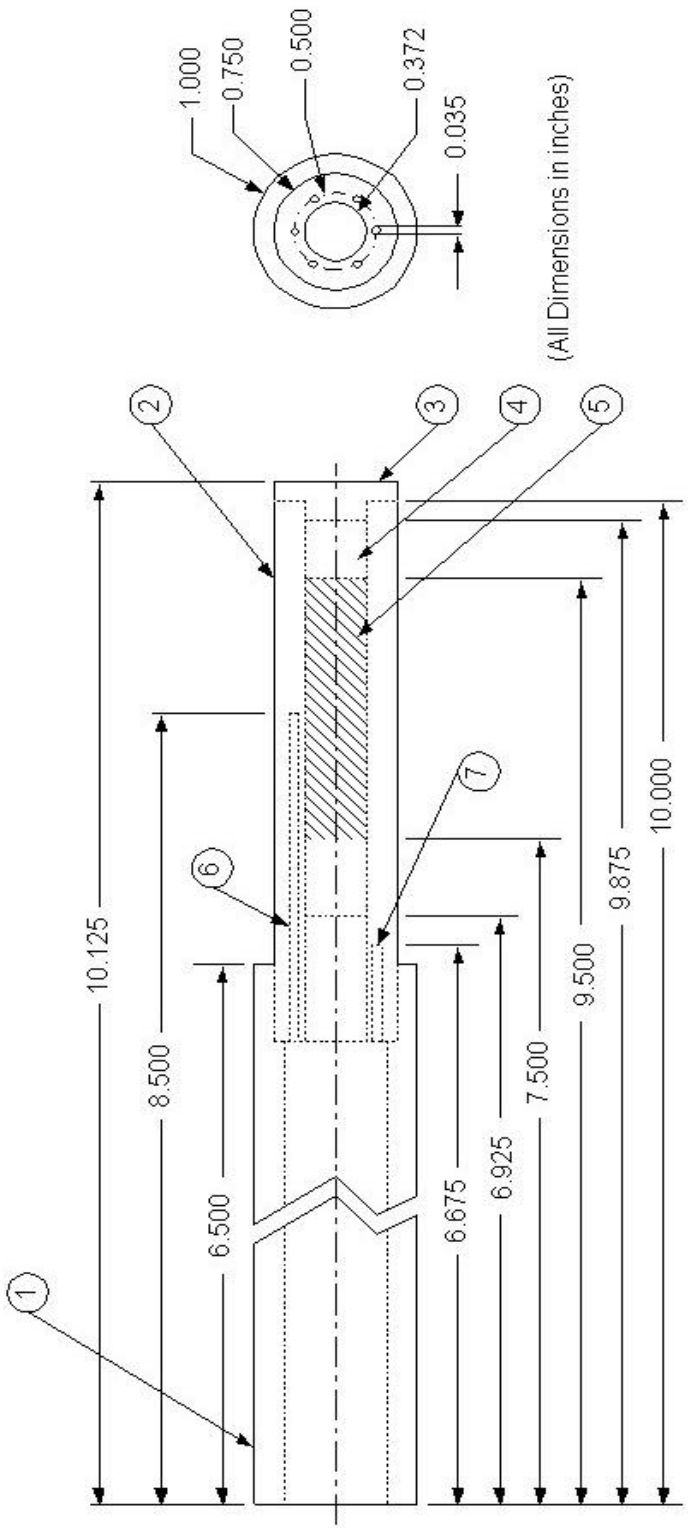

Figure 2.3-First test section with smooth copper surface. Legend: 1-stainless steel holder, 2-copper sleeve, 3-stainless steel cap, 4-graphite plug, 5-resistance heater (heated length shown as shaded region), 6-centerline thermocouple well, 7-error estimation thermocouple well.

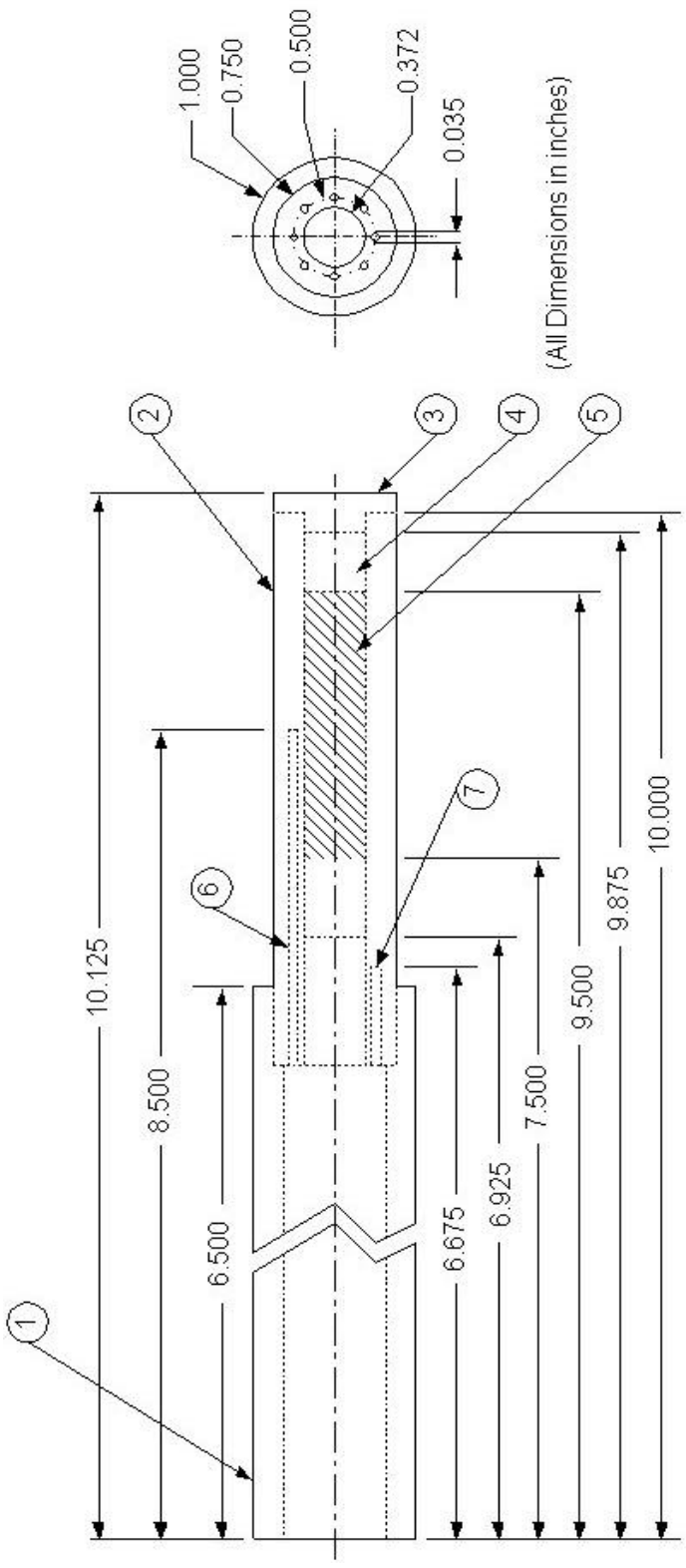

Figure 2.4-Second test section with smooth copper surface. Legend: 1-stainless steel holder, 2-copper sleeve, 3-stainless steel cap, 4-graphite plug, 5-resistance heater (heated length shown as shaded region), 6-centerline thermocouple well, 7-error estimation thermocouple well.

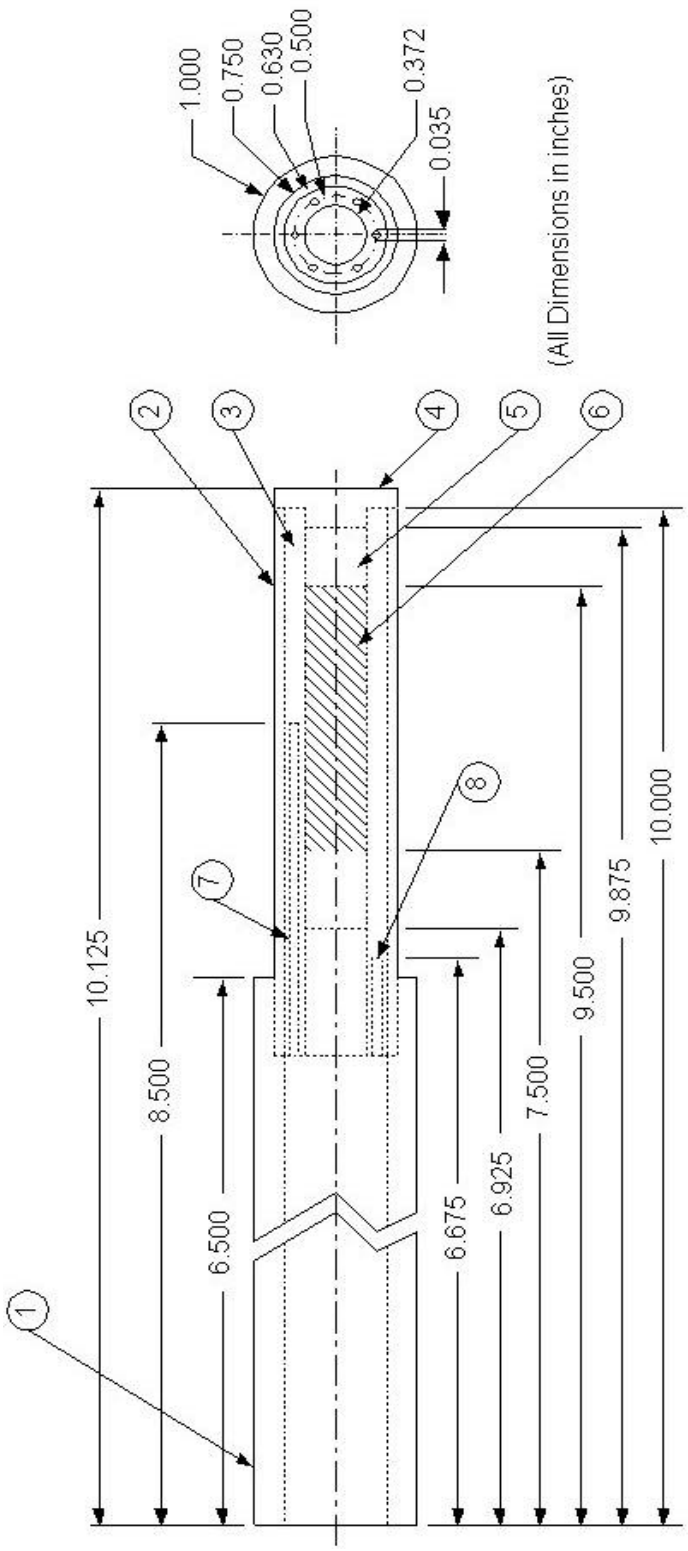

Figure 2.5-Test section with Turbo BIII surface. Legend: 1-stainless steel holder, 2-Turbo BIII surface, 3-copper sleeve, 4-stainless steel cap, 5-graphite plug, 6-resistance heater (heated length shown as shaded region), 7-centerline thermocouple well, 8-error estimation thermocouple well.

3.0 TEST FLUIDS

This investigation examined water-ethylene glycol, water-propylene glycol, and water-diethylene glycol mixtures at several different mole fraction mixtures. The following section lists the basic fluid properties and vapor-liquid equilibrium data.

An important parameter in characterizing mixture systems is the boiling range, denoted $?T_{bp}$. Boiling range is defined as the difference between the dew point and bubble point temperatures at the liquid phase mixture composition. The boiling range can be readily estimated for binary mixture systems from the vapor-liquid equilibrium diagram. This estimation is performed by first generating continuous bubble and dew point curves from the experimental VLE data. The boiling range at a specified liquid composition is then identified as the difference in the dew point and bubble point temperatures.

3.1 BASIC PROPERTIES

Parameter	Ethylene Glycol	Diethylene Glycol	Propylene Glycol
Formula	$C_2H_6O_2$	$C_4H_{10}O_3$	$C_3H_8O_2$
Molecular Weight	62.1	106.1	76.1
Boiling Point at 760 mm Hg (°C)	197.4	245.5	187.4
Density (g/cc) at 25°C	1.110	1.111	1.032
Viscosity (centipoise) at 25°C	16.9	25.3	48.6
at 60°C	5.2	7.3	8.42
Surface Tension (dynes/cm) at 25°C	48	44	36
Specific Heat (kJ/kg*K) at 25°C	2.428	2.303	2.512
Thermal Conductivity (W/m*K) at 25°C	0.2579	0.2034	0.2061
Heat of Vaporization (kJ/kg) at 25°C	1044.4	914.1	881.6

Table 3.1-Fluid properties table. Data taken from Dow (1999)

3.2 VAPOR-LIQUID EQUILIBRIUM DATA

This study is similar to many previous studies on binary mixture boiling in that the mixtures tested have a wide boiling range. However, in this study water is the light component, where in many studies examining water-hydrocarbon mixtures, water was the heavier component.

Tables 3.2 through 3.4 show the VLE data taken from Gmehling (1984) for the three mixture systems tested. The VLE data is then shown in graphical from in Figures 3.1 through 3.3. The wide boiling range is readily seen in these figures.

1-Water		
2-Diethylene Glycol		
P=1.013 Bar (760.0 mm Hg)		
Temp. (°C)	X_1	Y_1
245.50	0.0000	0.0000
159.35	0.1642	0.9519
147.85	0.2224	0.9752
142.25	0.2691	0.9809
129.45	0.3911	0.9921
120.35	0.5209	0.9960
109.25	0.7332	0.9989
101.85	0.9430	0.9999
100.00	1.0000	1.0000

Table 3.2-Tabular vapor liquid equilibrium data for water/diethylene glycol system from Gmehling (1984)

1-Water		
2-Ethylene Glycol		
P=0.996 Bar (747.0 mm Hg)		
Temp. (°C)	X_1	Y_1
196.7	0.0000	0.0000
196	0.0034	0.0336
182.6	0.0434	0.4469
171.6	0.0688	0.6396
168.6	0.0842	0.6859
151.2	0.1750	0.8489
140.8	0.2746	0.9160
136.5	0.3196	0.9319
133	0.3398	0.9439
127	0.4032	0.9591
125	0.4421	0.9667
120	0.5514	0.9793
112	0.6850	0.9917
110.5	0.6984	0.9941
103.7	0.9017	0.9991
99.5	1.0000	1.0000

Table 3.3-Tabular vapor liquid equilibrium data for water/ethylene glycol system from Gmehling (1984)

1-Water		
2-Propylene Glycol		
P=0.987 Bar (740.0 mm Hg)		
Temp. (°C)	X_1	Y_1
187.4	0.0000	0.0000
141.0	0.1250	0.8100
138.0	0.1350	0.8930
130.6	0.2300	0.9370
125.5	0.2800	0.9450
120.0	0.3470	0.9580
117.5	0.3820	0.9650
111.4	0.4510	0.9770
109.2	0.5400	0.9800
106.5	0.6200	0.9840
104.4	0.6960	0.9900
102.5	0.7730	0.9920
100.2	0.8950	0.9940
99.27	1.0000	1.0000

Table 3.3-Tabular vapor liquid equilibrium data for water/propylene glycol system from Gmehling (1984)

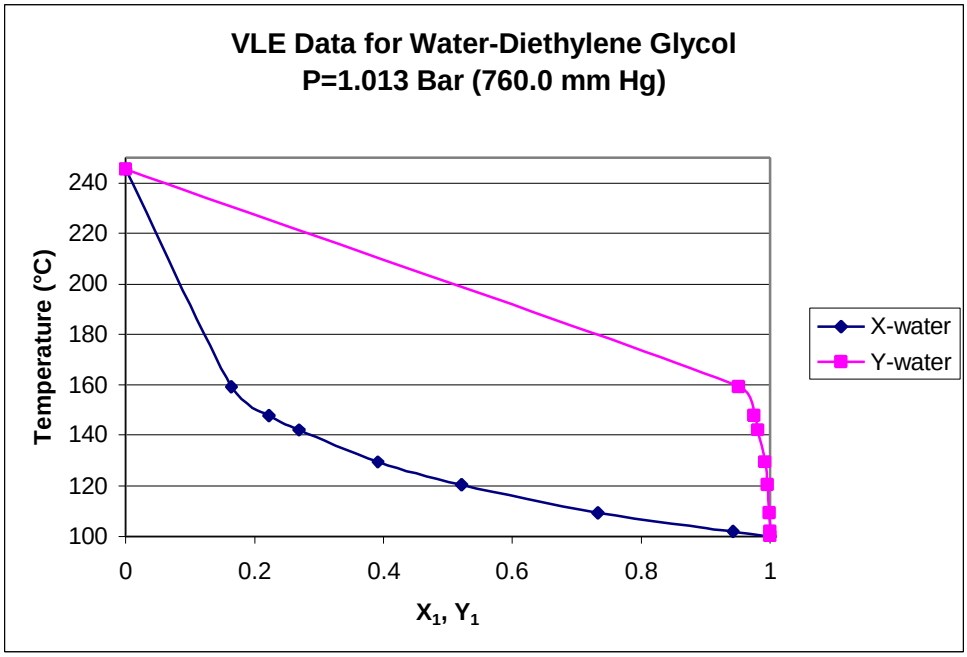

Figure 3.1 – Graphical vapor liquid equilibrium data for water-diethylene Glycol from Gmehling (1984)

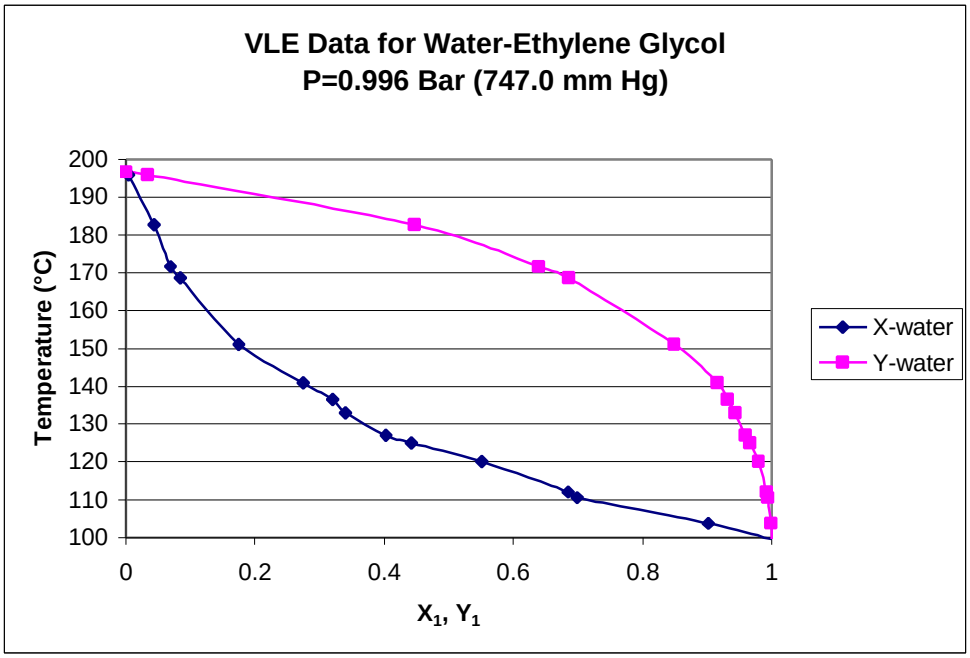

Figure 3.2 - Graphical vapor liquid equilibrium data for water-ethylene glycol from Gmehling (1984)

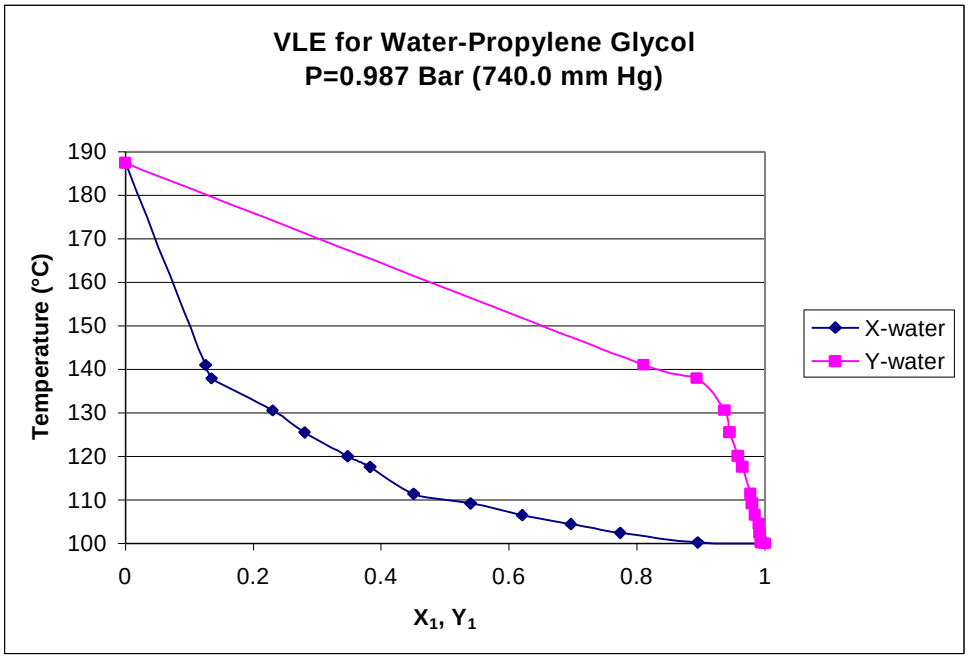

Figure 3.3 - Graphical vapor liquid equilibrium data for water-propylene glycol from Gmehling (1984)

4.0 EXPERIMENTAL PROCEDURE

4.1 TESTING PROCEDURE

Before recording measurements from a test section, the surface of each tube was aged by boiling each tube at a heat flux of at least 200 kW/m^2 for several hours. This allows the surface to oxidize slightly, and helps ensure that the tests that followed would be repeatable.

Reagent grade liquids and distilled water were used in the preparation of all mixtures. The mixture components were measured using a balance accurate to ±1.0 g.

The pressure vessel was filled to a level of 70 mm above the top of the test section. During the time that the vessel was being filled, water was flowing through the condensing coil to ensure that any vapor that might evaporate was condensed. After reaching the desired level, both the liquid inlet line and the degassing vent were closed. The immersion heaters were turned on and when the pressure exceeded 1.01 bar, the degassing vent was momentarily opened in order to degas the system. This was continued until saturation conditions for that fluid were attained. This usually required approximately 1.5 hours. Once the system was at saturation, power was applied to the test section, and increased until the heat flux was at least 200 kW/m^2. This heat flux was maintained for approximately 5 minutes in order to remove trapped gases from the nucleation sites. The power to the test section was then slowly decreased to zero so that the surface deactivated and attained equilibrium with the bulk fluid. The process was then repeated to ensure that all trapped gases were removed from the boiling surface.

After the pre-test cycling was complete, the surface heat flux was increased in small increments starting from zero, and the temperatures of the thermocouples in the test section and in the bulk fluid were recorded. The voltage and current through the test section were also recorded to determine the applied power. The heat flux was increased to the maximum level that could be attained while maintaining the vessel at the test pressure and maintaining a temperature that was safe for the heater.

The recorded measurements were then used to estimate the wall surface temperature, superheat, surface heat flux, and the heat transfer coefficient. Conductive

losses through the holder, which were minor, were accounted for in these estimations. The source code for PBDATA, the computer program used to perform these calculations, can be found in the Appendix as well as sample input and output files.

4.2 TEST REPEATABILITY AND UNCERTAINTY

The measurement error associated with the wall superheat was estimated to be ± 0.2 K. This value assumes that the Omega Trendicator was in error by ± 0.1 K. The combined uncertainty in heat flux due to error in the electrical current and voltage measurements is estimated to be ± 2%. The uncertainty in the heat transfer coefficient due to these errors was ± 4%.

For several of the mixtures, the temperature measurements would see some fluctuations up to ± 0.5 K about a mean value. These fluctuations were most likely due to condensation and reflux in the lines leading to the pressure transducer and the pressure relief valve. Taking this into account we can see that even if the temperature measurement errors resulted in a 1.0 K superheat error, the error in the heat transfer coefficient would still be no larger than ± 5%. If we assume the error in heat flux measurements remained ± 2%, the maximum error in the heat transfer coefficient was estimated to be ± 7.5%.

Another important concern in boiling experimentation is reproducibility of results. To demonstrate the reproducibility of the experimental data, several tests for pure components were repeated on the same surface throughout the testing life of the heaters. Figure 4.1 shows four boiling curves for pure water at 1.0 bar which were obtained on the same smooth surface heater. At q'' = 200 kW/m^2, the variation in heat transfer coefficients was from 14.78 kW/m^2°C to 19.17 kW/m^2°C. The average value of the heat transfer coefficient was 17.15 kW/m^2°C. These values ranged from 11.8% below to 13.8% above the average heat transfer coefficient at this heat flux. This range is slightly larger than our uncertainty range, but examining the results can offer an explanation. Tests #319 and #330, the top two boiling curves on the graph, were taken early in the lifetime of the heater. Soon after these tests, the heater surface required refinishing. The

tests #351 and #372 were then taken. The surface refinishing is most likely the reason for the large gap between the two sets of tests.

Figure 4.2 shows four boiling curves for pure water at 1.0 bar which were obtained on the heater with the Turbo BIII surface. At q'' = 200 kW/m^2, the variation in heat transfer coefficients was from 25.17 kW/m^2°C to 27.18 kW/m^2°C. The average value of the heat transfer coefficient was 25.86 kW/m^2°C. These values ranged from 5.1% below to 2.7% above the average heat transfer coefficient at this heat flux.

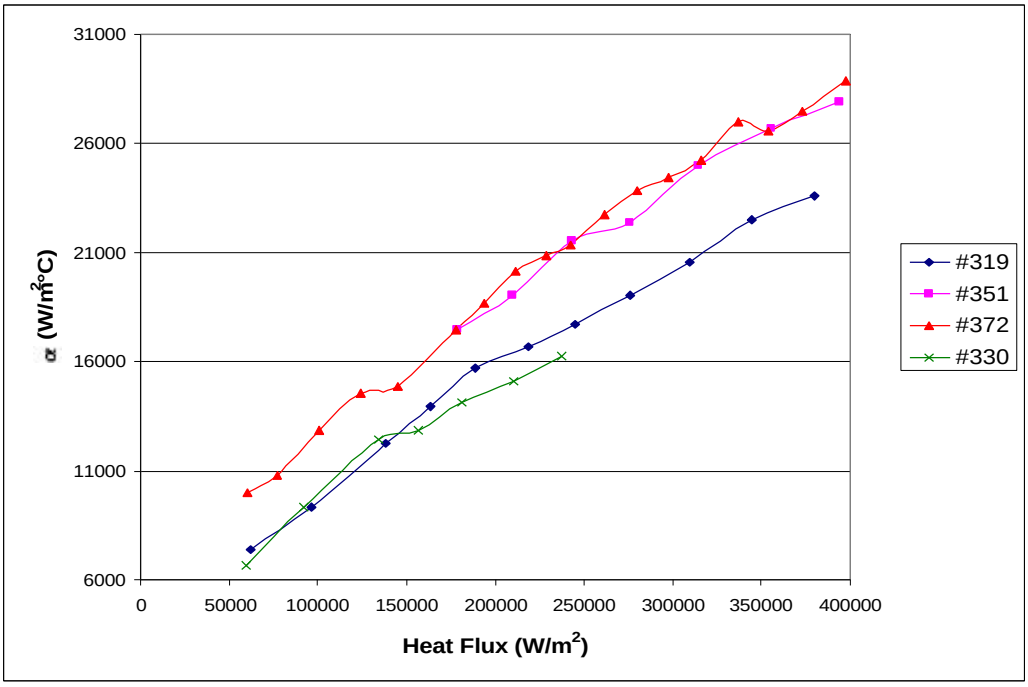

Figure 4.1- Boiling curves for pure water at 1.0 bar on the smooth tube.

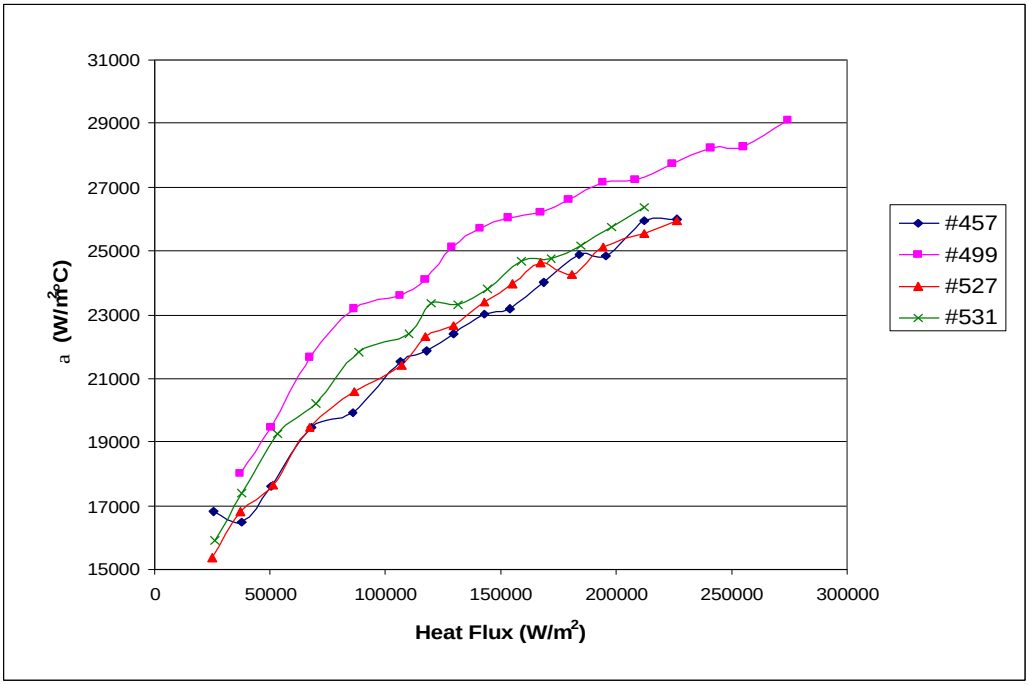

Figure 4.2- Boiling curves for pure water at 1.0 bar on the Turbo BIII heater.

5.0 EXPERIMENTAL RESULTS FOR SMOOTH TUBE

Experimental data were obtained for three binary mixture systems on a smooth, copper surface at a pressure of 1.0 bar. The binary systems tested were: water-propylene glycol, water-ethylene glycol, and water-diethylene glycol. Overall the systems were chosen because of the availability of VLE data. Some previous experimental data was available for ethylene glycol and propylene glycol mixture systems in a flow boiling situation, however, there was no pure component data for comparison. Also there was data available for the ethylene glycol mixture system including pure components on a horizontal platinum wire, but this is difficult to compare to our data on a horizontal cylinder. For the current experiments it was necessary to have smooth tube data for mixtures to compare to the enhanced tube data. Each test was assigned an individual identification number to distinguish it from the other tests. These numbers can be seen in the legends on the graphs.

The lines shown connecting the data points in the figures are meant only as a visual aid. They are not meant to show correlation between points. For the purpose of keeping the figures clear from clutter, experimental uncertainty is shown only in the first graph of a given type.

The degradation in heat transfer coefficient for a mixture can be characterized by comparing its value to the value of the heat transfer coefficient obtained from a linear combination of pure component values using the liquid mole fraction. This heat transfer coefficient, α_{id}, is termed the ideal heat transfer coefficient and is defined as

$$a_{id} = X_1 a_1 + (1 - X_1) a_2 \qquad (1)$$

for a_1 and a_2 at equivalent heat fluxes. When the measured heat transfer coefficient is less than this ideal heat transfer coefficient, it is considered to have undergone degradation.

5.1 WATER-PROPYLENE GLYCOL MIXTURES

The boiling curves obtained for the water-propylene glycol system at 1.0 bar on the smooth tube are shown in Figures 5.1 through 5.3. The boiling curves are presented first with the heat flux as a function of wall superheat since this is representative of the way the tests were conducted. Next the curves are presented as boiling heat transfer coefficient versus wall superheat. Finally the ratio of the measured boiling heat transfer coefficient to the ideal boiling heat transfer coefficient is shown as a function of mixture concentration.

The mixture effect on the boiling heat transfer coefficient in this mixture system is clearly evident. Figure 5.1 clearly shows that the mixtures lie well to the right of the pure component curves. This indicates that it requires a much larger superheat to maintain a given heat flux for the mixtures. In Figure 5.2 it can be seen that the heat transfer coefficient degradation increases as the water concentration decreases. This degradation reaches a maximum at 0.230 mole fraction of water and then begins to decrease.

In Figure 5.3 the amount of degradation at a given heat flux for each mixture composition is shown. Within the bounds of our uncertainty it can be seen that there is a small reduction due to heat flux for all but the solutions with the highest mole fraction water. Even at the most dilute solution we see very little change in the degradation due to the change in heat flux. This leads us to believe that the heat flux plays a very small role in the degradation when compared to the role played by mixture composition in this mixture system.

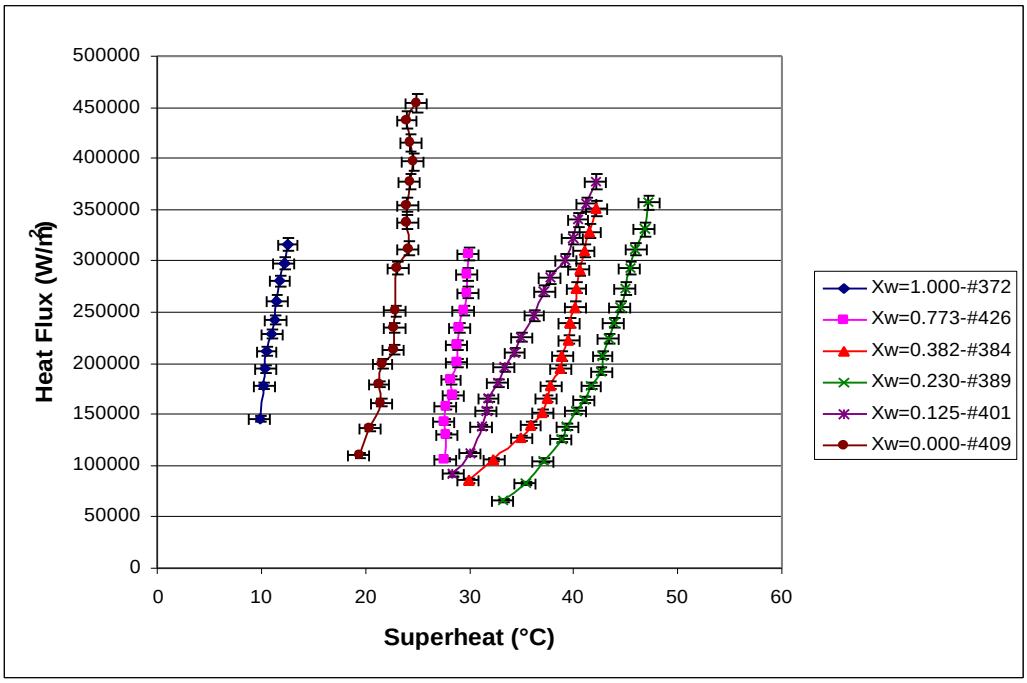

Figure 5.1-Heat flux vs. superheat boiling curves for water/propylene glycol mixtures at saturation at 1.0 bar on the smooth tube.

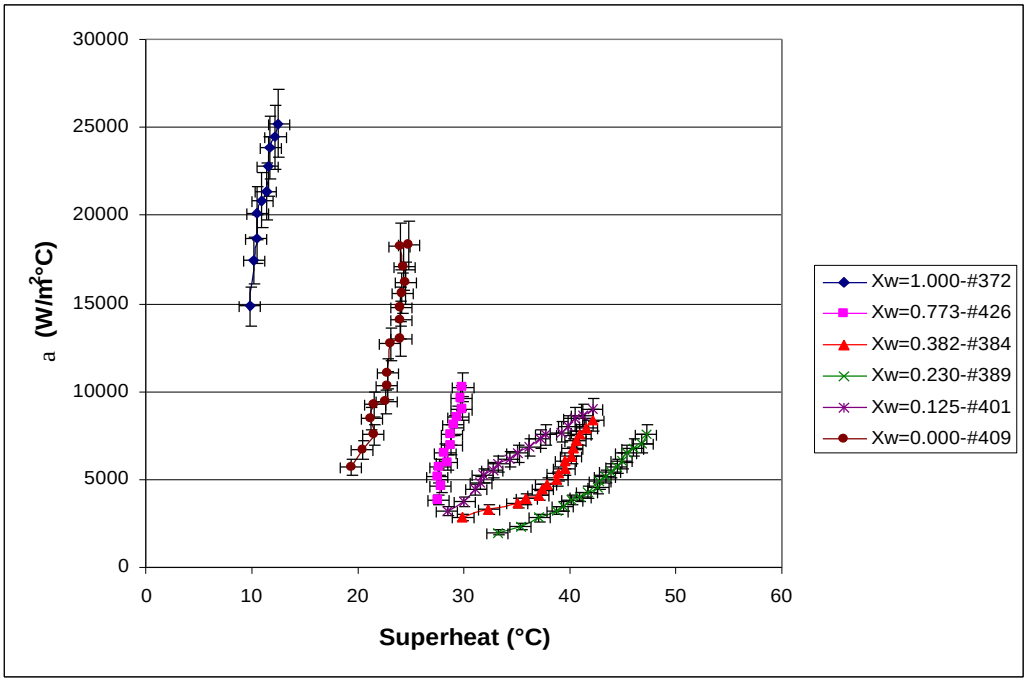

Figure 5.2-Heat transfer coefficient vs. superheat boiling curves for water/propylene glycol mixtures at saturation on the smooth tube

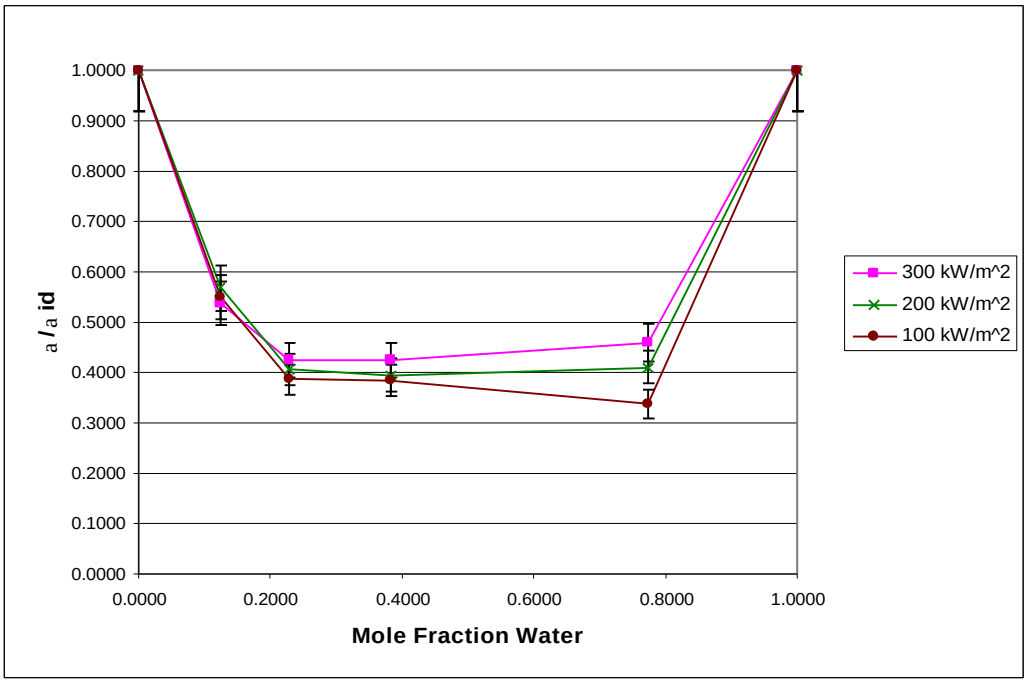

Figure 5.3- a/a_{id} ***vs. mole fraction water in a water/propylene glycol mixture at saturation at 1.0 bar on the smooth tube.***

5.2 WATER-ETHYLENE GLYCOL MIXTURES

The boiling curves obtained for the water-ethylene glycol system at 1.0 bar on the smooth tube are shown in Figures 5.4 through 5.6. The boiling curves are presented first with the heat flux as a function of wall superheat since this is representative of the way the tests were conducted. Next the curves are presented as boiling heat transfer coefficient versus wall superheat. Finally, the ratio of the measured boiling heat transfer coefficient to the ideal boiling heat transfer coefficient is shown as a function of mixture concentration.

The mixture effect on the boiling heat transfer coefficient can clearly be seen in all the figures. Figure 5.4 shows that all of the mixture curves lie to the right of the pure component boiling curves. The heat transfer coefficient degradation increases as the mole fraction of water decreases until it reaches a maximum degradation at between 0.400 and 0.250 mole fraction water. This maximum degradation point is very close to the maximum boiling range for this mixture, which occurs at approximately $X_w = 0.4$ with ? $T_{bp} = 58°C$.

The amount of degradation at a given heat flux for each mixture composition is seen in Figure 5.6. There is virtually no change in the degradation due to heat flux for all but the highest concentration of water and that change is insignificant when compared to our uncertainty. Once again, heat flux plays an insignificant role in the degradation when compared to the degradation due to mixture effects for this mixture system.

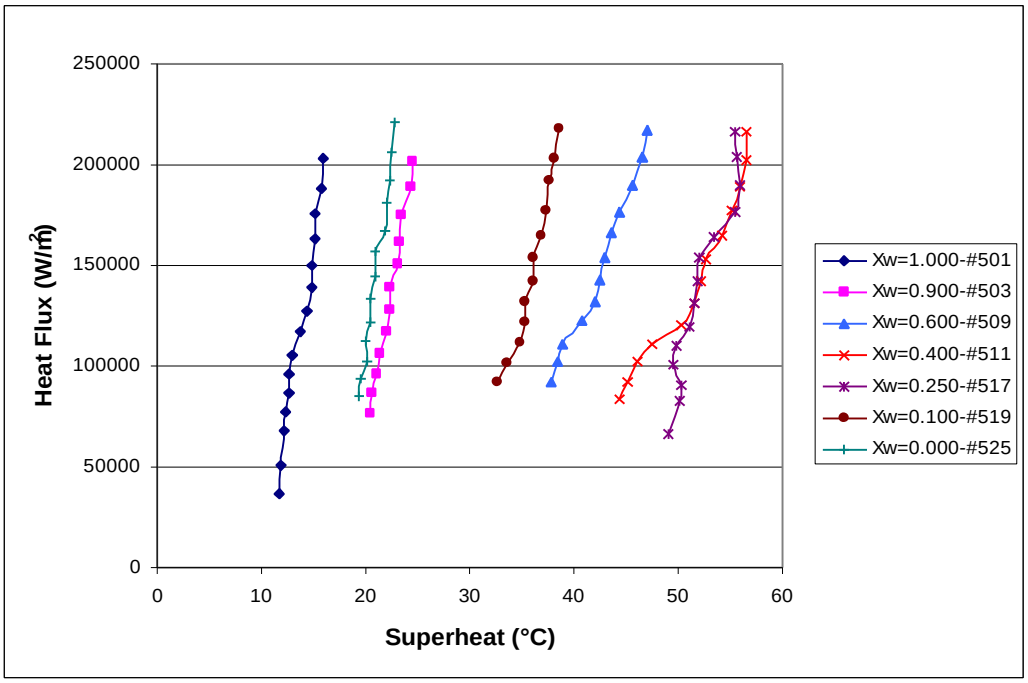

Figure 5.4-Heat flux vs. superheat boiling curves for water/ethylene glycol mixtures at saturation at 1.0 bar on the smooth tube.

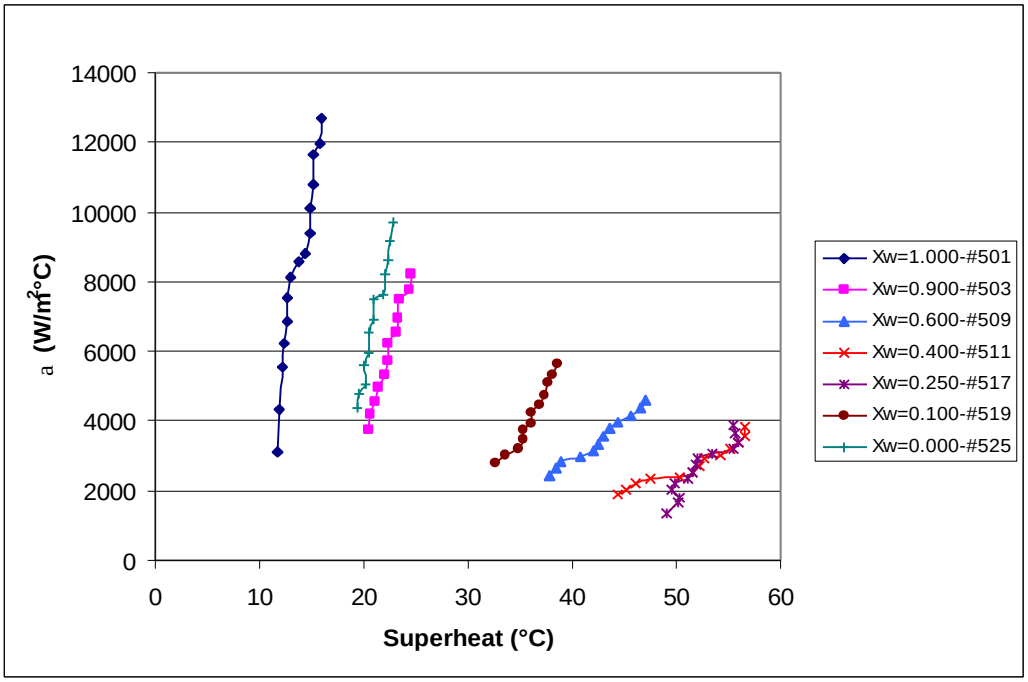

Figure 5.5-Heat transfer coefficient vs. superheat boiling curves for water/ethylene glycol mixtures at saturation at 1.0 bar on the smooth tube.

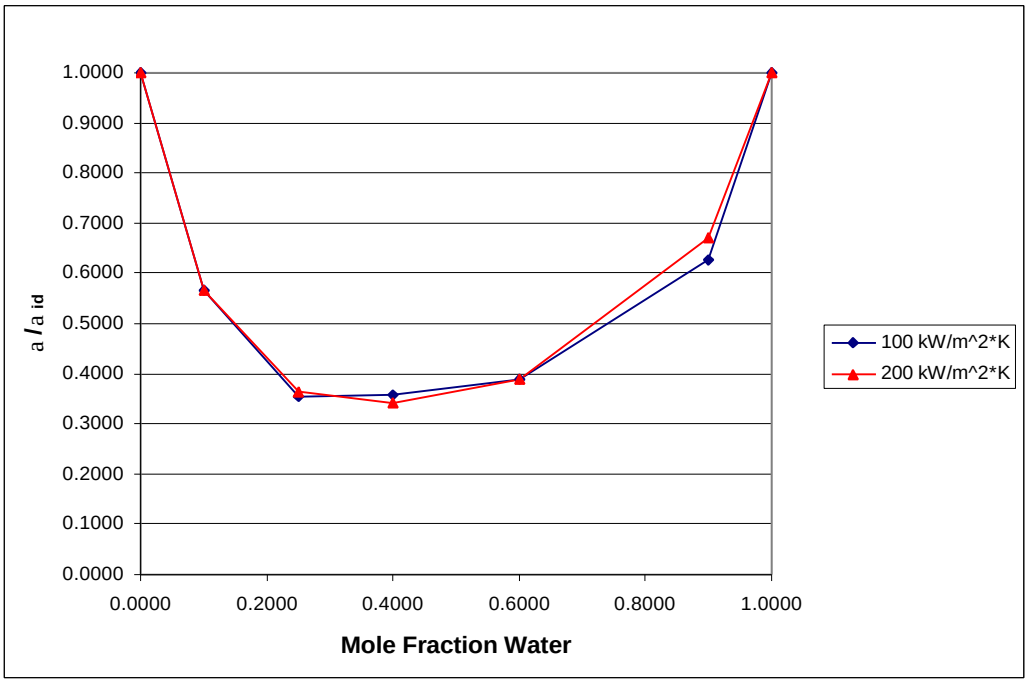

Figure 5.6- a/a_{id} ***vs. mole fraction water in a water/ethylene glycol mixture at saturation at 1.0 bar on a smooth tube.***

5.3 WATER-DIETHYLENE GLYCOL MIXTURES

The boiling curves obtained for the water-diethylene glycol system at 1.0 bar on the smooth tube are shown in Figures 5.7 through 5.9. The boiling curves are presented first with the heat flux as a function of wall superheat since this is representative of the way the tests were conducted. Next the curves are presented as boiling heat transfer coefficient versus wall superheat. Finally, the ratio of the measured boiling heat transfer coefficient to the ideal boiling heat transfer coefficient is shown as a function of mixture concentration.

Due to the high saturation temperature of diethylene glycol it was not feasible to obtain a boiling curve for pure diethylene glycol. However, this study did obtain boiling curves for four other mixtures which are shown with a pure water boiling curve as a reference. Although there is no boiling curve for pure diethylene glycol in the figures it is clear that there is a large mixture boiling effect at work.

In order to obtain a heat transfer coefficient for pure diethylene glycol it was necessary to use the Stephan-Abdelsalam correlation (1978). Using the heat transfer coefficients obtained in this manner the relative degradation in the heat transfer coefficients at each mixture was determined, and is shown in Figure 5.9. This figure confirms that there is a large degradation in the boiling heat transfer coefficient due to the mixture effect. It also shows us that there is a rather large degradation with only a small addition of water to the pure diethylene glycol.

Heat flux seems to have a greater effect on the amount of degradation for this mixture system than was seen in the water/ethylene glycol and water/propylene glycol systems. At the lower fluxes greater degradation occurs than at the higher heat fluxes. This result is similar to what that observed in the water-propylene glycol mixture with the highest mole fraction water.

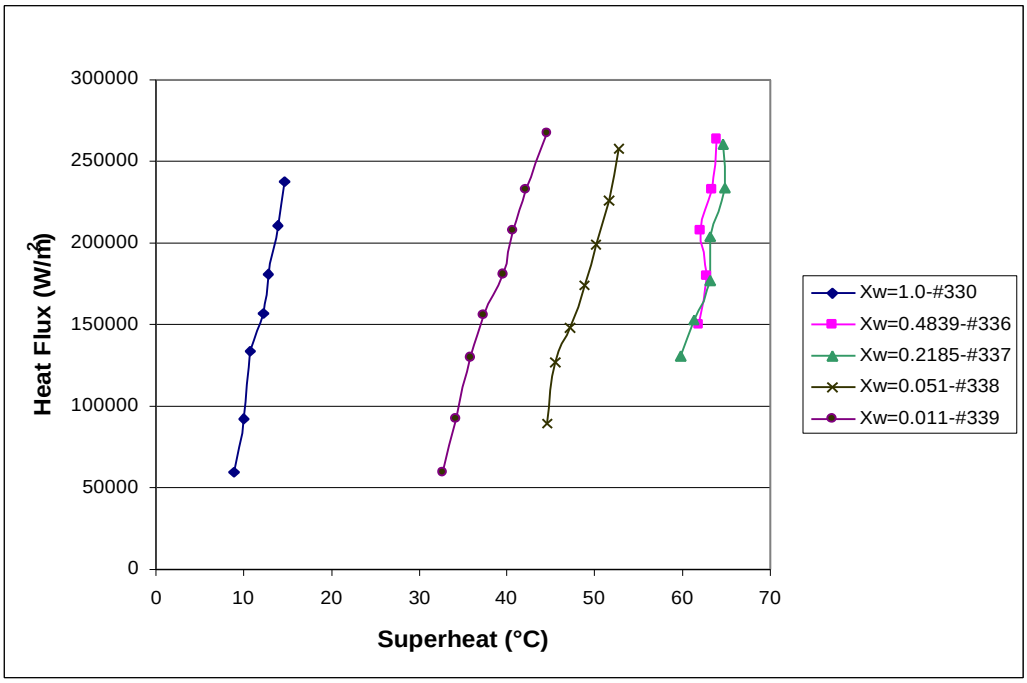

Figure 5.7- Heat flux vs. superheat boiling curves for water/diethylene glycol mixtures at saturation at 1.0 bar on the smooth tube.

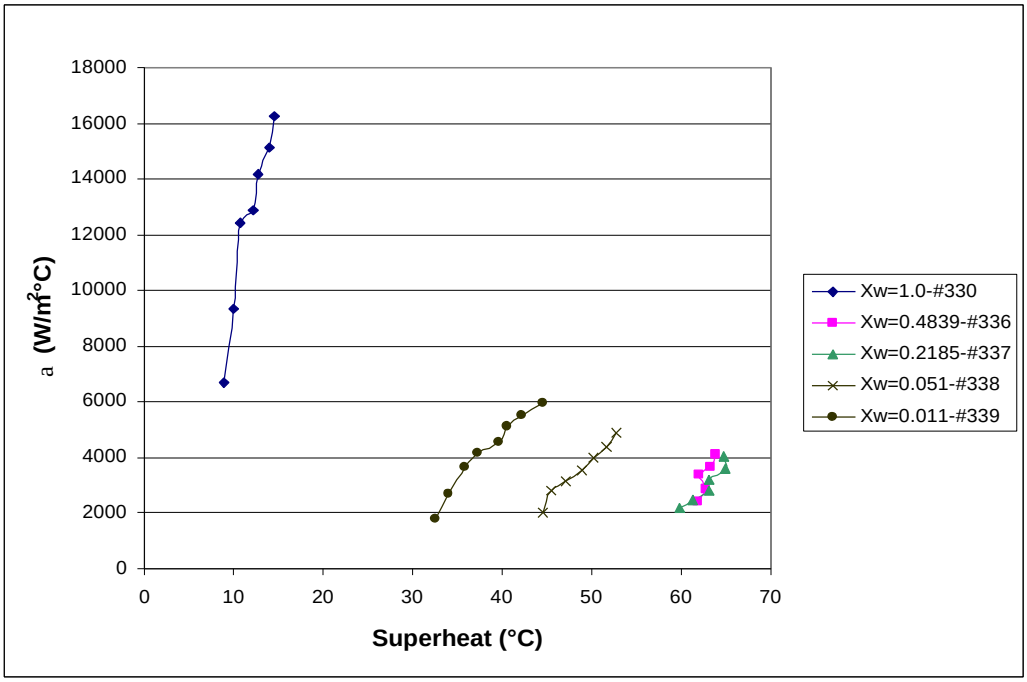

Figure 5.8-Heat transfer coefficient vs. superheat boiling curves for water/diethylene glycol mixtures at saturation at 1.0 bar on the smooth tube.

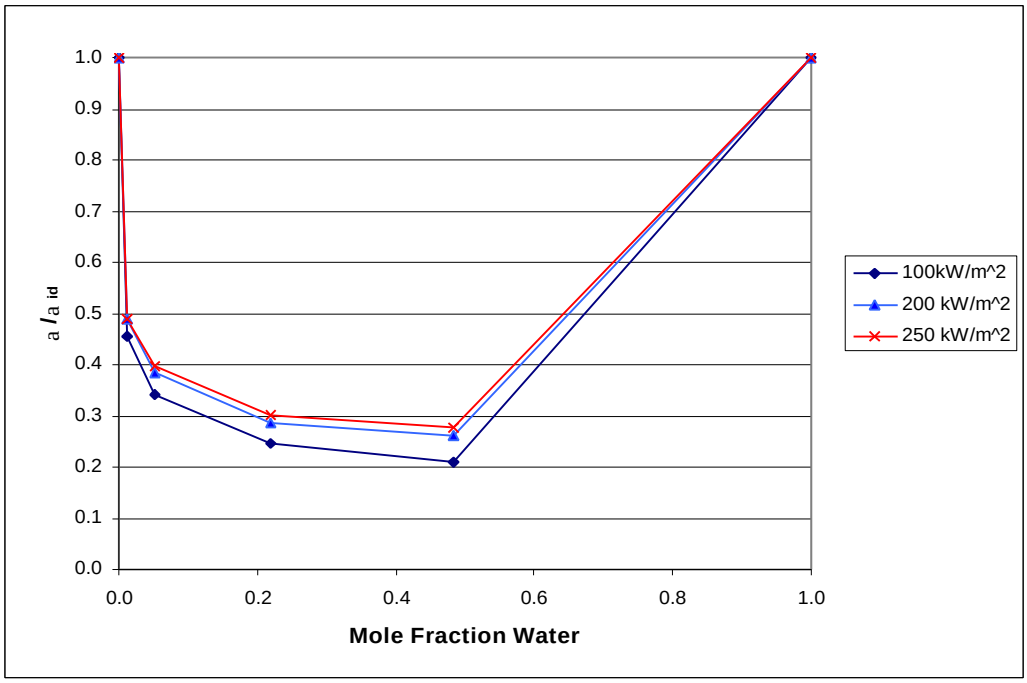

Figure 5.9- a/a_{id} ***vs. mole fraction water in a water/diethylene glycol mixture at saturation at 1.0 bar on a smooth tube.***

6.0 EXPERIMENTAL RESULTS FOR TURBO BIII SURFACE

Experimental data were obtained for two binary mixture systems on the Wolverine Tube Turbo BIII surface. The same mixture concentrations were used as were used for the smooth tube testing, except that diethylene glycol was omitted because of its high boiling point. Therefore, nearly all tests that were done with propylene glycol and ethylene glycol on the smooth surface heater have a counterpart for comparison on the Turbo BIII surface.

6.1 WATER-PROPYLENE GLYCOL MIXTURES

The boiling curves obtained for the water-propylene glycol system at 1.0 bar on the Turbo BIII surface are shown in Figures 6.1 through 6.3. The mixture effect on the boiling heat transfer degradation is once again clearly evident. It is also seen that the degradation increases as the mole fraction of water decreases. The maximum degradation occurs at 0.125 mole fraction water.

In Figure 6.3 the results are seen to differ somewhat from those observed for the smooth tube. Heat flux seems to play a more significant role in the degradation of the heat transfer coefficient. At the lower concentrations of water a greater effect of heat flux can be seen than at higher concentrations of water. The degradation in the boiling heat transfer coefficient is also seen to be quite large for low concentrations of water, but is much smaller for higher concentrations of water.

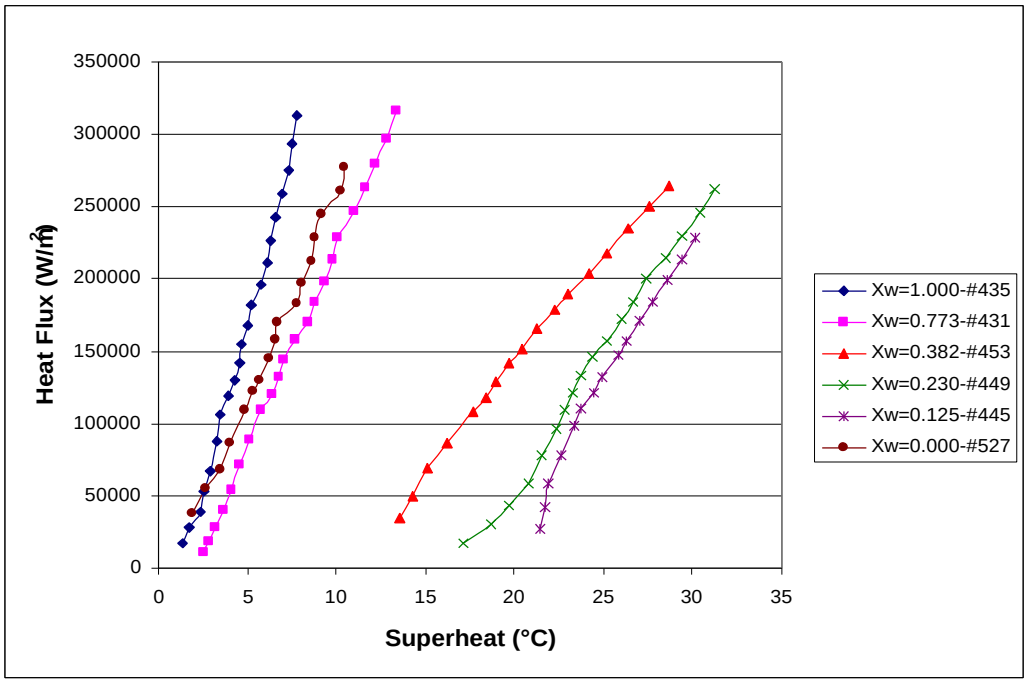

Figure 6.1-Heat flux vs. superheat boiling curves for water/propylene glycol mixtures at saturation at 1.0 bar on the Turbo BIII tube.

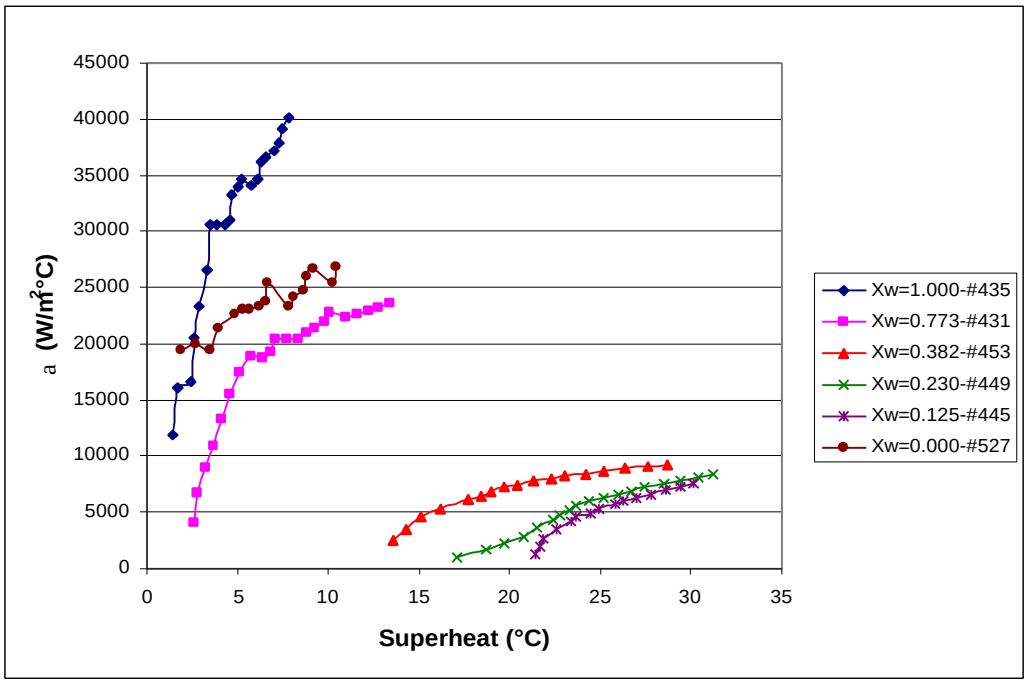

Figure 6.2-Heat transfer coefficient vs. superheat boiling curves for water/propylene glycol mixtures at saturation at 1.0 bar on the Turbo BIII tube.

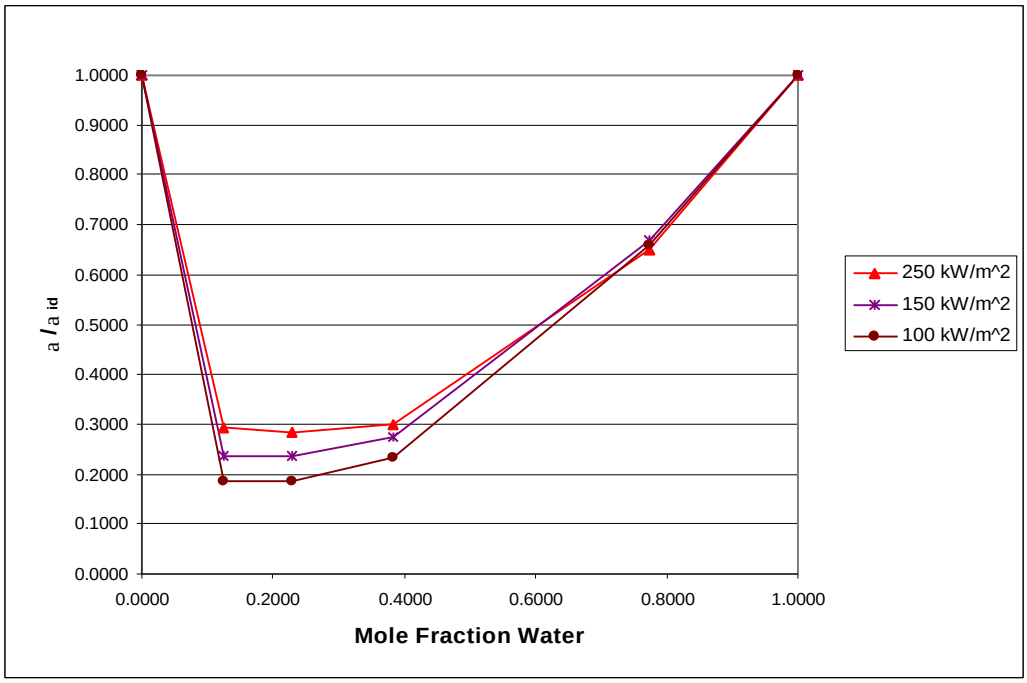

Figure 6.3- a/a_{id} ***vs. mole fraction water in a water/propylene glycol mixture at saturation at 1.0 bar on a Turbo BIII tube.***

6.2 WATER-ETHYLENE GLYCOL MIXTURES

The boiling curves obtained for the water-ethylene glycol system at 1.0 bar on the Turbo BIII surface are shown in Figures 6.4 through 6.6. The mixture effect on the boiling heat transfer degradation is once again clearly evident. The degradation is also seen to increase as the mole fraction of water decreases. However, the degradation reaches a maximum at between 0.400 and 0.250 mole fraction water.

In Figure 6.6 the heat flux is seen to play a much greater role in the degradation at all the mixture concentrations. As heat flux increases the degradation in the boiling heat transfer coefficient seems to decrease. The figure also shows that for mixtures having a lower mole fraction water, the degradation is quite large when compared to the same mole fraction of ethylene glycol.

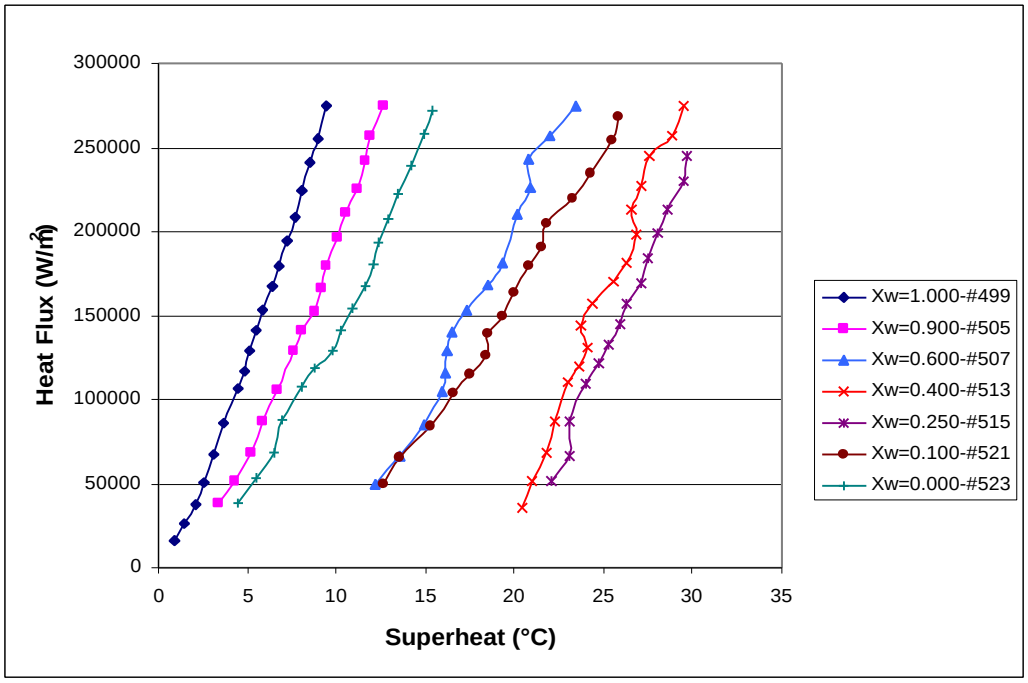

Figure 6.4-Heat flux vs. superheat boiling curves for water/ethylene glycol mixtures at saturation at 1.0 bar on the Turbo BIII tube.

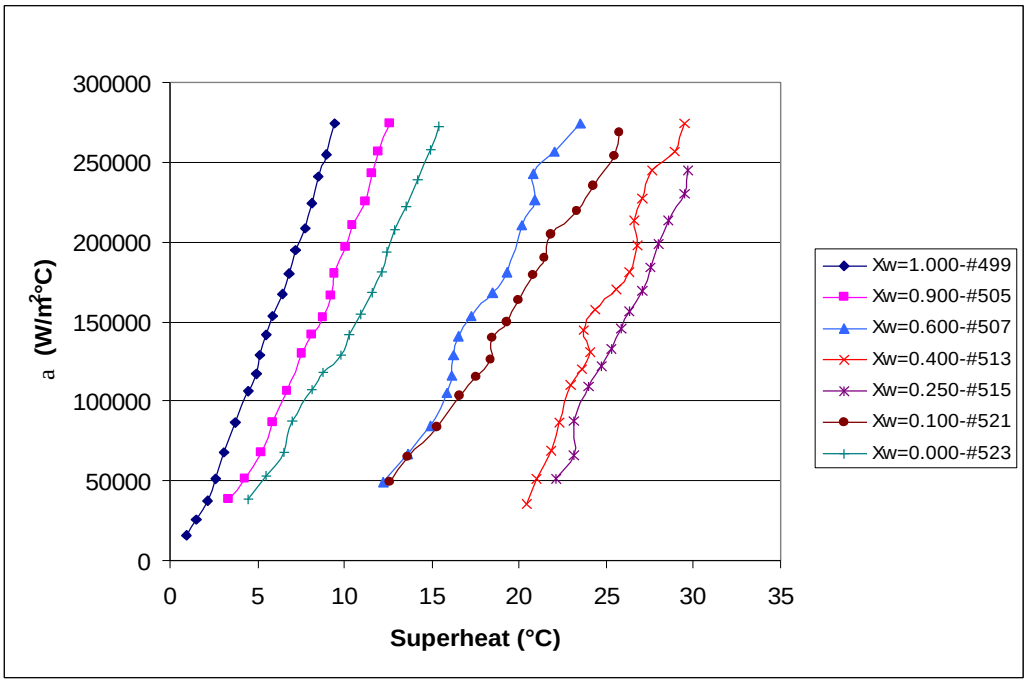

Figure 6.5-Heat transfer coefficient vs. superheat boiling curves for water/ethylene glycol mixtures at saturation on the Turbo BIII tube.

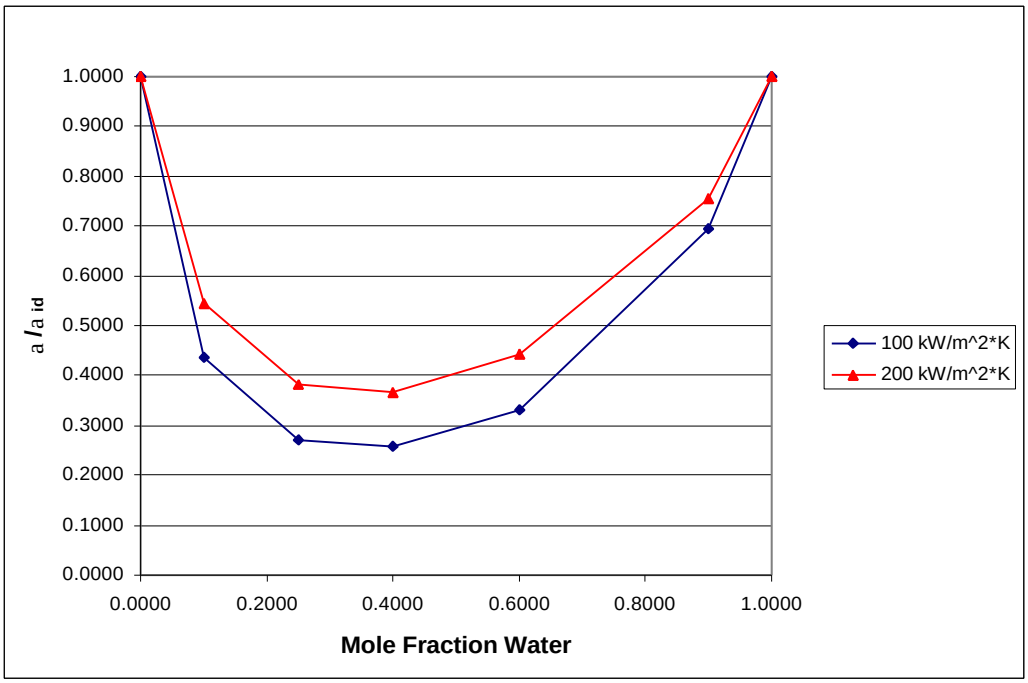

Figure 6.6- a/a_{id} vs. mole fraction water in a water/ethylene glycol mixture at saturation on a Turbo BIII tube.

7.0 EVALUATION OF RESULTS

This chapter will examine the factors that affect the heat transfer coefficient. First, the effect of the mixture composition will be examined. Then, the heat transfer coefficient observed on the enhanced surface as compared to that observed on the smooth surface is examined. Finally, the effect of subcooling on the heat transfer coefficient is shown.

7.1 MIXTURE COMPOSITION EFFECT

The mixture composition effect is summarized in Figures 7.1 and 7.2. These figures clearly show that the boiling heat transfer coefficient undergoes significant degradation due to mixture effects. Figure 7.1 shows that the water-diethylene glycol mixture experiences the most degradation at lower mole fractions water followed by the water-ethylene glycol and then the water-propylene glycol mixtures. However, at concentrations above 0.5 mole fraction water the trend seems to disappear. It is difficult to say at what point exactly with the limited number of data sets. It is even more interesting to note that in Figure 7.2 the opposite trend is seen when comparing the water-ethylene glycol and water-propylene glycol mixtures. The water-propylene glycol mixtures exhibit a larger degradation than the water-ethylene glycol mixtures at concentrations of less than 0.5 mole fraction water. This suggests that the surface has a large effect on the amount of degradation experienced at a given mole fraction.

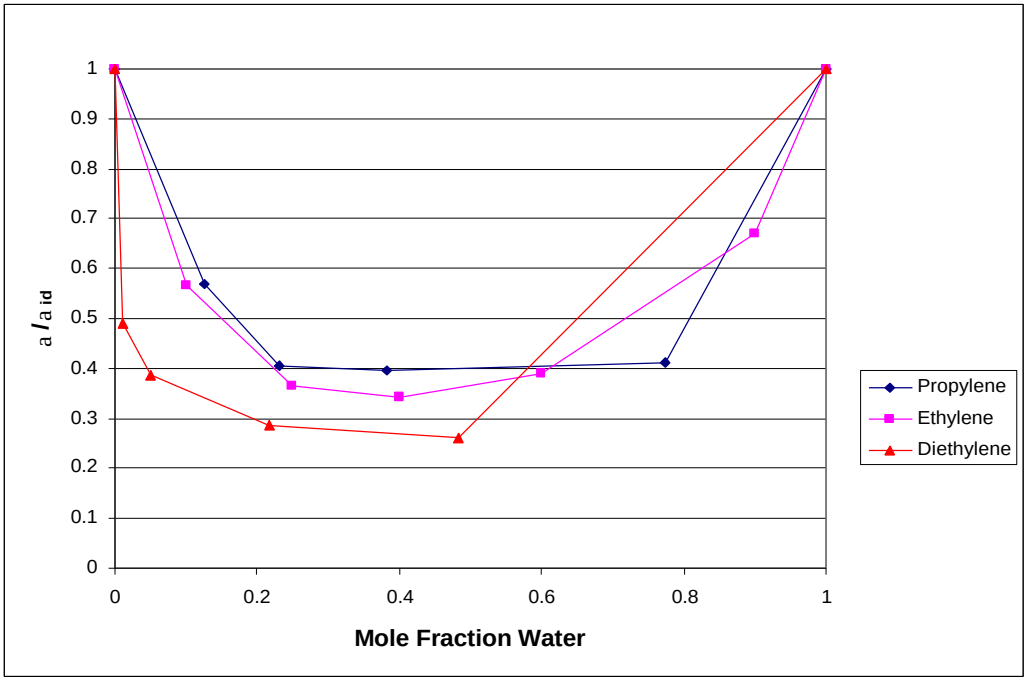

Figure 7.1- a/a_{id} vs. mole fraction water comparison of water-propylene glycol, water-ethylene glycol, and water-diethylene glycol mixtures at saturation at 1.0 bar on a smooth tube at 200 kW/m^2

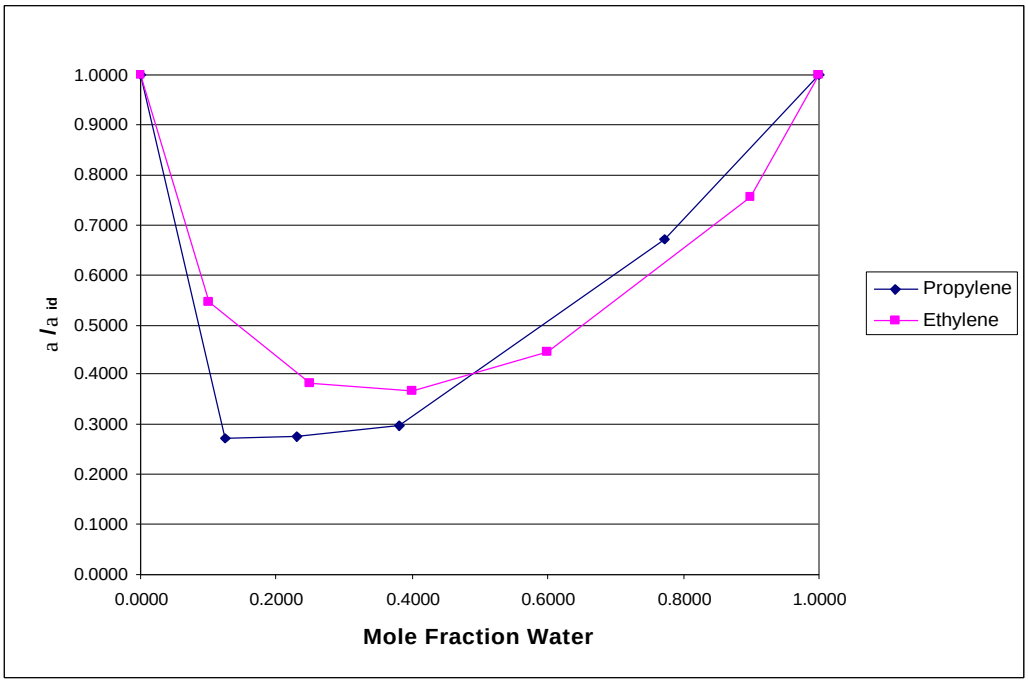

Figure 7.2- a/a_{id} ***vs. mole fraction water comparison of water-propylene glycol mixtures to water-ethylene glycol mixtures at saturation at 1.0 bar on a Turbo BIII tube at 200 kW/m^2***

7.2 SURFACE EFFECT

In this study, three separate heaters were used for testing. The first two had smooth copper surfaces and the third had a Wolverine Tube Turbo BIII surface to enhance its boiling characteristics. Enhanced surfaces are discussed in detail in Section 1.3.

7.2.1 Water/Propylene Glycol Mixtures

Figures 7.3 through 7.9 show the effect of the surface on the boiling heat transfer coefficient for water/propylene glycol mixtures. Figures 7.3 through 7.8 are in the form heat flux versus superheat followed by Figure 7.9 which is in the form α/α_{id} vs. mole fraction water.

In Figures 7.3 through 7.8 it is clearly seen that the heater with the Turbo BIII surface requires a substantially lower superheat to maintain a given heat flux. This increase in the boiling heat transfer coefficient is rather significant.

In Figure 7.9, at lower mole fractions of water, the Turbo BIII surface exhibits a larger reduction in the heat transfer coefficient than the smooth surface. It is worth noting, however, that even with this much larger reduction in the heat transfer coefficient, the Turbo BIII still out performs the smooth surface significantly.

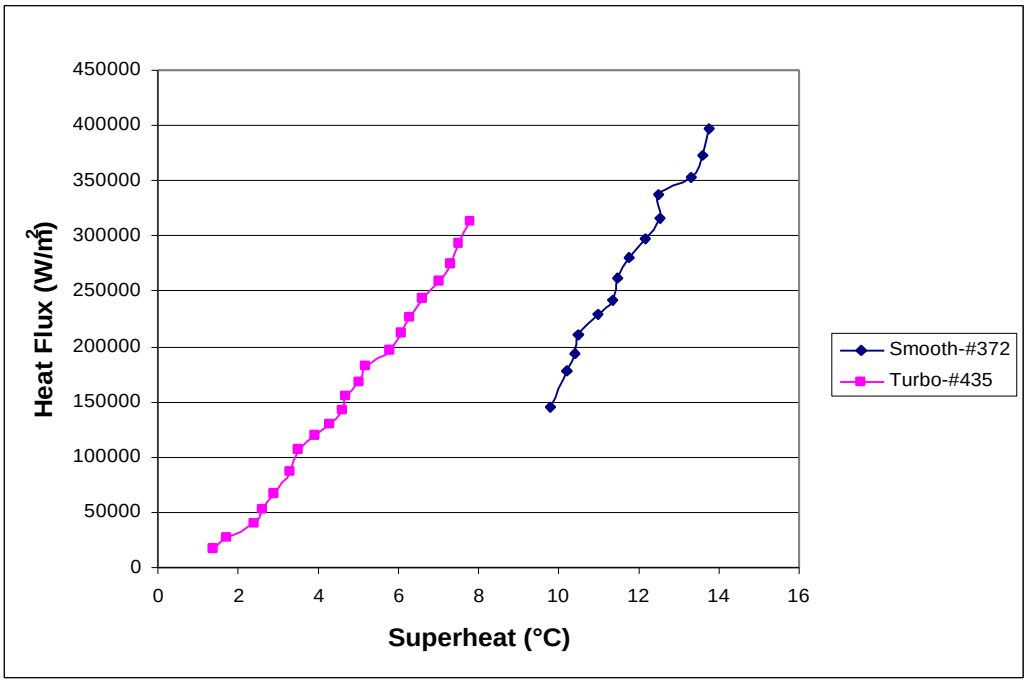

Figure 7.3-Boiling curve comparison between smooth and Turbo BIII tubes in X_w=1.0, X_{pg}=0.0 at saturation at 1.0 bar.

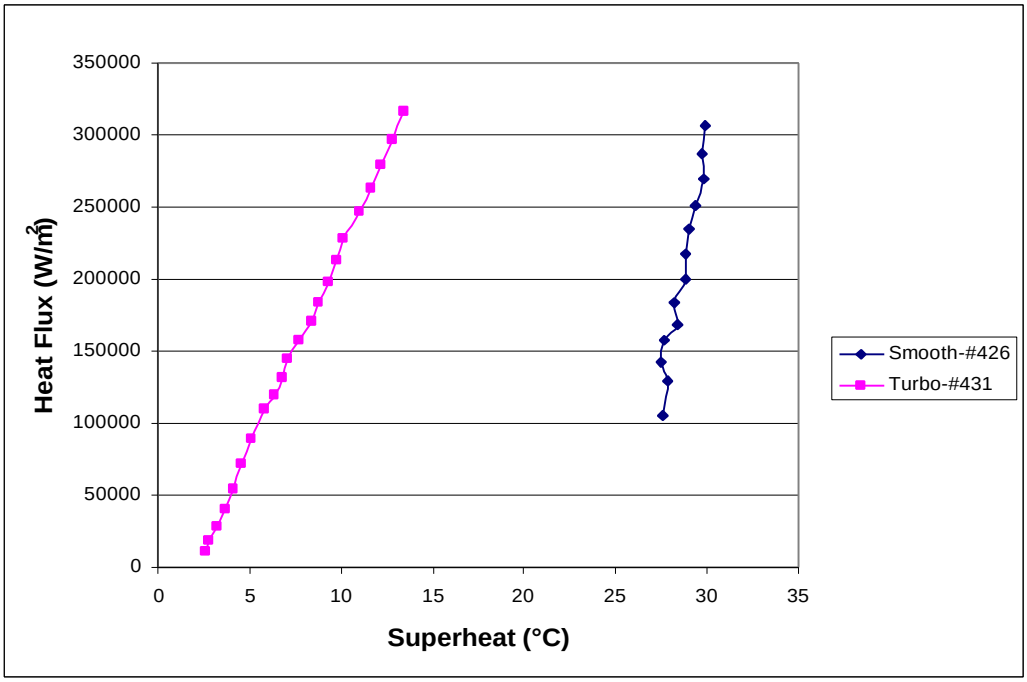

Figure 7.4-Boiling curve comparison between smooth and Turbo BIII tubes in X_w=0.773, X_{pg}=0.227 at saturation at 1.0 bar.

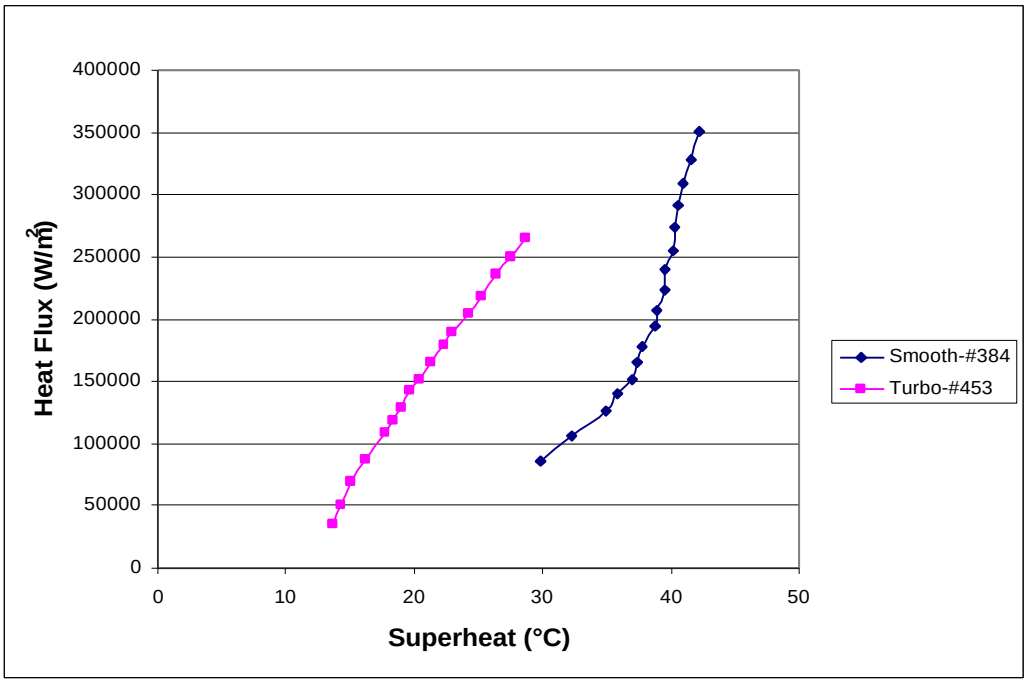

Figure 7.5-Boiling curve comparison between smooth and Turbo BIII tubes in X_w=0.382, X_{pg}=0.618 at saturation at 1.0 bar.

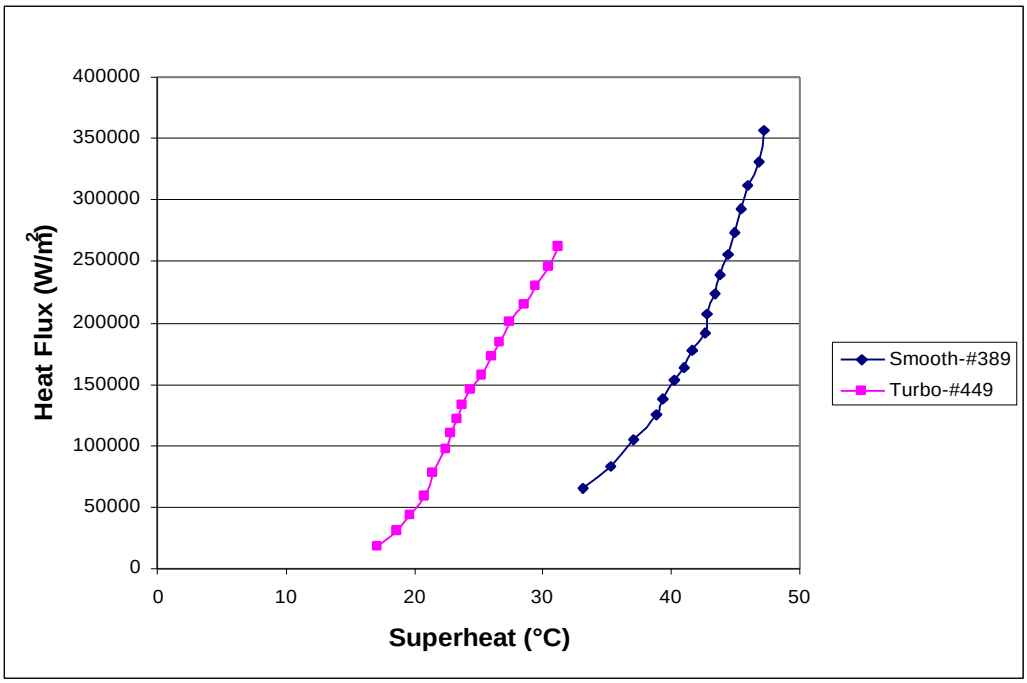

Figure 7.6-Boiling curve comparison between smooth and Turbo BIII tubes in X_w=0.230, X_{pg}=0.770 at saturation at 1.0 bar.

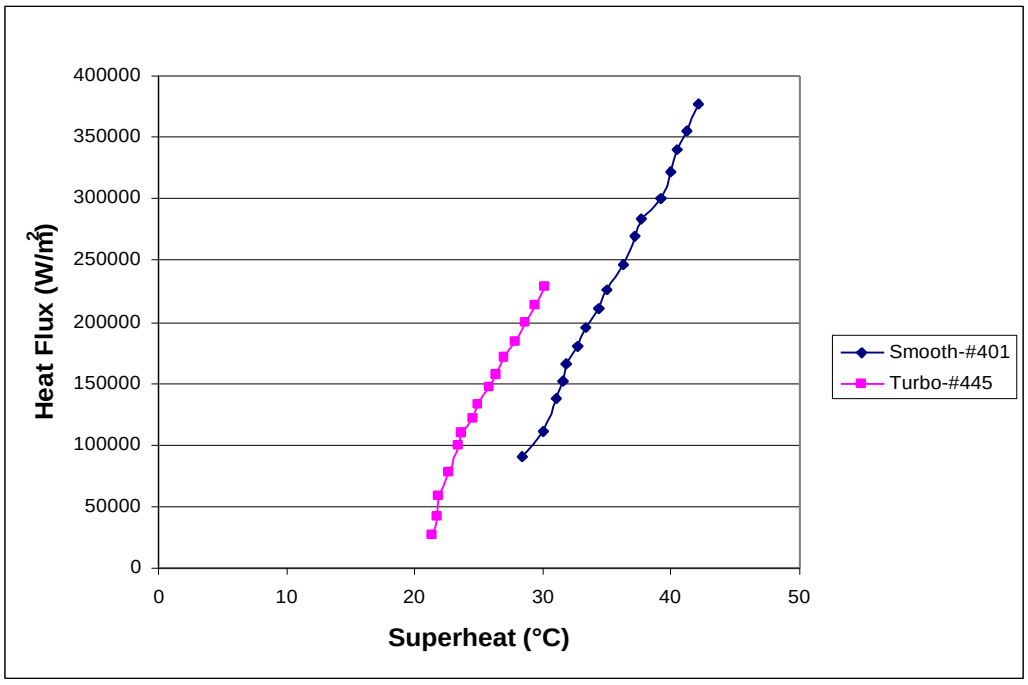

Figure 7.7-Boiling curve comparison between smooth and Turbo BIII tubes in X_w=0.125, X_{pg}=0.875 at saturation at 1.0 bar.

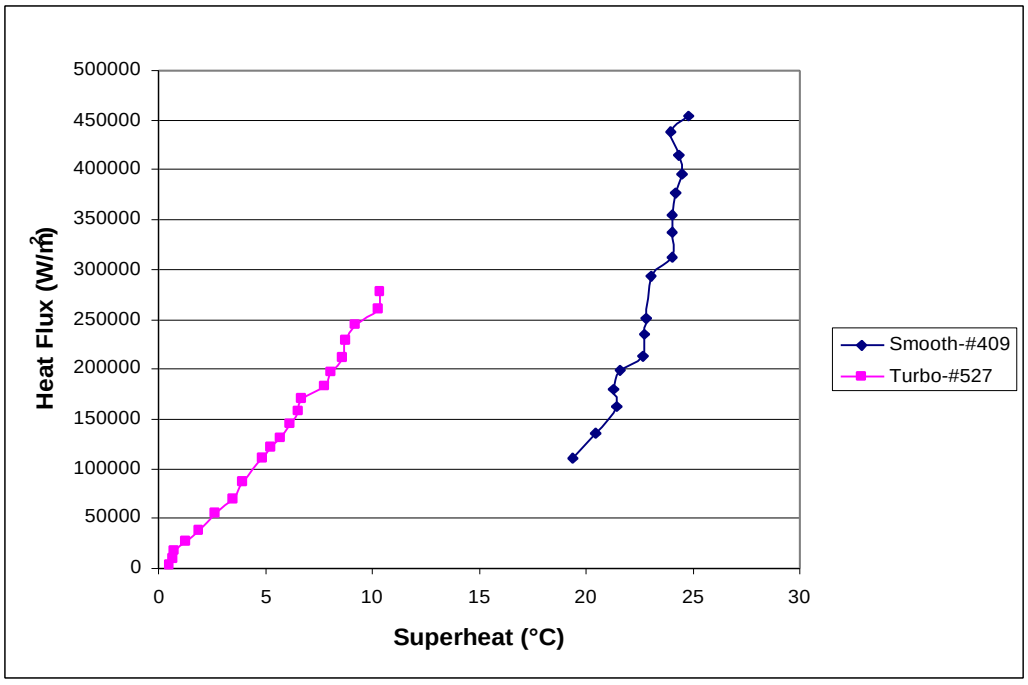

Figure 7.8-Boiling curve comparison between smooth and Turbo BIII tubes in X_w=0.0, X_{pg}=1.0 at saturation at 1.0 bar.

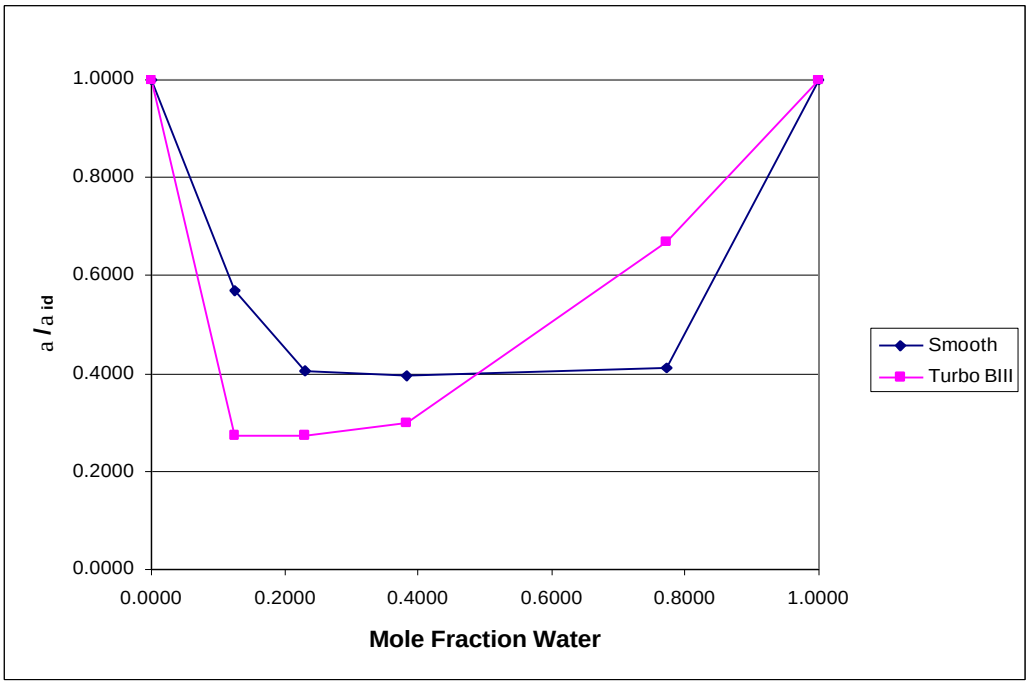

Figure 7.9- a/a_{id} ***vs. mole fraction water comparison between smooth and Turbo BIII tube for Water-Propylene Glycol Mixtures at saturation at 1.0 bar at 200 kW/m^2***

7.2.2 Water/Ethylene Glycol Mixtures

Figures 7.10 through 7.17 show the effect of the surface on the boiling heat transfer coefficient for water/ethylene glycol mixtures. Figures 7.10 through 7.16 are in the form heat flux versus superheat followed by Figure 7.17 which is in the form α/α_{id} vs. mole fraction water.

In Figures 7.10 through 7.16 it is clear that the heater with the Turbo BIII surface requires a substantially lower superheat to maintain a given heat flux. This increase in the boiling heat transfer coefficient is rather significant.

In Figure 7.17, at water mole fractions below approximately 0.20, there is virtually no difference between the degradation experienced on the smooth surface and the Turbo BIII surface. Above a mole fraction of 0.20 the Turbo BIII surface appears to have somewhat less degradation than the smooth tube, however, the degradation is not greater than the experimental uncertainty.

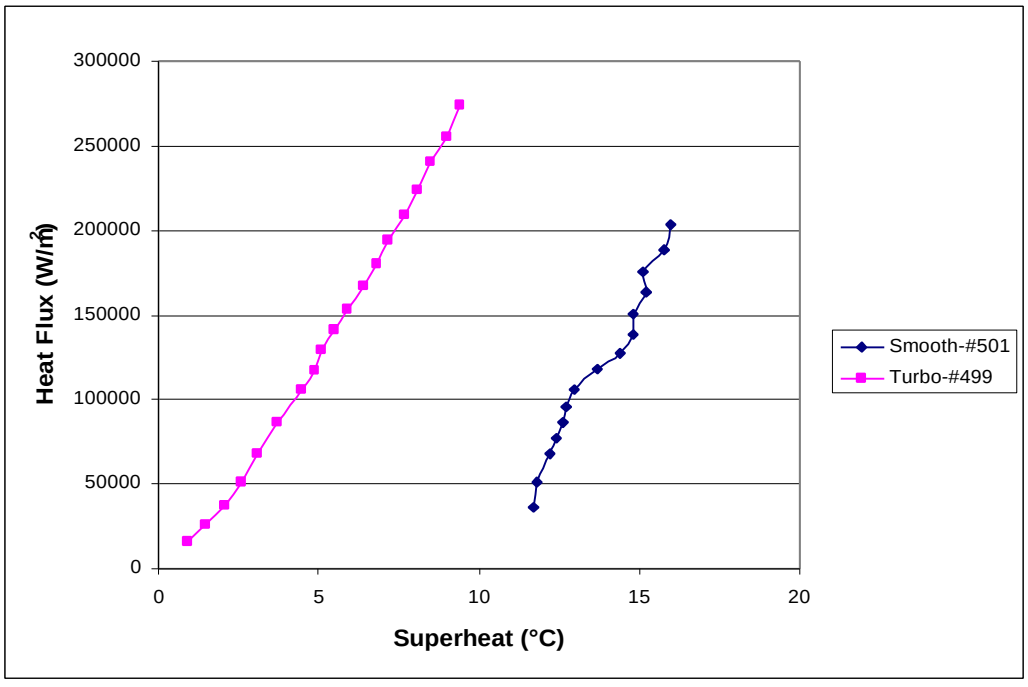

Figure 7.10-Boiling curve comparison between smooth and Turbo BIII tubes in X_w =1.0, X_{eg}=0.0 at saturation at 1.0 bar.

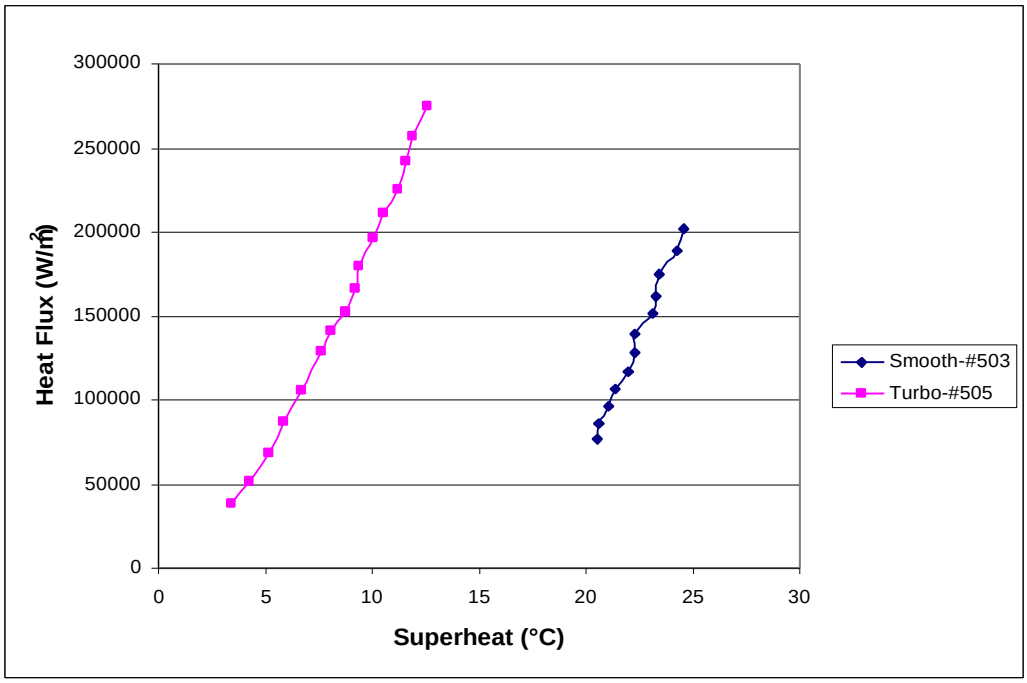

Figure 7.11-Boiling curve comparison between smooth and Turbo BIII tubes in X_w =0.9, X_{eg} =0.1 at saturation at 1.0 bar.

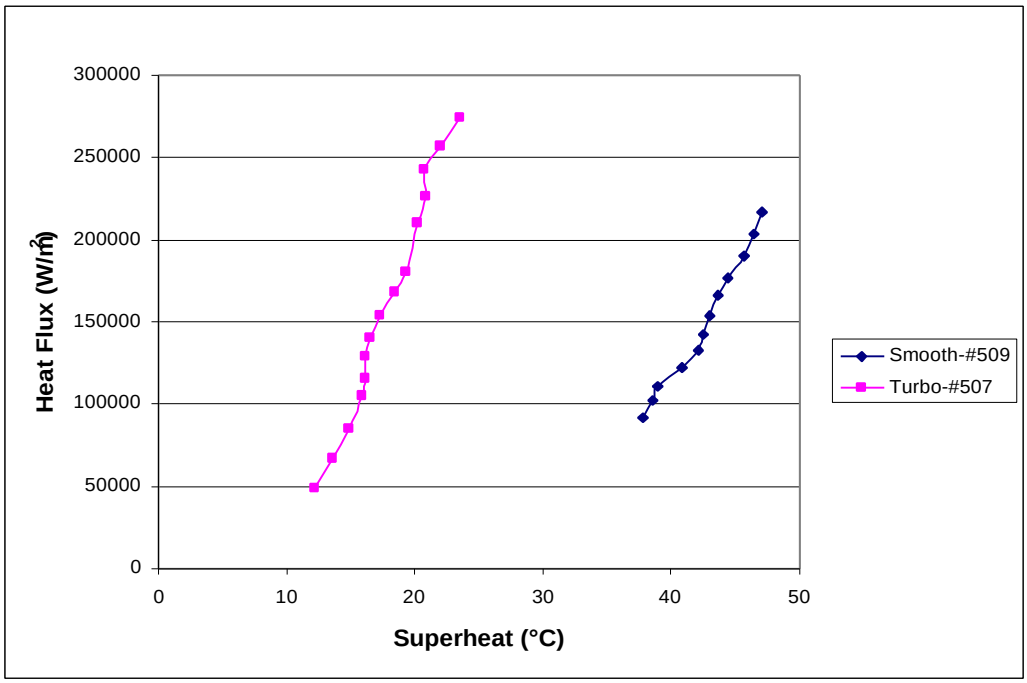

Figure 7.12-Boiling curve comparison between smooth and Turbo BIII tubes in X_w =0.6, X_{eg} =0.4 at saturation at 1.0 bar.

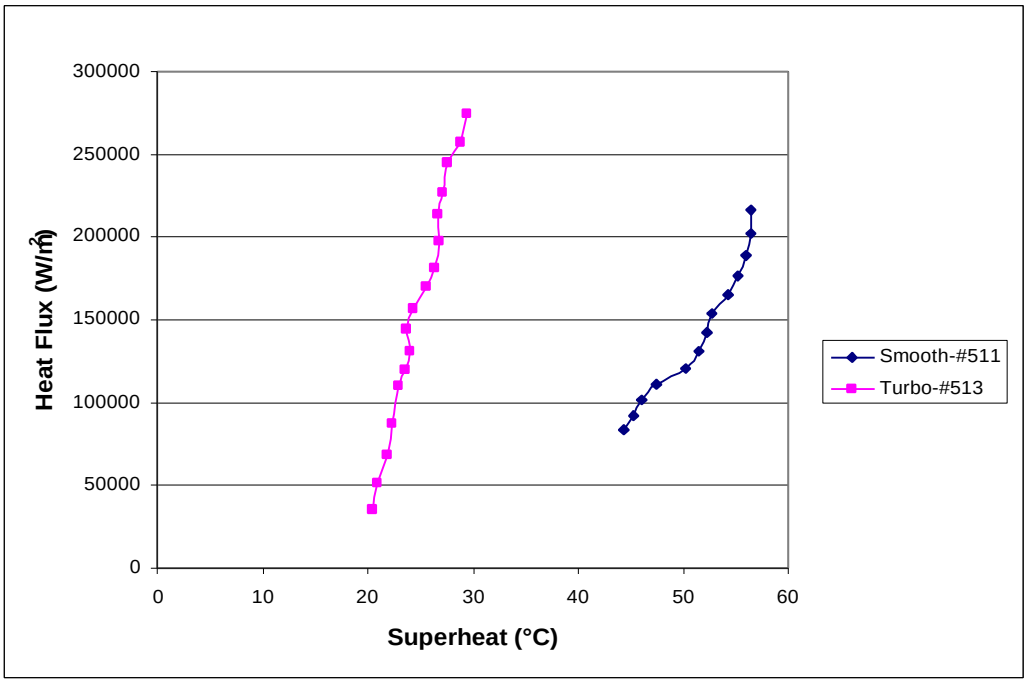

Figure 7.13-Boiling curve comparison between smooth and Turbo BIII tubes in X_w =0.4, X_{eg} =0.6 at saturation at 1.0 bar.

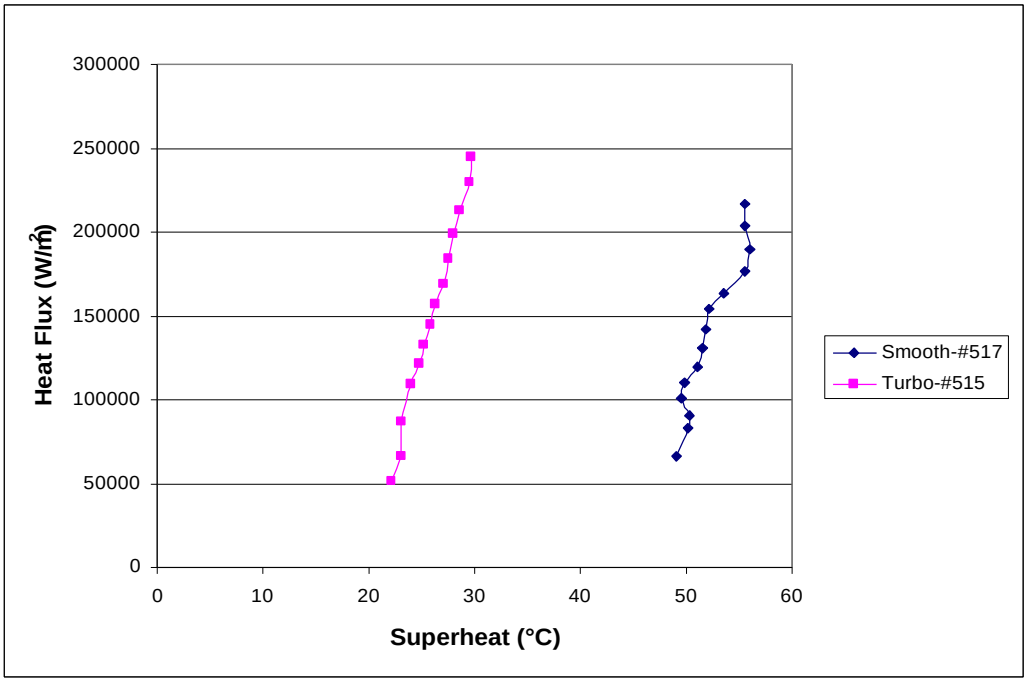

Figure 7.14-Boiling curve comparison between smooth and Turbo BIII tubes in X_w =0.75, X_{eg} =0.25 at saturation at 1.0 bar.

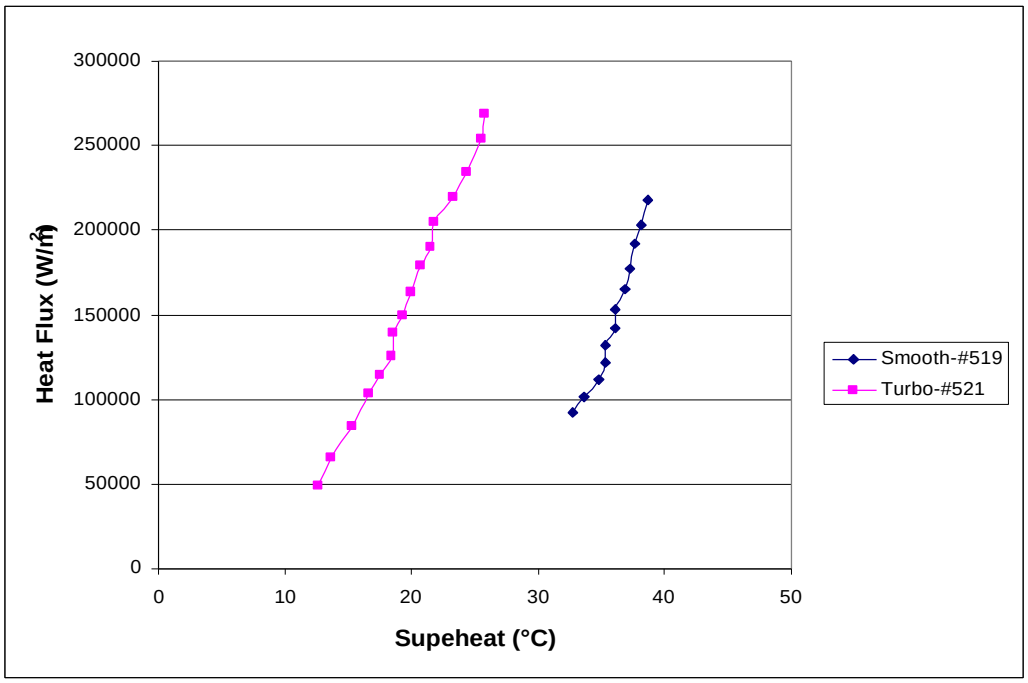

Figure 7.15-Boiling curve comparison between smooth and Turbo BIII tubes in X_w =0.1, X_{eg} =0.9 at saturation at 1.0 bar.

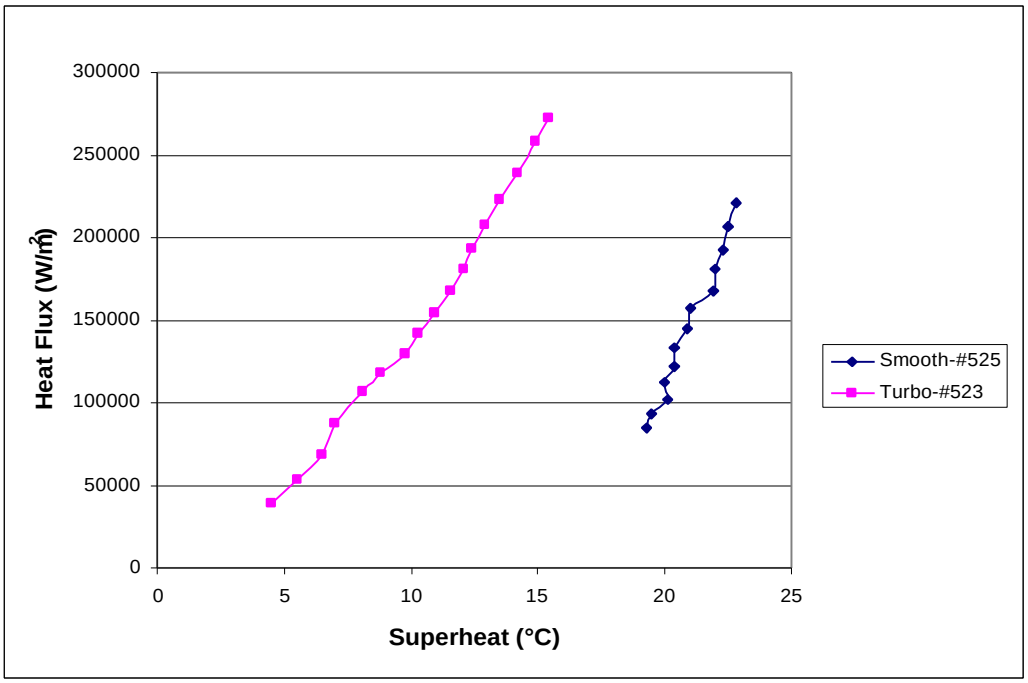

Figure 7.16-Boiling curve comparison between smooth and Turbo BIII tubes in X_w =0.0, X_{eg} =1.0 at saturation at 1.0 bar.

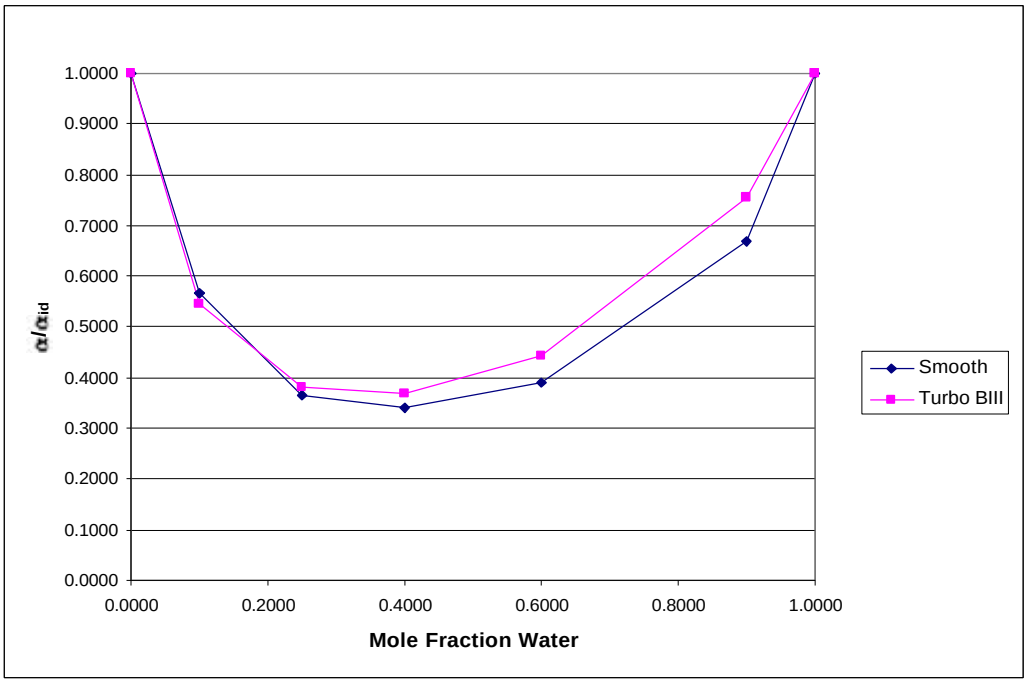

Figure 7.17- a/a_{id} ***vs. mole fraction comparison between smooth and Turbo BIII tube for water-ethylene glycol mixtures at saturation at 1.0 bar at 200 kW/m^2***

7.3 SUBCOOLING EFFECT

Subcooled boiling can significantly affect the boiling characteristics of a given surface. The effect of subcooling on the boiling on both smooth and Turbo BIII surfaces is presented in this section. First the water/propylene glycol mixture system is examined, followed by the water/ethylene glycol system. The mixture $X_w = 0.773$, $X_{pg} = 0.227$, presented in Figure 7.19, was not performed on the smooth surface heater due to premature failure of the heater's electrical resistance heating element.

It is important to remember that the heat transfer coefficient (a) is defined as follows:

For saturated mixtures $$a = \frac{q''}{(T_{wall} - T_{sat})} \quad (3)$$

For subcooled mixtures $$a = \frac{q''}{(T_{wall} - T_{bulk})} \quad (4)$$

7.3.1 Water/Propylene Glycol Mixtures

Figure 7.18 shows the subcooling effect for pure water. On the smooth tube, the subcooling reduces the heat transfer coefficient. However, on the Turbo BIII tube the subcooling actually increases the heat transfer coefficient. This could be due in part to the fact that the Turbo BIII has much more surface area, therefore the convective contribution to the heat transfer could play a larger role than bubble nucleation and departure on the Turbo BIII tube at subcooled conditions. This implies that the surface is a significant determining factor in subcooling effect.

Figures 7.19 through 7.22 show the boiling curves for the mixtures of water and propylene glycol. These figures show that on the Turbo BIII tube subcooling increases the heat transfer coefficient in all but the $X_w = 0.125$ mixture, where it seems to have no effect. These figures also show that on the smooth tube subcooling also increases the heat transfer coefficient.

Pure propylene glycol boiling curves are shown in Figure 7.23. In it is seen that on the Turbo BIII tube the subcooling increases the heat transfer coefficient. We also see that on the smooth tube the effect is not clearly defined. The data suggests that the subcooling increases the heat transfer coefficient below a heat flux of approximately 225 kW/m^2 and decreases the heat transfer coefficient above that flux.

The reduction in the heat transfer coefficient due to subcooling on both surfaces is then compared in Figures 7.24 and 7.25. Figure 7.24 shows that the smooth surface experiences close to twice as much degradation in the saturated trial as is seen in the subcooled trial. However, in Figure 7.27 it should be noted that although the Turbo BIII tube behaves quite similarly below $X_w = 0.382$, above that mixture it behaves in a completely opposite manner. Unfortunately, only one data set above that mixture was obtained so it is difficult to say exactly where this trend changes.

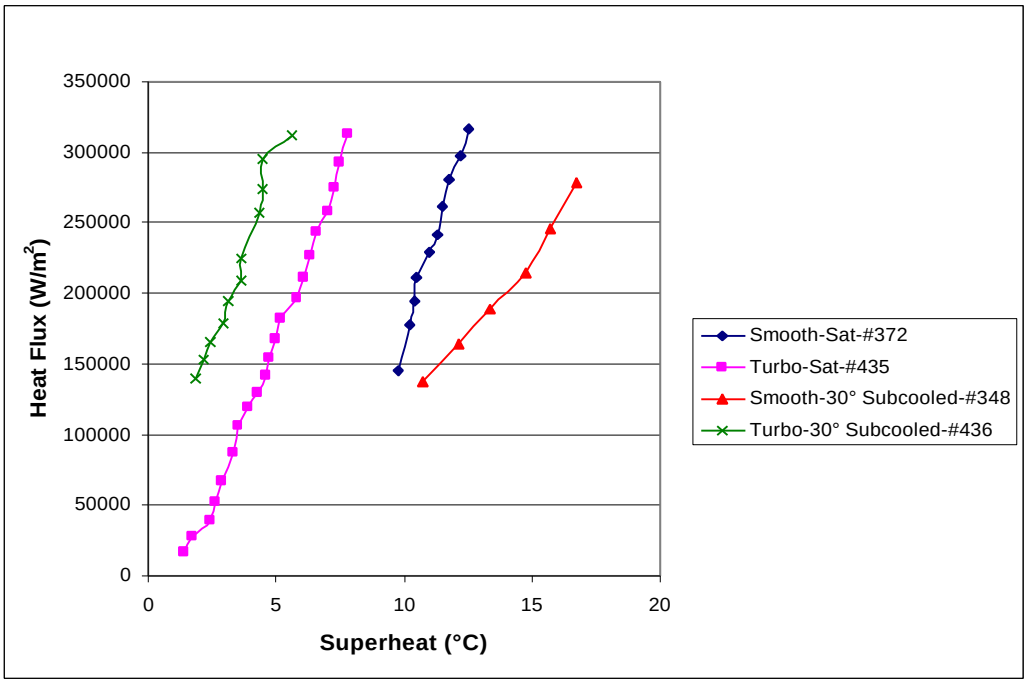

Figure 7.18-Subcooling effect at X_w =1.0, X_{pg}=0.0 on both smooth and Turbo tubes at saturation at 1.0 bar.

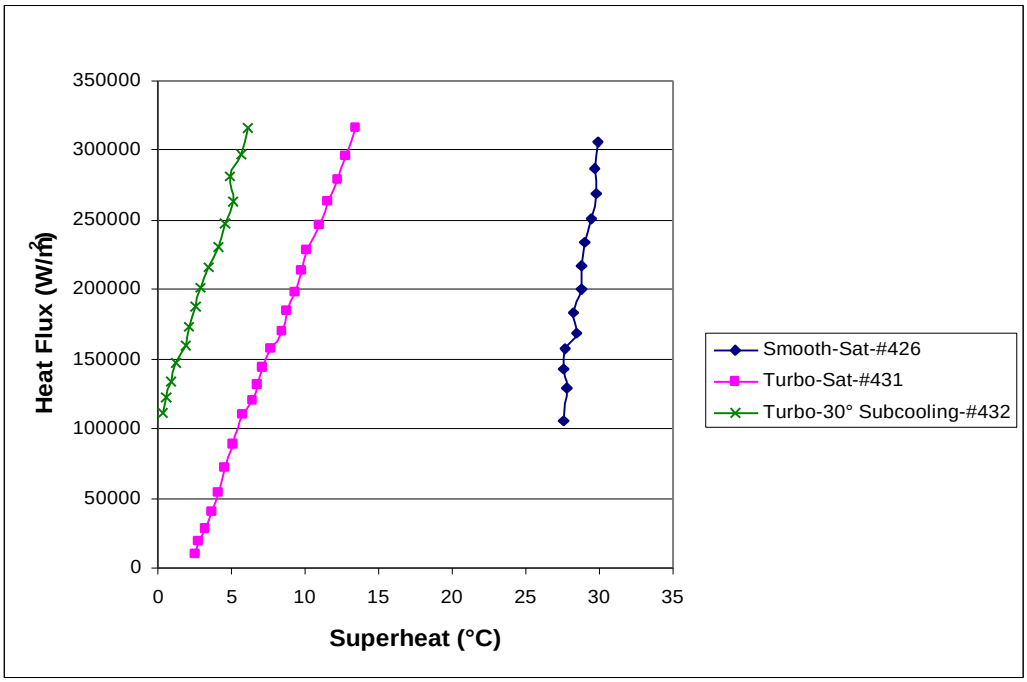

Figure 7.19-Subcooling effect at X_w =0.773, X_{pg} =0.227 on the Turbo tube (smooth tube data not available).

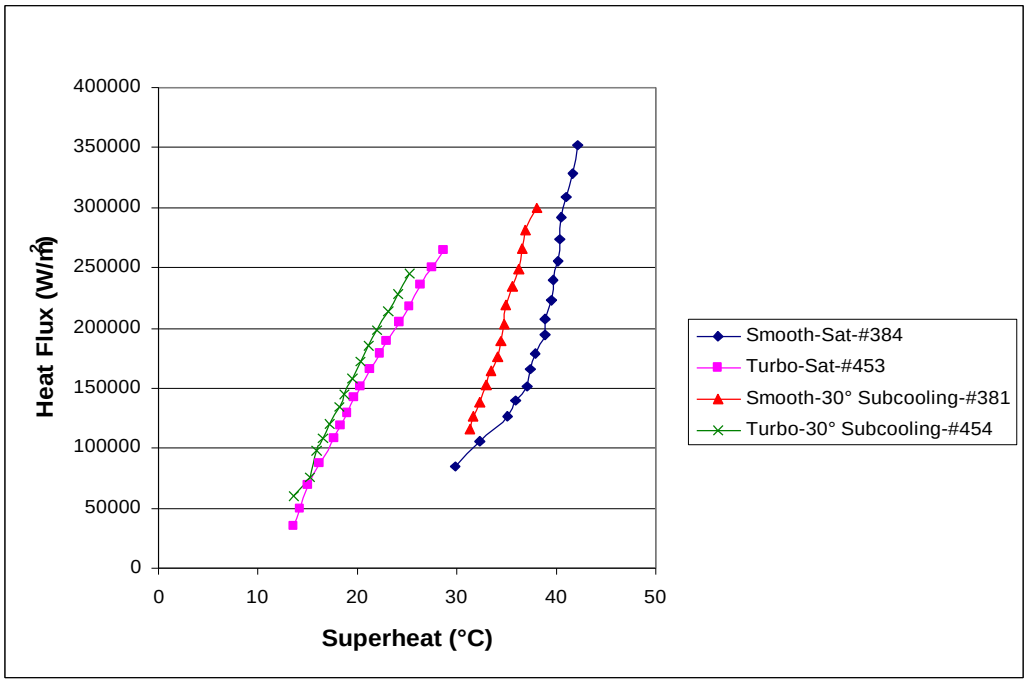

Figure 7.20-Subcooling effect at X_w =0.382, X_{pg} =0.618 on both smooth and Turbo tubes at saturation at 1.0 bar.

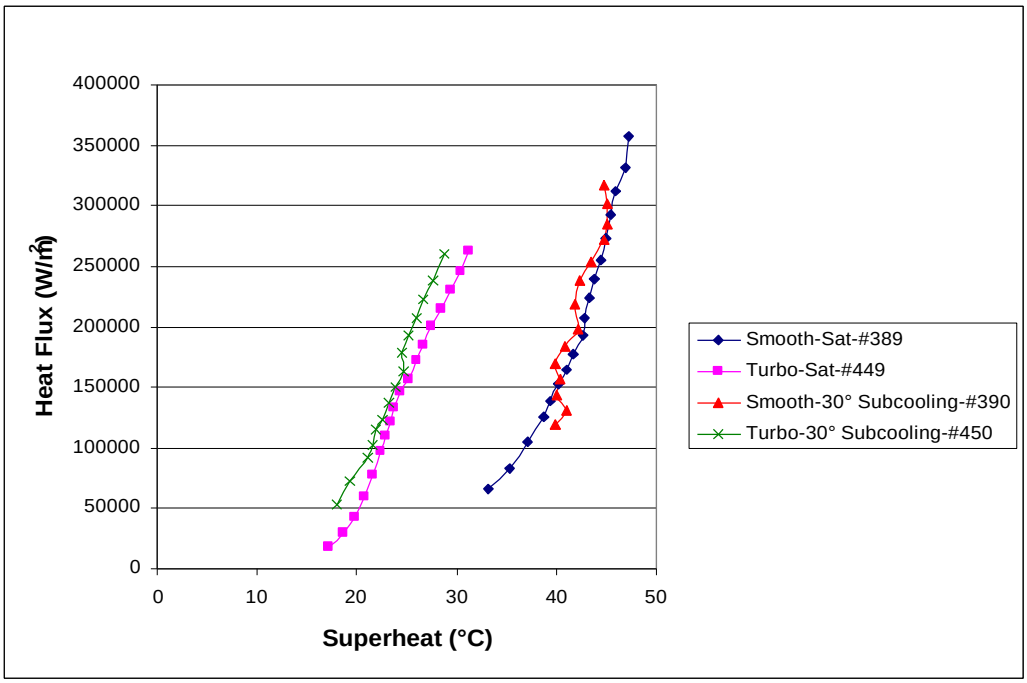

Figure 7.21-Subcooling effect at X_w =0.230, X_{pg} =0.770 on both smooth and Turbo tubes at saturation at 1.0 bar.

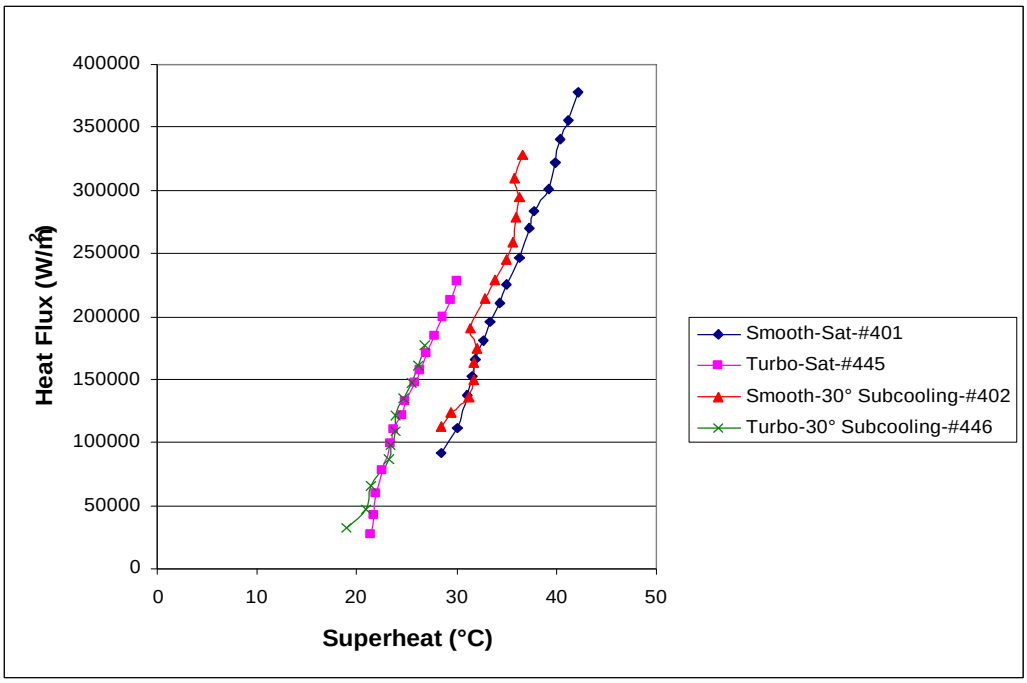

Figure 7.22-Subcooling effect at X_w =0.125, X_{pg} =0.875 on both smooth and Turbo tubes at saturation at 1.0 bar.

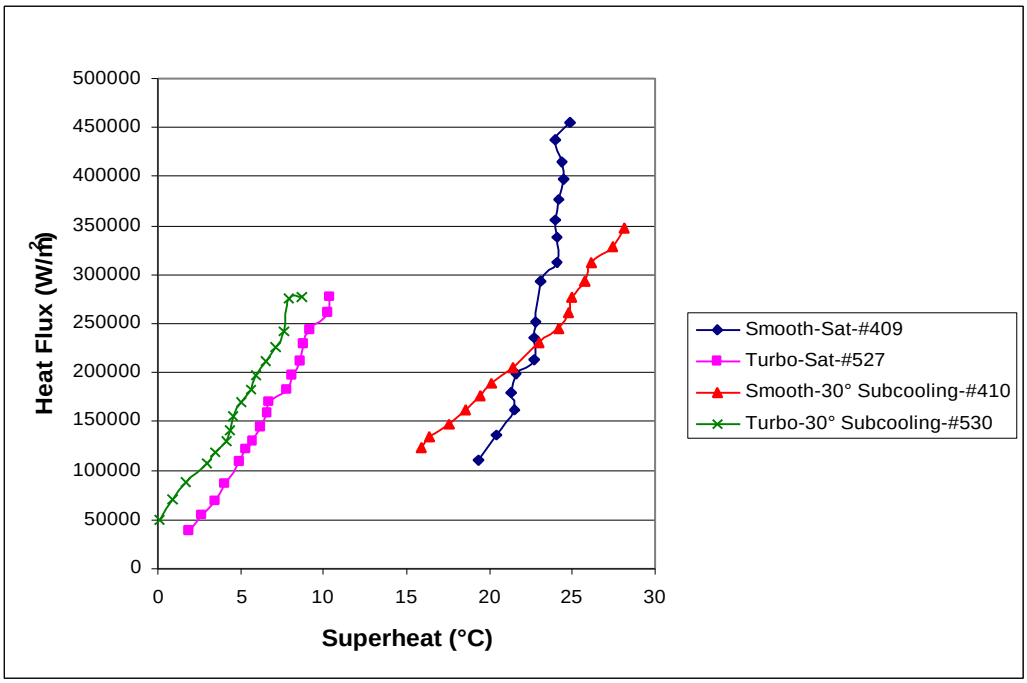

Figure 7.23-Subcooling effect at X_w =0.0, X_{pg} =1.0 on both smooth and Turbo tubes at saturation at 1.0 bar.

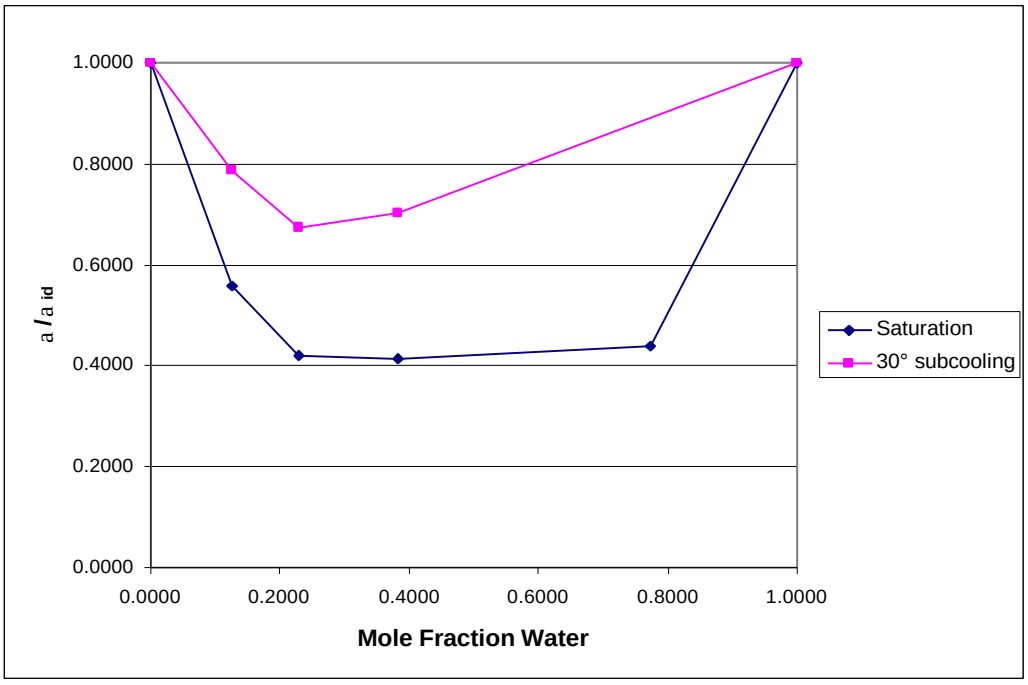

Figure 7.24-Subcooling effect shown as a/a_{id} vs. mole fraction water in the water/propylene glycol system at 1 bar on the smooth surface at 250 kW/m^2 heat flux.

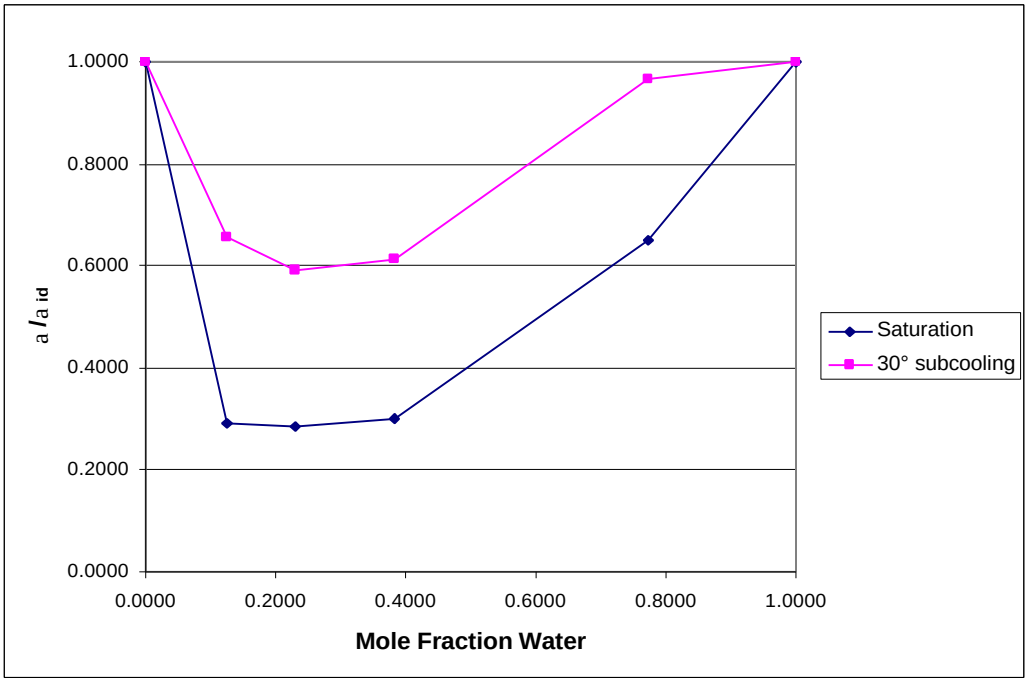

Figure 7.25-Subcooling effect shown as a/a_{id} vs. mole fraction water in the water/propylene glycol system at 1 bar on the Turbo BIII surface at 250 kW/m^2 heat flux.

7.3.2 Water/Ethylene Glycol Mixtures

The water/ethylene glycol mixture tests were done using a different smooth tube heater than the one used for the water/propylene glycol mixtures. The pure water results, shown in Figure 7.26, differ slightly on this heater. Similar to the water/propylene glycol mixtures, on the smooth tube the subcooling decreases the heat transfer coefficient above a heat flux of approximately 150 kW/m^2. However, subcooling actually increases the heat transfer coefficient below that heat flux. Similar to the previous pure water test on the Turbo BIII, the subcooling increases the heat transfer.

Figures 7.27 through 7.31 show the boiling curves for the mixtures of water and ethylene glycol. These figures show that on the Turbo BIII tube subcooling increases the heat transfer coefficient in all but the $X_w = 0.25$ mixture, where it seems to have no effect. These figures also show that on the smooth tube subcooling also increases the heat transfer coefficient in all but the $X_w = 0.90$ mixture, where it decreases the heat transfer coefficient.

Pure ethylene glycol boiling curves are shown in Figure 7.32. In this figure, similar to the pure propylene glycol trial on the Turbo BIII tube, the subcooling increases the heat transfer coefficient. However, unlike the pure propylene glycol trial on the smooth tube it is clear that subcooling decreases the heat transfer coefficient for all heat fluxes tested in pure ethylene glycol.

The reduction in the heat transfer coefficient due to subcooling is then compared for both surfaces in Figures 7.33 and 7.34. Figure 7.33 shows that the smooth surface experiences close to twice as much degradation in the saturated trial as is seen in the subcooled trial. Figure 7.34 shows that the Turbo BIII tube behaves similarly with almost twice the reduction at saturation than at 30° subcooled.

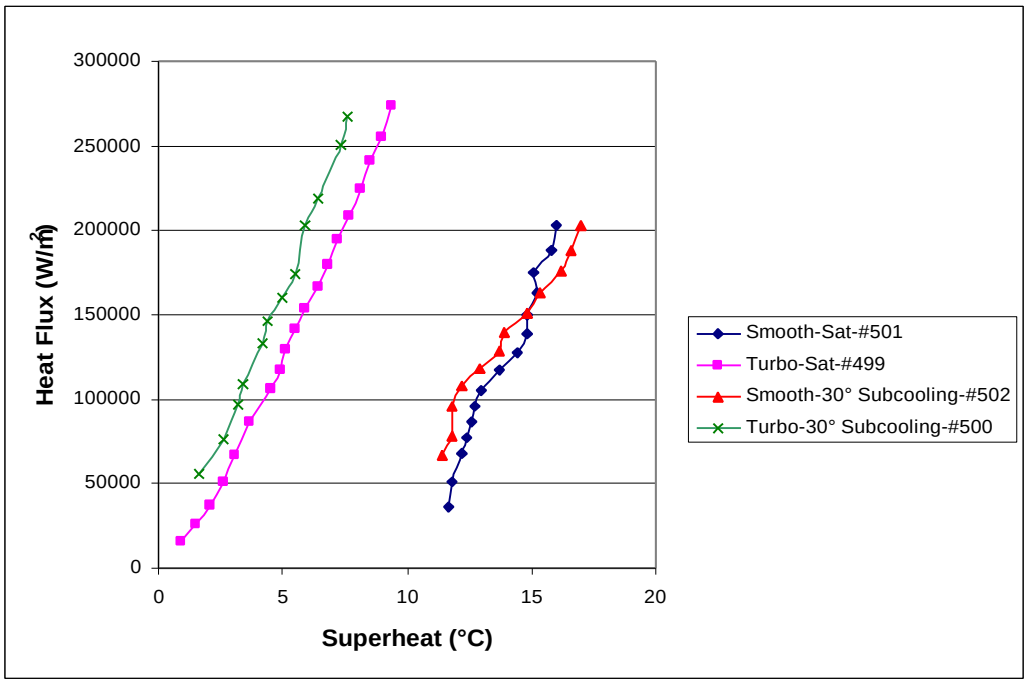

Figure 7.26-Subcooling effect at X_w =1.0, X_{eg}=0.0 on both smooth and Turbo tubes at saturation at 1.0 bar.

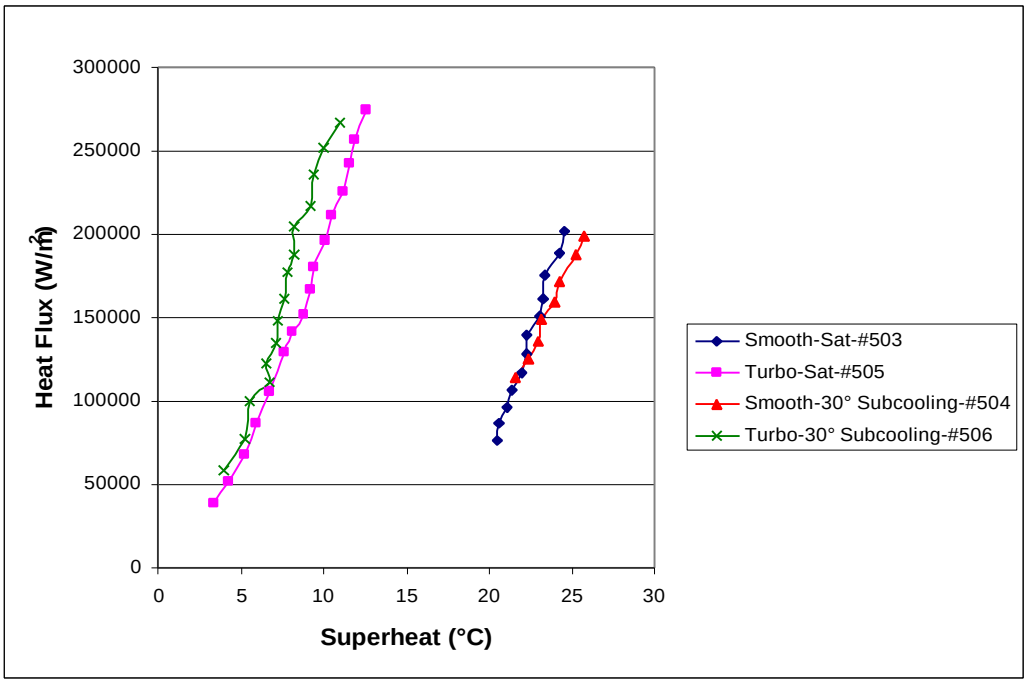

Figure 7.27-Subcooling effect at X_w =0.9, X_{eg} =0.1 on both smooth and Turbo tubes at saturation at 1.0 bar.

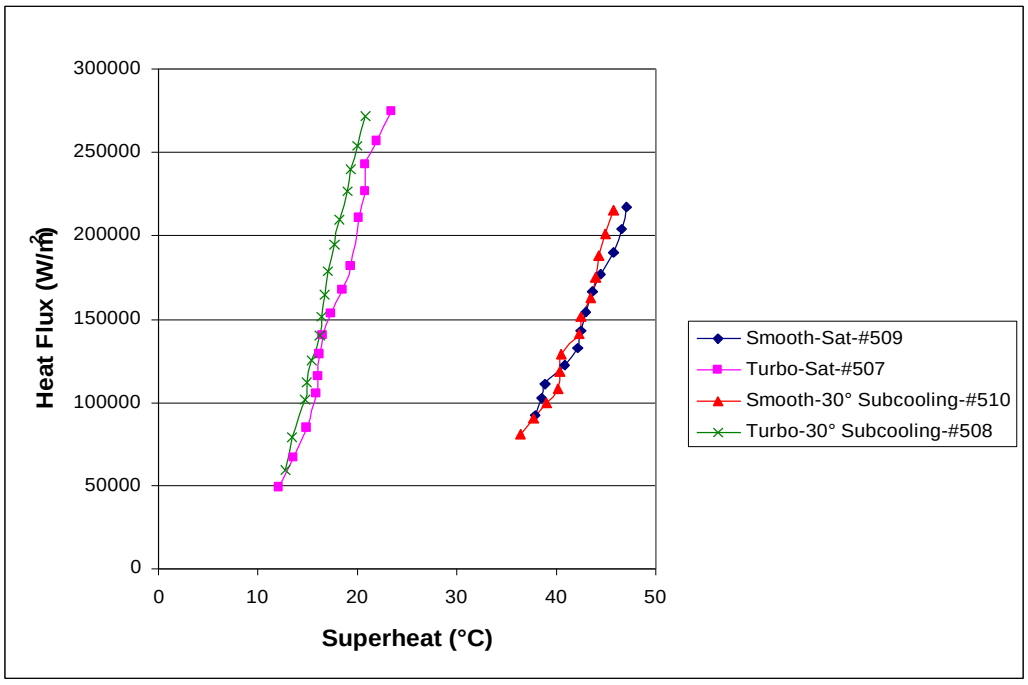

Figure 7.28-Subcooling effect at X_w =0.6, X_{eg} =0.4 on both smooth and Turbo tubes at saturation at 1.0 bar.

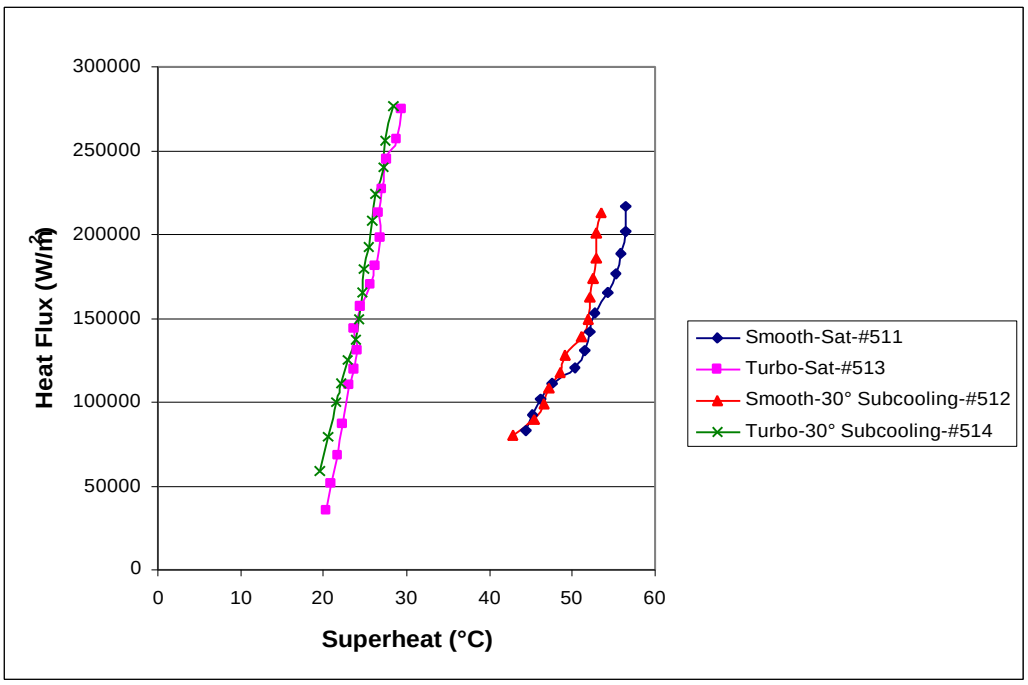

Figure 7.29-Subcooling effect at X_w =0.4, X_{eg} =0.6 on both smooth and Turbo tubes at saturation.

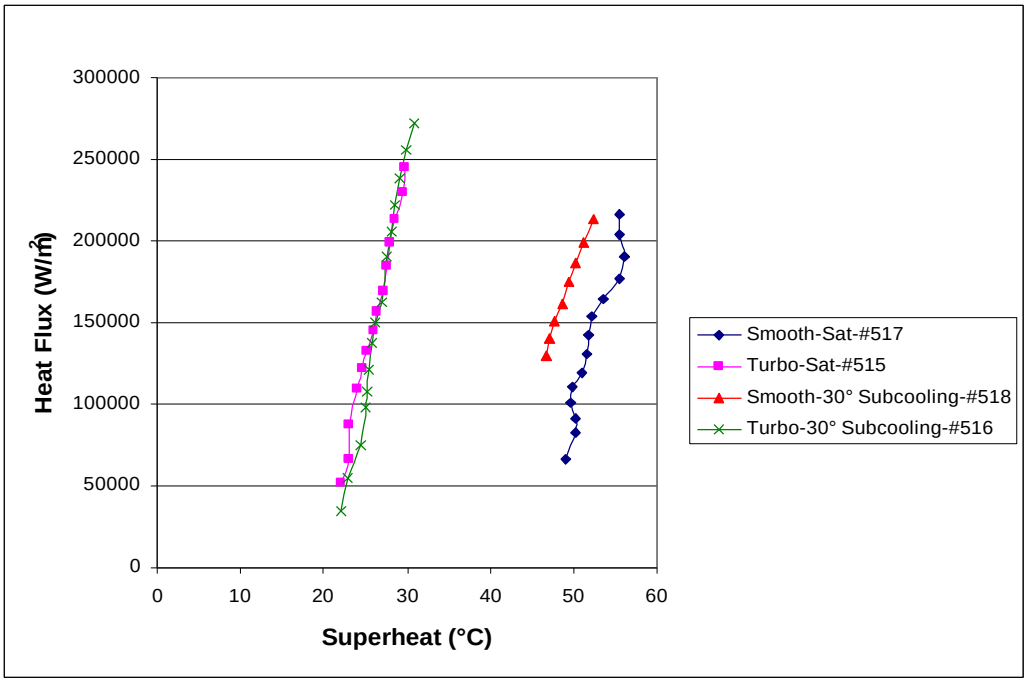

Figure 7.30-Subcooling effect at X_w =0.25, X_{eg} =0.75 on both smooth and Turbo tubes at saturation at 1.0 bar.

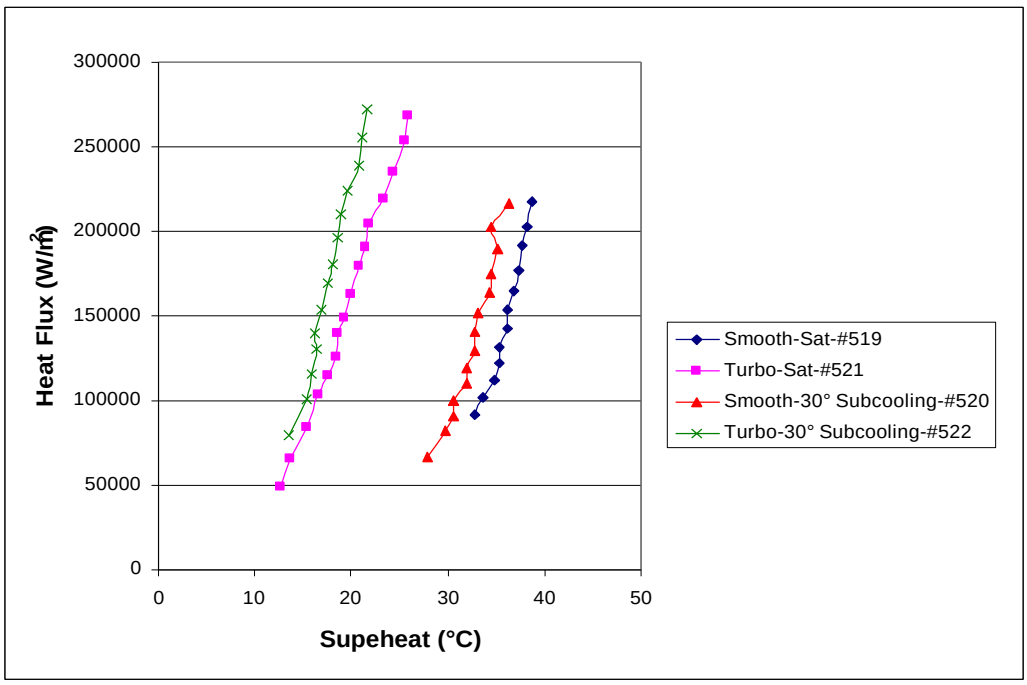

Figure 7.31-Subcooling effect at X_w =0.9, X_{eg} =0.1 on both smooth and Turbo tubes at saturation at 1.0 bar.

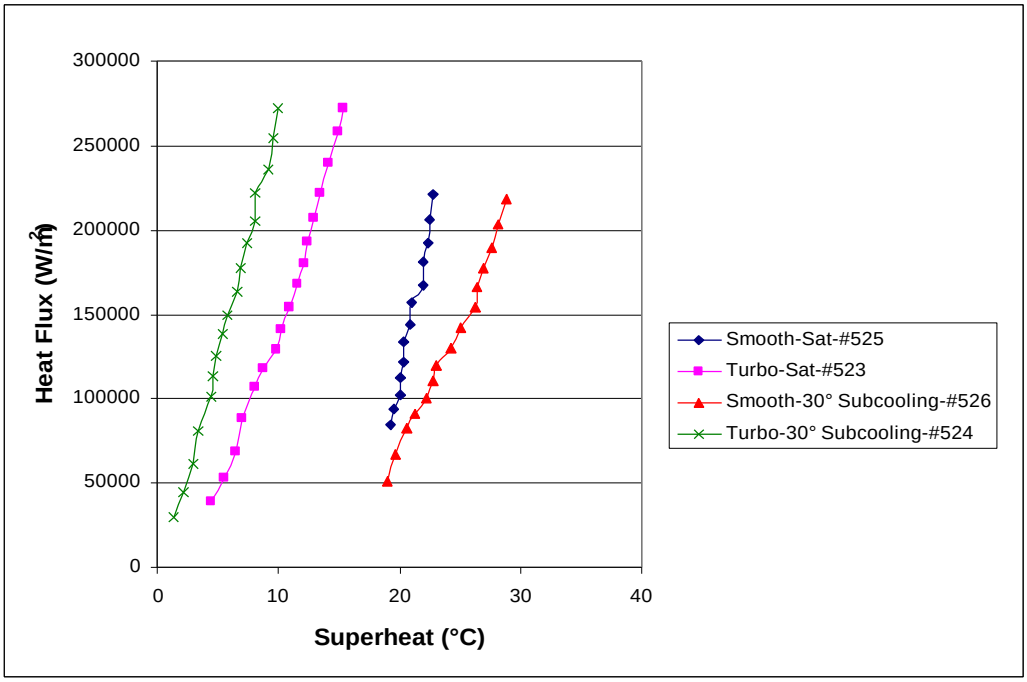

Figure 7.32-Subcooling effect at X_w =0.0, X_{eg} =1.0 on both smooth and Turbo tubes at saturation at 1.0 bar.

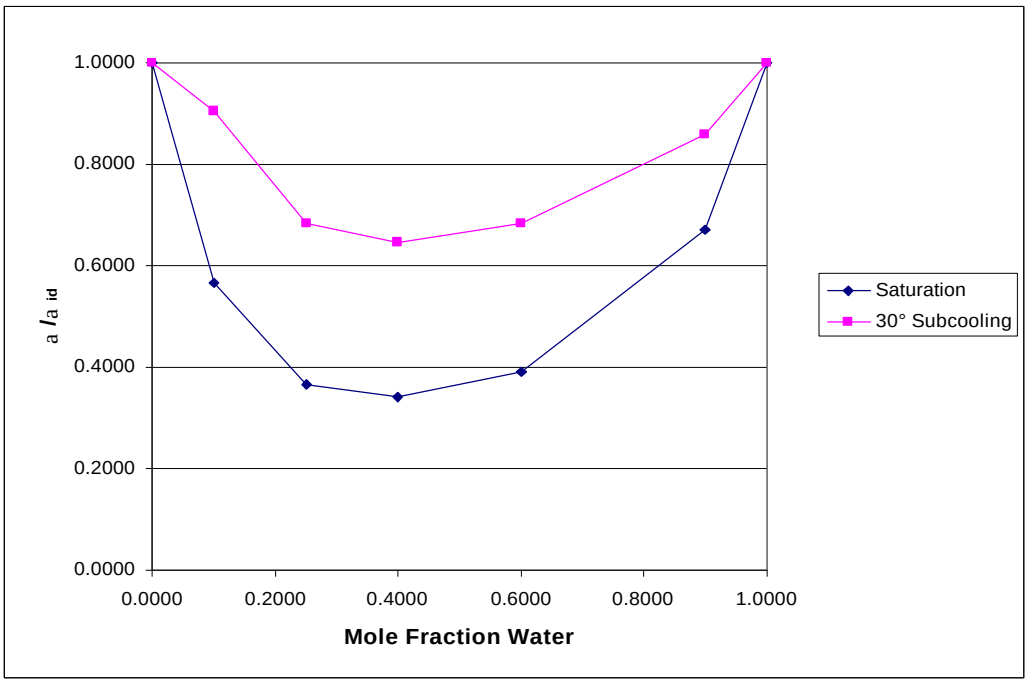

Figure 7.33-Subcooling effect shown as a/a_{id} vs. mole fraction water in the water/ethylene glycol system at 1 bar on the smooth surface at 200 kW/m^2 heat flux.

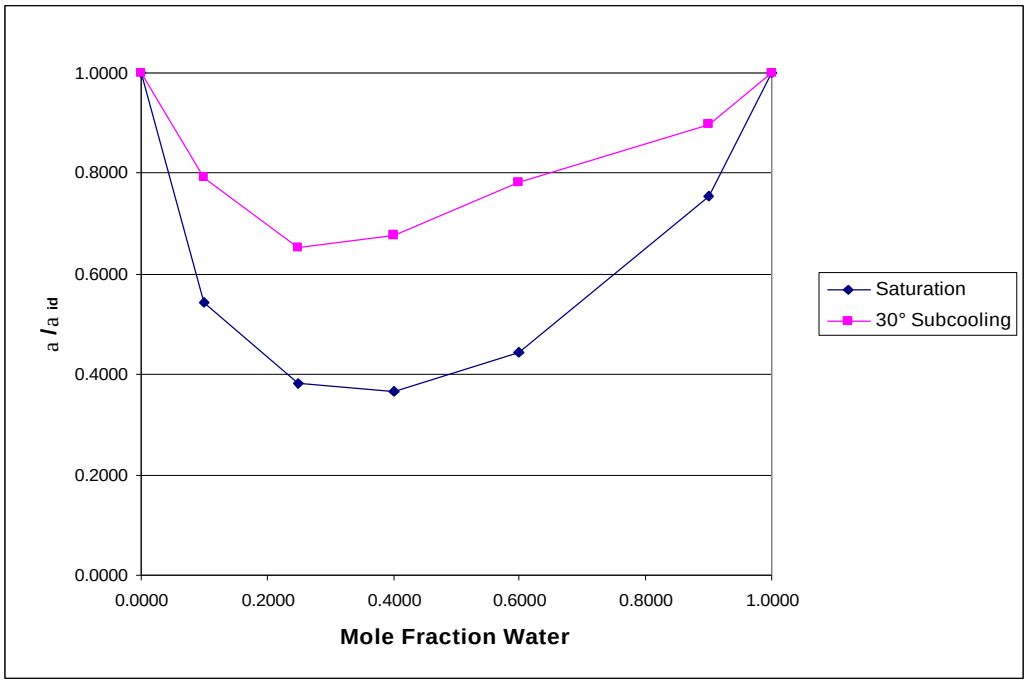

Figure 7.34-Subcooling effect shown as a/a_{id} vs. mole fraction water in the water/ethylene glycol system at 1 bar on the Turbo BIII surface at 200 kW/m^2 heat flux.

8.0 SUMMARY AND CONCLUSIONS

This investigation generated a database of emperical information for aqueous glycol mixtures on smooth and Turbo BIII surfaces at saturation and various subcoolings.

The experimental apparatus was previously used in investigations by Bajorek (1988), Shakir (1986), Hui (1985), and Thome (1984). The data generated by this investigation complements the data previously taken using this apparatus.

Experimental data were obtained for aqueous mixtures of propylene glycol, ethylene glycol, and diethylene glycol. The propylene glycol and ethylene glycol tests were performed on both smooth and Turbo BIII surfaces. Subcooled tests were also performed for these mixtures. The water-diethylene glycol mixture system was only tested at saturation on the smooth tube due to its high saturation temperature.

Inspection of the experimental results clearly show that mixture composition has a large effect on the boiling heat transfer coefficient. Ideal heat transfer coefficients are calculated for a mixture by a linear mixing law from pure component data. When the observed heat transfer coefficients are compared to the calculated ideal heat transfer coefficients, it is seen that the heat transfer coefficients for the mixtures are severely degraded. For the water-ethylene glycol mixture system reductions on the order of 65% are observed on the smooth and the Turbo BIII tubes at $X_w = 0.5$. For the water-propylene glycol mixture system at $X_w = 0.5$ reductions on the order of 60% and 65% are observed for the smooth and Turbo BIII tubes, respectively. The water-diethylene glycol mixture system has reductions in the heat transfer coefficient of nearly 75% on the smooth tube at $X_w = 0.5$. These reductions are rather large, but are consistent with results previously observed for mixture systems with large boiling ranges.

The experimental results also clearly show that the surface had a large effect on the heat transfer coefficient. Throughout all the tests conducted in which the smooth surface was compared to the Turbo BIII surface, the Turbo BIII surface consistently had much higher heat transfer coefficients.

9.0 REFERENCES

Bajorek, S. M., (1988). An experimental and theoretical investigation of multicomponent pool boiling on smooth and finned surfaces. Doctoral dissertation: Michigan State University, East Lansing.

Bajorek, S. M., Lloyd, J. R., and Thome, J. R., (1991). Prediction methods for boiling of pure and multicomponent fluids on a low finned tube. *Fouling and Enhancement Interactions,* ASME, HTD-Vol. 164.

Bhowmick, S., Branchi, C., McAssey, Jr., E. V., and Gollin, M., (1996). Heat transfer performance of engine coolants under sub-cooled boiling conditions. *ASME ICE*, *26*(2), 53-59.

Branchi, C., Bhowmick, S., McAssey, Jr., E. V., Gollin, M., and Cozzone, G., (1997). Comparison of aqueous mixtures of propylene-glycol and ethylene-glycol under simulated engine cooling conditions. *Society of Automotive Engineers, Inc.*, 133-138.

Collier, John G., and Thome, John R., (1994). *Convective boiling and condensation* (3rd ed.). New York: Oxford University Press Inc.

Dow Chemical Company, (1992). *A Guide to Glycols*. Midland, MI.

El-Sayed, Y.M., and Tribus, M., "A Theoretical Comparison of the Rankine and Kalina Cycles," ASME Winter Annual Meeting, pp. 97-102, 1985.

Fujita, Yasunobu, Bai, Qiang, and Tsutsui, Masayuki., (1996) heat transfer of binary mixtures in nucleate pool boiling. In G. P. Celata, P. Di Marco and A. Mariani (Eds.) 2nd European Thermal-Sciences and 14th UIT National Heat Transfer Conference 1996. (pp. 1639-1646). Pisa, Italy: Edizioni ETS.

Gmehling, J., Onken, U., and Rarey-Nies, J. R., (1984). *Vapor-liquid equilibrium data collection: Aqueous systems*. Germany: DECHEMA.

Grigor'ev, L. N., (1962). Studies of heat transfer to two component mixtures. *Teplo Masso Perenos, 2*, 120-127.

Hui, T. O. and Thome, J. R., (1985). A study of binary mixture boiling: Boiling site density and subcooled heat transfer. *International Journal of Heat and Mass Transfer, 28*, 919-928.

Kalina, A. I., "Combined Cycle System with Novel Bottoming Cycle," ASME J. Heat Transfer, Vol. 106, 1984.

McAssey, E. V. Stinson, C., and Gollin M., (1995). Evaluation of engine coolants under flow boiling conditions. *Proceedings of the ASME Heat Transfer Division*, *317*(1), 193-200.

Shakir, S., (1986). *Boiling incipience and heat transfer on smooth and enhanced surfaces.* Doctoral dissertation: Michigan State University, East Lansing.

Stephan, K. and Abdelsalam, M., (1978). Heat-transfer correlations for natural convection boiling. *International Journal of Heat and Mass Transfer, 23*, 73-87.

Stephan, K. and Korner, M., (1969). Calculation of heat transfer in evaporating binary liquid mixtures. *Chemie-Ingenieur Technik, 41*(7), 409-417.

Stephan, K. and Preusser, P., (1979). Heat transfer and critical heat flux in pool boiling of binary and ternary mixtures. *German Chemical Engineering*, *2*, 161-169.

Sternling, C. V. and Tickacek, L. J., (1961). Heat transfer coefficients for boiling mixtures. *Chemical Engineering Science, 16*(4), 297-337.

Thome, J. R., (1981). Nucleate pool boiling in binary liquids---an analytical equation. *AIChE Symposium*, *77*(208), 238-250.

Thome, J. R., (1983). Prediction of binary mixture boiling heat transfer coefficients using only phase equilibrium data. *International Journal of Heat and Mass Transfer*, *26*, 965-974.

Thome, John R., (1990). *Enhanced boiling heat transfer*. New York: Hemisphere Publishing Corporation.

Thome, John R. and Shock, Richard A. W., (1984). Boiling of multicomponent liquid mixtures. *Advances in Heat Transfer*, *16*, 59-156.

Thome, J. R., (1982). Boiling heat transfer in binary liquid mixtures. *NATO Advanced Research Workshop on Advances in Two-Phase Flow and Heat Transfer*, Spitzingsee, FRG, August 31-Septermber 3.

Van Wijk, W. R., Vos, A. S., and Van Stralen, S. J. D., (1956). Heat transfer to boiling binary liquid mixtures. *Chemical Engineering Science*, *5*, 68-80.

Webb, R. L., (1981). The evolution of enhanced surface geometries for nucleate boiling. *Heat Transfer Engineering*, *2*(3), 46-69.

APPENDIX

Fortran source code for PBDATA, the computer program used to estimate the wall surface temperature, superheat, surface heat flux, and the heat transfer coefficient

```
PROGRAM PBDATA
C
C       PBDATA_06   February 21, 2001 Version
C
C
C       Modified by S.M.Bajorek
C
     COMMON/XDATA/ IDNUM,IDATE,ISURF,ICOMP(5),FRAC(5),NPTS, IUNITS
     COMMON/XDATA/ VOLTS(40),AMPS(40),P(40)
     COMMON/XDATA/ TB(2,40),TC(4,40),TE(4,40)
     COMMON/XOUTP/ DELT(40),QLOSS(40),ALPHA(40),TWALL(40),FLUX(40)
     COMMON/XOUTP/ TCVAR1(40),TCVAR2(40)
     CHARACTER*20 INPFIL, DATFIL, SDFFIL
C
     JIN  = 1
     JINP = 2
     JDAT = 3
     JSDF = 4
     JBAN = 5
C
     OPEN(JIN,FILE='A:PBDATA.INP',STATUS='OLD')
     OPEN(JBAN,FILE='PBDATA.TXT',STATUS='UNKNOWN')
     READ(JIN,10)
  10  FORMAT( )
     READ(JIN,10)
     READ(JIN,15) NFILES
  15  FORMAT(3X,I3)
     READ(JIN,10)
     DO 900 IFILE=1,NFILES
     READ(JIN,20) INPFIL, DATFIL, SDFFIL
  20  FORMAT(3A20)
     WRITE(*,25) INPFIL
  25  FORMAT(/,10X,'BEGIN DATA REDUCTION FOR FILE ',A20)
C
     OPEN(JINP,FILE=INPFIL,STATUS='OLD')
     OPEN(JDAT,FILE=DATFIL,STATUS='NEW')
     OPEN(JSDF,FILE=SDFFIL,STATUS='NEW')
C
     CALL INPUT(JINP)
```

```
C
      PI= 3.141593
      TWOPI= 6.283185
C
      IF (IDNUM.GE.1000) GO TO 1000
      GO TO (130,140,150,160,555,170,130,130,180,190,580,590) ISURF
C
  130  CONTINUE
C     ISURF = 1,7,8  Smooth Tube - See section B.2, pg. 101 Shakir
      RI=  0.00630
      RT=  0.00870
      RO=  0.01110
C     This heater had a 3 inch boiling length
      ZLB= 0.07620
      ZLNC=0.01270
      ZL = ZLB + ZLNC
      CONDCU= 391.0
C
      DO 135 I=1,NPTS
      WATTS = VOLTS(I)*AMPS(I)
      Q = WATTS
      TCAVE=(TC(1,I)+TC(2,I)+TC(3,I)+TC(4,I))/4.
      TBAVE=(TB(1,I)+TB(2,I))/2.
      TLAVE=(TE(1,I)+TE(2,I))/2.
      TVAR = 0.
      DO 133 J=1,4
      TVAR = TVAR + (TCAVE - TC(J,I))**2
  133  CONTINUE
      TCVAR1(I)= SQRT(TVAR)
      TCVAR2(I)= 100.*TCVAR1(I)/(TCAVE-TBAVE)
      TWALL(I)= TCAVE - Q*(1./(TWOPI*CONDCU*ZLB))*ALOG(RO/RT)
      DELT(I)= TWALL(I) - TBAVE
      FLUX(I)= Q/(TWOPI*RO*ZL)
      ALPHA(I)= FLUX(I)/DELT(I)
      DELTL= TCAVE - TLAVE
      DELTM= TLAVE - TBAVE
      QLOSS(I)= CONDCU*PI*(RO*RO-RI*RI)*DELTL/(0.5*ZL) +
     &          ALPHA(I)*TWOPI*RO*ZLNC*DELTM
      Q = Q - QLOSS(I)
      QLOSS(I)= 100.*QLOSS(I)/WATTS
      TWALL(I)= TCAVE - Q*(1./(TWOPI*CONDCU*ZLB))*ALOG(RO/RT)
      DELT(I)= TWALL(I) - TBAVE
      FLUX(I)= Q/(TWOPI*RO*ZLB)
      ALPHA(I)= FLUX(I)/DELT(I)
  135  CONTINUE
```

```
      GO TO 200
C
 140  CONTINUE
C     ISURF = 2, High Flux  (Bajorek)
      RO= 0.009335
      RC= 0.008382
      RT= 0.007798
      RI= 0.004763
      ZLB= 0.0508
      ZLNC= 0.041625
      ZL= ZLB + ZLNC
      CONDHF= 242.0
C
      DO 145 I=1,NPTS
      WATTS = VOLTS(I)*AMPS(I)
      Q = WATTS
      TCAVE=(TC(1,I)+TC(2,I)+TC(3,I)+TC(4,I)+2.*(TE(2,I)+TE(4,I)))/8.
      TBAVE=(TB(1,I)+TB(2,I))/2.
      TLAVE=(TE(1,I)+TE(3,I))/2.
      TVAR = 0.
      DO 143 J=1,4
      TVAR = TVAR + (TCAVE - TC(J,I))**2
 143  CONTINUE
      TCVAR1(I)= SQRT(TVAR)
      TCVAR2(I)= 100.*TCVAR1(I)/(TCAVE-TBAVE)
      TWALL(I)= TCAVE - Q*(1./(TWOPI*CONDHF*ZLB))*ALOG(RO/RT)
      DELT(I)= TWALL(I) - TBAVE
      FLUX(I)= Q/(TWOPI*RO*ZL)
      ALPHA(I)= FLUX(I)/DELT(I)
      DELTL= (TE(2,I)+TE(4,I))/2. - TLAVE
      DELTM= TLAVE - TBAVE
      QLOSS(I)= CONDHF*PI*(RO*RO-RI*RI)*DELTL/(0.5*ZLNC) +
     &          ALPHA(I)*TWOPI*RO*ZLNC*DELTM
      Q = Q - QLOSS(I)
      QLOSS(I)= 100.*QLOSS(I)/WATTS
      TWALL(I)= TCAVE - Q*(1./(TWOPI*CONDHF*ZLB))*ALOG(RO/RT)
      DELT(I)= TWALL(I) - TBAVE
      FLUX(I)= Q/(TWOPI*RO*ZLB)
      ALPHA(I)= FLUX(I)/DELT(I)
 145  CONTINUE
      GO TO 200
C
 150  CONTINUE
C     ISURF = 3, Finned Tube, 19 Fins per Inch (Bajorek)
      RI   = 0.00470
```

```
      RT   = 0.00591
      RO   = 0.00800
      RFIN = 0.009535
      ZLB  = 0.0508
      ZLNC = 0.03175
      ZL   = ZLB + ZLNC
      CONDCU = 391.0
C
      DO 155 I=1,NPTS
      WATTS = VOLTS(I)*AMPS(I)
      Q = WATTS
      TCAVE=(TC(1,I)+TC(2,I)+TC(3,I)+TC(4,I))/4.
      TBAVE=(TB(1,I)+TB(2,I))/2.
      TVAR = 0.
      DO 153 J=1,4
      TVAR = TVAR + (TCAVE - TC(J,I))**2
 153  CONTINUE
      TCVAR1(I)= SQRT(TVAR)
      TCVAR2(I)= 100.*TCVAR1(I)/(TCAVE-TBAVE)
      TWALL(I)= TCAVE - Q*(1./(TWOPI*CONDCU*ZLB))*ALOG(RO/RT)
      DELT(I)= TWALL(I) - TBAVE
      FLUX(I)= Q/(TWOPI*RFIN*ZL)
      ALPHA(I)= FLUX(I)/DELT(I)
      DELTM= 0.5 * DELT(I)
      QLOSS(I)=  ALPHA(I)*TWOPI*RO*ZLNC*DELTM
      Q = Q - QLOSS(I)
      QLOSS(I)=  100.*QLOSS(I)/WATTS
      TWALL(I)= TCAVE - Q*(1./(TWOPI*CONDCU*ZLB))*ALOG(RO/RT)
      DELT(I)= TWALL(I) - TBAVE
      FLUX(I)= Q/(TWOPI*RFIN*ZLB)
      ALPHA(I)= FLUX(I)/DELT(I)
 155  CONTINUE
      GO TO 200
C
 160  CONTINUE
C     ISURF = 4    (Schnelle)
C     Smooth surface, 0.75 inch diameter, 2.5 inch boiling length
C     Four thermocouples at midpoint of heated length.
      RI=  0.47625E-02
      RT=  0.71438E-02
      RO=  0.95250E-02
      ZLB= 0.0635
C     The length for natural convection is 1/2 + 7/8 in.
      ZLNC=0.0349
      ZL = ZLNC + ZLB
```

```
C *** ZLOSS = 0.675 in. = 0.017145 m
          ZLOSS = 0.017145
      CONDCU= 391.0
          CONDCU = 339.
C
      DO 165 I=1,NPTS
      WATTS = VOLTS(I)*AMPS(I)
      Q = WATTS
      TCAVE=(TC(1,I)+TC(2,I)+TC(3,I)+TC(4,I))/4.
      TBAVE=(TB(1,I)+TB(2,I))/2.
C     TLAVE=(TE(1,I)+TE(2,I)+TE(3,I)+TE(4,I))/4.
      TVAR = 0.
      DO 163 J=1,4
      TVAR = TVAR + (TCAVE - TC(J,I))**2
 163  CONTINUE
      TCVAR1(I)= SQRT(TVAR)
      TCVAR2(I)= 100.*TCVAR1(I)/(TCAVE-TBAVE)
      TWALL(I)= TCAVE - Q*(1./(TWOPI*CONDCU*ZLB))*ALOG(RO/RT)
      DELT(I)= TWALL(I) - TBAVE
      FLUX(I)= Q/(TWOPI*RO*ZL)
      ALPHA(I)= FLUX(I)/DELT(I)
      DELTL= (TE(3,I)+TE(4,I))/2. - (TE(1,I)+TE(2,I))/2.
      DELTM= ((TE(1,I)+TE(2,I))/2. + TLAVE)/2. - TBAVE
      QLOSS(I)= CONDCU*PI*(RT*RT-RI*RI)*DELTL/ZLOSS
      Q = Q - QLOSS(I)
      QLOSS(I)= 100.*QLOSS(I)/WATTS
      TWALL(I)= TCAVE - Q*(1./(TWOPI*CONDCU*ZLB))*ALOG(RO/RT)
      DELT(I)= TWALL(I) - TBAVE
      FLUX(I)= Q/(TWOPI*RO*ZLB)
      ALPHA(I)= FLUX(I)/DELT(I)
 165  CONTINUE
      GO TO 200
C
 555  CONTINUE
C     ISURF = 5   Smooth Tube - 0.75 in. OD  (Bajorek)
C     Three valid thermocouples at center of tube.
      RI=  0.47625E-02
      RT=  0.71438E-02
      RO=  0.95250E-02
      ZLB= 0.05080
      ZLNC=0.01905
      ZL = 0.03810 + 0.05080
      CONDCU= 391.0
C
      DO 575 I=1,NPTS
```

```
      WATTS = VOLTS(I)*AMPS(I)
      Q = WATTS
      TCAVE=(TC(1,I)+TC(2,I)+TC(3,I))/3.
      TBAVE=(TB(1,I)+TB(2,I))/2.
      TLAVE=(TE(1,I)+TE(2,I)+TE(3,I)+TE(4,I))/4.
      TVAR = 0.
      DO 573 J=1,4
      TVAR = TVAR + (TCAVE - TC(J,I))**2
  573  CONTINUE
      TCVAR1(I)= SQRT(TVAR)
      TCVAR2(I)= 100.*TCVAR1(I)/(TCAVE-TBAVE)
      TWALL(I)= TCAVE - Q*(1./(TWOPI*CONDCU*ZLB))*ALOG(RO/RT)
      DELT(I)= TWALL(I) - TBAVE
      FLUX(I)= Q/(TWOPI*RO*ZL)
      ALPHA(I)= FLUX(I)/DELT(I)
      DELTL= TCAVE - (TE(1,I)+TE(2,I))/2.
      DELTM= ((TE(1,I)+TE(2,I))/2. + TLAVE)/2. - TBAVE
      QLOSS(I)= CONDCU*PI*(RO*RO-RI*RI)*DELTL/(0.00635) +
     &          ALPHA(I)*TWOPI*RO*ZLNC*DELTM
          QLOSS1 = CONDCU*PI*(RO*RO-RI*RI)*DELTL/(0.00635)
          QLOSS2 = ALPHA(I)*TWOPI*RO*ZLNC*DELTM
          QLOSS(I) = QLOSS2
C         WRITE(JDAT,577) I, Q, QLOSS(I), DELTM, DELTL, ALPHA(I)
C 577  FORMAT(1X,"I=",I3," Q=",F8.1," QLOSS=",F8.1," DM=",F5.1,
C     &      " DL=",F5.1," A=",F7.1)
C         WRITE(JDAT,578) QLOSS1, QLOSS2
C 578  FORMAT(1X," QLOSS1=",F6.1," QLOSS2=",F6.1)
      Q = Q - QLOSS(I)
      QLOSS(I)= 100.*QLOSS(I)/WATTS
      TWALL(I)= TCAVE - Q*(1./(TWOPI*CONDCU*ZLB))*ALOG(RO/RT)
      DELT(I)= TWALL(I) - TBAVE
      FLUX(I)= Q/(TWOPI*RO*ZLB)
      ALPHA(I)= FLUX(I)/DELT(I)
  575  CONTINUE
C
      GO TO 200
C
  170  CONTINUE
C     ISURF = 6   Smooth Tube - 0.75 in. OD  (Bajorek)
C     Four valid thermocouples at center of tube.
      RI=  0.47625E-02
      RT=  0.71438E-02
      RO=  0.95250E-02
      ZLB= 0.05080
      ZLNC=0.01905
```

```
      ZL = 0.03810 + 0.05080
      CONDCU= 391.0
C
      DO 175 I=1,NPTS
      WATTS = VOLTS(I)*AMPS(I)
      Q = WATTS
      TCAVE=(TC(1,I)+TC(2,I)+TC(3,I)+TC(4,I))/4.
      TBAVE=(TB(1,I)+TB(2,I))/2.
      TLAVE=(TE(3,I)+TE(4,I))/2.
      TVAR = 0.
      DO 173 J=1,4
      TVAR = TVAR + (TCAVE - TC(J,I))**2
 173  CONTINUE
      TCVAR1(I)= SQRT(TVAR)
      TCVAR2(I)= 100.*TCVAR1(I)/(TCAVE-TBAVE)
      TWALL(I)= TCAVE - Q*(1./(TWOPI*CONDCU*ZLB))*ALOG(RO/RT)
      DELT(I)= TWALL(I) - TBAVE
      FLUX(I)= Q/(TWOPI*RO*ZL)
      ALPHA(I)= FLUX(I)/DELT(I)
      DELTL= TCAVE - (TE(1,I)+TE(2,I))/2.
      DELTM= ((TE(1,I)+TE(2,I))/2. + TLAVE)/2. - TBAVE
      QLOSS(I)= CONDCU*PI*(RO*RO-RI*RI)*DELTL/(0.00635) +
     &          ALPHA(I)*TWOPI*RO*ZLNC*DELTM
      Q = Q - QLOSS(I)
      QLOSS(I)= 100.*QLOSS(I)/WATTS
      TWALL(I)= TCAVE - Q*(1./(TWOPI*CONDCU*ZLB))*ALOG(RO/RT)
      DELT(I)= TWALL(I) - TBAVE
      FLUX(I)= Q/(TWOPI*RO*ZLB)
      ALPHA(I)= FLUX(I)/DELT(I)
 175  CONTINUE
      GO TO 200
C
 180     CONTINUE
C        ISURF = 9
C        Nuclear clad heater - 17x17 Vantage 5A clad with
C                              2-inch long cartridge heater.
C        The heater diameter after press fit is 0.245 in.
      RI=  0.003111
C        The thermocouples are on a 0.329 in diameter circle.
      RT=  0.004178
C        The outside diameter is 0.374 in
      RO=  0.00475
C        The length of the boiling region is 2.0 in.
      ZLB= 0.0508
C        Assume the length of tube in natural convection is 2 in
```

```
      ZLNC=0.0508
      ZL = ZLB + ZLNC
C         Thermal conductivities for copper and zircalloy
      CONDCU= 391.0
          CONDZR= 7.51
C
      DO 185 I=1,NPTS
      WATTS = VOLTS(I)*AMPS(I)
      Q = WATTS
      TCAVE=(TC(1,I)+TC(2,I)+TC(3,I))/3.
      TBAVE=(TB(1,I)+TB(2,I))/2.
C         Since this heater lacks error TCs, assume that TLAVE
C         is equal to TBAVE.
      TLAVE=(TE(1,I)+TE(2,I))/2.
      TVAR = 0.
      DO 183 J=1,3
      TVAR = TVAR + (TCAVE - TC(J,I))**2
  183  CONTINUE
      TCVAR1(I)= SQRT(TVAR)
      TCVAR2(I)= 100.*TCVAR1(I)/(TCAVE-TBAVE)
C     TWALL(I)= TCAVE - Q*(1./(TWOPI*CONDCU*ZLB))*ALOG(RO/RT)
          RC = 0.0002/(TWOPI*RT*ZLB)
          TWALL(I) = TCAVE - Q*(ALOG(RO/RT)/(TWOPI*CONDZR*ZLB)+RC)
      DELT(I)= TWALL(I) - TBAVE
      FLUX(I)= Q/(TWOPI*RO*ZL)
      ALPHA(I)= FLUX(I)/DELT(I)
      DELTL= TCAVE - TLAVE
      DELTM= TLAVE - TBAVE
      QLOSS(I)= CONDZR*PI*(RO*RO-RI*RI)*DELTL/(0.5*ZL) +
     &          ALPHA(I)*TWOPI*RO*ZLNC*DELTM
      Q = Q - QLOSS(I)
      QLOSS(I)= 100.*QLOSS(I)/WATTS
      TWALL(I)= TCAVE - Q*(1./(TWOPI*CONDZR*ZLB))*ALOG(RO/RT)
      DELT(I)= TWALL(I) - TBAVE
      FLUX(I)= Q/(TWOPI*RO*ZLB)
      ALPHA(I)= FLUX(I)/DELT(I)
  185  CONTINUE
      GO TO 200
C
  190     CONTINUE
C         ISURF = 10
C         Nuclear clad heater - 17x17 Vantage 5A clad with
C                               1-inch long cartridge heater.
C         The heater diameter after press fit is 0.245 in.
      RI=  0.003111
```

```
C     The copper sleeve has radius:
          RCI= 0.004178
C         The thermocouples are on a 0.329 in diameter circle.
C      RT=  0.004178
C     Assume the TCs are centrally located between the sleeve
C      and the heating element.
          RT= 0.003645
C         The outside diameter is 0.374 in
      RO=  0.00475
C         The length of the boiling region is 1.0 in.
      ZLB= 0.0254
C         Assume the length of tube in natural convection is 1 in
      ZLNC=0.0254
      ZL = ZLB + ZLNC
C         Thermal conductivities for copper and zircalloy
      CONDCU= 391.0
C
      DO 195 I=1,NPTS
      WATTS = VOLTS(I)*AMPS(I)
      Q = WATTS
      TCAVE=(TC(1,I)+TC(2,I)+TC(3,I))/3.
          TKAVE= TCAVE + 273.15
          CONDZR = 7.51 + 0.0209*TKAVE - 1.45E-5*TKAVE**2 +
     &       7.67E-9*TKAVE**3
C         CONDZR = 10.0
C     In current input files, TE-4 is the TC for conduction loss.
      TBAVE=TB(1,I)
      TLAVE= max(TC(4,I),TBAVE)
      TVAR = 0.
      DO 193 J=1,3
      TVAR = TVAR + (TCAVE - TC(J,I))**2
  193  CONTINUE
      TCVAR1(I)= SQRT(TVAR)
      TCVAR2(I)= 100.*TCVAR1(I)/(TCAVE-TBAVE)
C       TWALL(I)= TCAVE - Q*(1./(TWOPI*CONDCU*ZLB))*ALOG(RO/RT)
C     RC is the contact resistance between the copper sleeve and
C     the Zr clad.  Based on natural conv. cooling tests.
          RC = 0.0002/(TWOPI*RT*ZLB)
C         RC = 1.4516E-4/(TWOPI*RT*ZLB)
      RC = 0.000692/(TWOPI*RT*ZLB)
          TWALL(I) = TCAVE - Q*(ALOG(RO/RT)/(TWOPI*CONDZR*ZLB)+RC)
      DELT(I)= TWALL(I) - TBAVE
      FLUX(I)= Q/(TWOPI*RO*ZL)
      ALPHA(I)= FLUX(I)/DELT(I)
      DELTL= TCAVE - TLAVE
```

```
      DELTM= TLAVE - TBAVE
C
      FMIN = 0.1
           FMAX = 1.0
           TSAT = 100.0
C          RC = max((1.0+(FMIN-FMAX)*(TCAVE-TSAT)/100.),FMIN)*RC
      FRC = (TSAT-TCAVE)/50.
C          TCHF = TSAT+75.
C          FRC = ((TCHF-TCAVE)/(TCHF-70.))**3
           FRC = min(FMAX,max(FRC,FMIN))
           RC =  FRC*RC
C          FRC = max((1.0+(FMIN-FMAX)*(TCAVE-TSAT)/100.),FMIN)
C     Heat loss in the nuclear clad heater is assumed to be due to
C     conduction through the copper sleeve.
      DTC = 0.0015875
      ACU = PI*(RCI*RCI-RI*RI) - PI*DTC**2
C     The low TC is assumed to be pulled out 2.54 cm based on
C     conditions at nucleation.
           ZERR = 2.00*0.0254
           QLOSS(I) = CONDCU*ACU*DELTL/ZERR
C      QLOSS(I) = 0.
C     QLOSS(I)= CONDZR*PI*(RO*RO-RI*RI)*DELTL/(0.5*ZL) +
C     &          ALPHA(I)*TWOPI*RO*ZLNC*DELTM
      Q = Q - QLOSS(I)
C          PRINT *," I=",I," TCAVE=",TCAVE," TLAVE=",TLAVE
C          PRINT *," POWER=",WATTS," Q=",Q," QLOSS=",QLOSS(I)
C          PRINT *," DTGAP =",Q*RC," RC=",RC
           RCLAD = ALOG(RO/RCI)/(TWOPI*CONDZR*ZLB)
C          PRINT *," DTCLAD=",Q*RCLAD," RCLAD=",RCLAD
           WRITE(JDAT,800) I, TCAVE,TLAVE,TBAVE
 800  FORMAT(1X,"I =",I3," TC=",F8.2," TL=",F8.2," TB=",F8.2)
           WRITE(JDAT,801) Q, WATTS, QLOSS(I)
 801  FORMAT(1X,"Q=",F8.3," POWER=",F8.3," QLOSS=",F8.3)
      WRITE(JDAT,802) Q*RC, RC
 802  FORMAT(1X,"DTgap =",F8.2," RC=",F10.5)
      WRITE(JDAT,803) Q*RCLAD, RCLAD, CONDZR
 803  FORMAT(1X,"DTclad=",F8.2," RCLAD=",F9.5," CONDZR=",F8.3)
      QLOSS(I)= 100.*QLOSS(I)/WATTS
C      TWALL(I)= TCAVE - Q*(1./(TWOPI*CONDZR*ZLB))*ALOG(RO/RT)
           TWALL(I) = TCAVE - Q*(ALOG(RO/RCI)/(TWOPI*CONDZR*ZLB)+RC)
      DELT(I)= TWALL(I) - TBAVE
      FLUX(I)= Q/(TWOPI*RO*ZLB)
      ALPHA(I)= FLUX(I)/DELT(I)
           RCONV = 1./((ALPHA(I)*TWOPI*RO*ZLB))
           PRINT *," TWALL=",TWALL(I)," ALPHA=",ALPHA(I)," FLUX=",FLUX(I)
```

```
          WRITE(JDAT,804) Q*RCONV, RCONV, TWALL(I)
 804     FORMAT(1X,"DTwall=",F8.3," RCONV=",F10.5," Twall=",F8.3)
      WRITE(JDAT,805) FRC
 805  FORMAT(1X," FRC=",F10.5)
 195  CONTINUE
C
      GO TO 200
C ***************************************************************
C *** ISURF = 11 ****** Turbo-BIII Enhanced Tube
 580  CONTINUE
C     ISURF = 11   Turbo-III Tube - 0.740 in. OD  (Schnelle)
C     Four valid thermocouples at center of tube.
C     Two thermocouples are assumed for estimating heat loss.
C     The loss TCs are located at the heater edge, and
C          0.675 inch (0.017145 m) inside the heated region.
C *** The heater diameter is 0.372 in (0.0094488 m)
      RI=  0.47244E-02
C *** The thermocouple diameter is (0.372+0.630)/2 = 0.501 in
C ***                                  = 0.0127254 m
      RT=  0.63627E-02
C *** The copper sleeve OD is 0.630 in. (0.016002 m)
      RSDO = 0.008001
C *** The outside diameter of the tube is 0.740 in. = 0.018796 m
      RO=  0.93980E-02
C *** The heater has a heated length of 2.5 in = 0.0635 m
      ZLB= 0.06350
      ZLNC=0.02530
      ZL = ZLB + ZLNC
C *** The error TCs are located 0.25 in off of the heater
          ZLOSS = 0.039065
C *** The thermal conductivity of Alloy C12200 (ASTM B359)
C     is k = 196 Btu/ft2-hr-F = 339.2 W/m2-K
      CONDCU= 339.2
          RC = 0.03
C
      DO 585 I=1,NPTS
      WATTS = VOLTS(I)*AMPS(I)
      Q = WATTS
      TCAVE=(TC(1,I)+TC(2,I)+TC(3,I)+TC(4,I))/4.
      TBAVE=(TB(1,I)+TB(2,I))/2.
      TLAVE=(TE(1,I)+TE(2,I))/2.
      TVAR = 0.
      DO 583 J=1,4
      TVAR = TVAR + (TCAVE - TC(J,I))**2
 583  CONTINUE
```

```
      TCVAR1(I)= SQRT(TVAR)
      TCVAR2(I)= 100.*TCVAR1(I)/(TCAVE-TBAVE)
C     TWALL(I)= TCAVE - Q*(1./(TWOPI*CONDCU*ZLB))*ALOG(RO/RT)
          TWALL(I)= TCAVE - Q*(ALOG(RO/RT)/(TWOPI*CONDCU*ZLB) + RC)
      DELT(I)= TWALL(I) - TBAVE
      FLUX(I)= Q/(TWOPI*RO*ZL)
      ALPHA(I)= FLUX(I)/DELT(I)
      DELTL= TCAVE - TLAVE
C     DELTM= ((TE(1,I)+TE(2,I))/2. + TLAVE)/2. - TBAVE
      QLOSS(I)= CONDCU*PI*(RSDO*RSDO-RI*RI)*DELTL/ZLOSS
      Q = Q - QLOSS(I)
      QLOSS(I)= 100.*QLOSS(I)/WATTS
C     TWALL(I)= TCAVE - Q*(1./(TWOPI*CONDCU*ZLB))*ALOG(RO/RT)
          TWALL(I)= TCAVE - Q*(ALOG(RO/RT)/(TWOPI*CONDCU*ZLB) + RC)
      DELT(I)= TWALL(I) - TBAVE
      FLUX(I)= Q/(TWOPI*RO*ZLB)
      ALPHA(I)= FLUX(I)/DELT(I)
 585  CONTINUE
C ***************************************************************
C *** ISURF = 12 ****** Turbo-BIII Enhanced Tube
 590  CONTINUE
C     ISURF = 12   Turbo-III Tube - 0.740 in. OD  (Schnelle)
C     Four valid thermocouples at center of tube inserted thru
C     sleeve to obtain contact with Turbo-III inner surface.
C     Two thermocouples are assumed for estimating heat loss.
C     The loss TCs are located at the heater edge, and
C          0.675 inch (0.017145 m) inside the heated region.
C *** The heater diameter is 0.372 in (0.0094488 m)
      RI=  0.47244E-02
C *** The thermocouple diameter is (0.559+0.035) = 0.594 in
C ***                                 = 0.0150876 m
      RT=  0.75438E-02
C *** The copper sleeve OD is 0.630 in. (0.016002 m)
      RSDO = 0.8001E-02
C *** The outside diameter of the tube is 0.740 in. = 0.018796 m
      RO=  0.93980E-02
C *** The heater has a heated length of 2.0 in = 0.0508 m
      ZLB= 0.05080
      ZLNC=0.02530
      ZL = ZLB + ZLNC
C *** The error TCs are located 0.25 in off of the heater
          ZLOSS = 0.00635
C *** The thermal conductivity of Alloy C12200 (ASTM B359)
C     is k = 196 Btu/ft2-hr-F = 339.2 W/m2-K
      CONDCU= 339.2
```

```
C
      DO 595 I=1,NPTS
      WATTS = VOLTS(I)*AMPS(I)
      Q = WATTS
      TCAVE=(TC(1,I)+TC(2,I)+TC(3,I)+TC(4,I))/4.
      TBAVE=(TB(1,I)+TB(2,I))/2.
      TLAVE=(TE(1,I)+TE(2,I))/2.
          DELTL= TCAVE - TLAVE
      TVAR = 0.
      DO 593 J=1,4
      TVAR = TVAR + (TCAVE - TC(J,I))**2
 593  CONTINUE
      TCVAR1(I)= SQRT(TVAR)
      TCVAR2(I)= 100.*TCVAR1(I)/(TCAVE-TBAVE)
      QLOSS(I)= CONDCU*PI*(RSDO*RSDO-RI*RI)*DELTL/ZLOSS
      Q = Q - QLOSS(I)
      QLOSS(I)= 100.*QLOSS(I)/WATTS
C     TWALL(I)= TCAVE - Q*(1./(TWOPI*CONDCU*ZLB))*ALOG(RO/RT)
          TWALL(I)= TCAVE - Q*(ALOG(RO/RT)/(TWOPI*CONDCU*ZLB))
      DELT(I)= TWALL(I) - TBAVE
      FLUX(I)= Q/(TWOPI*RO*ZLB)
      ALPHA(I)= FLUX(I)/DELT(I)
 595  CONTINUE
C ***************************************************************
      GO TO 200
C
 1000 CONTINUE
C *** FLAT DISK TEST SECTIONS
      CONDCU = 391.0
      RI = 0.0127
      RO = 0.0159
      AI = 0.507E-03
      AO = 0.792E-03
      THICK = 0.8E-03
      PERIM = 2. * TWOPI * RI + 2. * THICK
      AX = TWOPI * RI * THICK
      ZLB  = RO - RI
      ZLNC = 5.
      ZL = ZLNC * PERIM / CONDCU / AX
      D1 = 0.001
      D2 = 0.005
      D3 = 0.009
      DO 1050 I = 1, NPTS
      STC = TC(1,I) + TC(2,I) + TC(3,I)
      SX2 = D1*D1 + D2*D2 + D3*D3
```

```
      SX  = D1 + D2 + D3
      STCX= TC(1,I)*D1 + TC(2,I)*D2 + TC(3,I)*D3
      S2X = SX * SX
      TWALL(I) = (STC*SX2 - SX*STCX) / (3.*SX2 - S2X)
      TBAVE = (TB(1,I) + TB(2,I))/2.
      DELT(I) = TWALL(I) - TBAVE
      WATTS = VOLTS(I) * AMPS(I)
      QLOSS(I) = SQRT(ZLNC*PERIM*CONDCU*AX)*DELT(I)*TANH(ZL)
      FLUX(I) = (WATTS - QLOSS(I)) / AI
      ALPHA(I)= FLUX(I)/DELT(I)
      QLOSS(I)= 100.*QLOSS(I)/WATTS
      TCVAR1(I) = 0.
      TCVAR2(I) = 0.
 1050 CONTINUE
      GO TO 200
 200  CONTINUE
C
      CALL OUTPUT(JDAT)
      CALL SDFOUT(JSDF)
      WRITE(*,225) DATFIL
 225  FORMAT(10X,'OUTPUT FILE IS ',A20)
      WRITE(*,226) SDFFIL
 226  FORMAT(10X,'PLOT FILE IS   ',A20)
      IF(IFILE.EQ.NFILES) CALL BANNER(JBAN)
C
      CLOSE(JINP)
      CLOSE(JDAT)
      CLOSE(JSDF)
 900  CONTINUE
      CLOSE(JBAN)
      WRITE(*,950)
 950  FORMAT(/,1X,'Normal termination of Program PBDATA')
      STOP
      END
C ***************************************************************************
      SUBROUTINE BANNER(N)
C
      WRITE(N,10)
      WRITE(N,20)
      WRITE(N,30)
      WRITE(N,40)
      WRITE(N,50)
      WRITE(N,60)
      WRITE(N,60)
      WRITE(N,80)
```

```
      WRITE(N,90)
      WRITE(N,100)
      WRITE(N,110)
      WRITE(N,120)
   10 FORMAT(/)
   20
  FORMAT(15X,'PPPPPP',3X,'BBBBBB',3X,'DDDDDD',4X,'AAA',4X,'TTTTTTTT',
     &       5X,'AAA')
   30 FORMAT(15X,'PP   PP',2X,'BB   BB',2X,'DD   DD',3X,'AA AA',3X,
     &       'T  TT  T',3X,'AA AA')
   40 FORMAT(15X,'PP   PP',2X,'BB   BB',2X,'DD   DD',2X,'AA   AA',2X,
     &       'T  TT  T',2X,'AA   AA')
   50 FORMAT(15X,'PPPPPP',3X,'BBBBBB',3X,'DD   DD',2X,'AAAAAAA',5X,'TT',
     &       5X,'AAAAAAA')
   60 FORMAT(15X,'PP',7X,'BB   BB',2X,'DD   DD',2X,'AA   AA',5X,'TT',
     &       5X,'AA   AA')
   80 FORMAT(15X,'PP',7X,'BBBBBB',3X,'DDDDDD',3X,'AA   AA',4X,'TTTT',
     &       4X,'AA   AA')
   90 FORMAT( )
  100 FORMAT(15X,'PROGRAM PBDATA Version 06-Revised: February 20, 2001')
  110 FORMAT(30X,' --- Written by S. M. Bajorek')
  120 FORMAT( )
      WRITE(N,200)
      WRITE(N,210)
      WRITE(N,220)
      WRITE(N,230)
      WRITE(N,240)
      WRITE(N,250)
      WRITE(N,260)
      WRITE(N,270)
      WRITE(N,280)
      WRITE(N,290)
      WRITE(N,300)
      WRITE(N,310)
      WRITE(N,320)
      WRITE(N,330)
      WRITE(N,340)
      WRITE(N,350)
  200 FORMAT(15X,'COMPONENT INDEX:')
  210 FORMAT(15X,' 1 = ACETONE    ')
  220 FORMAT(15X,' 2 = 2-BUTANONE ')
  230 FORMAT(15X,' 3 = METHANOL   ')
  240 FORMAT(15X,' 4 = ETHANOL    ')
  250 FORMAT(15X,' 5 = BENZENE    ')
  260 FORMAT(15X,' 6 = WATER      ')
```

```
 270  FORMAT(15X,' 7 = 1-PROPANOL ')
 280  FORMAT(15X,' 8 = 2-PROPANOL ')
 290  FORMAT(15X,' 9 = ETHYLENE GLYCOL')
 300  FORMAT(15X,'10 = CYCLOHEXANE')
 310  FORMAT(15X,'11 = PROPYLENE GLYCOL')
 320  FORMAT(15X,'12 = METHYL ACETATE')
 330  FORMAT(15X,'13 = ETHYL ACETATE')
 340  FORMAT(15X,'14 = DIETHYLENE GLYCOL')
 350  FORMAT(15X,'15 = AMMONIA')
C
      WRITE(N,120)
      WRITE(N,500)
      WRITE(N,510)
      WRITE(N,520)
      WRITE(N,530)
      WRITE(N,540)
      WRITE(N,550)
      WRITE(N,560)
      WRITE(N,570)
      WRITE(N,580)
          WRITE(N,590)
          WRITE(N,595)
          WRITE(N,596)
          WRITE(N,597)
      WRITE(N,120)
      WRITE(N,700)
      WRITE(N,710)
      WRITE(N,720)
 500  FORMAT(15X,'SURFACE INDEX:')
 510  FORMAT(15X,' 1 = SMOOTH TUBE      Shakir')
 520  FORMAT(15X,' 2 = HIGH FLUX TUBE   Bajorek')
 530  FORMAT(15X,' 3 = FINNED TUBE      Bajorek')
 540  FORMAT(15X,' 4 = SMOOTH TUBE      Schnelle')
 550  FORMAT(15X,' 5 = SMOOTH TUBE      Bajorek')
 560  FORMAT(15X,' 6 = SMOOTH TUBE      Bajorek')
 570  FORMAT(15X,' 7 = SMOOTH TUBE      Shakir')
 580  FORMAT(15X,' 8 = SMOOTH TUBE      Shakir')
 590    FORMAT(15X,' 9 = NUCLEAR CLAD     Schnelle')
 595    FORMAT(15X,'10 = NUCLEAR CLAD     Schnelle')
 596  FORMAT(15X,'11 = TURBO-IIIB       Schnelle')
 597  FORMAT(15X,'12 = TURBO-IIIB       Schnelle')
 700  FORMAT(14X,'101 = SMOOTH CU FLAT DISK')
 710  FORMAT(14X,'102 = SMOOTH CU FLAT DISK')
 720  FORMAT(14X,'103 = 1.25 IN SI WAFER')
      RETURN
```

```
      END
C *****************************************************************
      SUBROUTINE INPUT(J)
      COMMON/XDATA/ IDNUM,IDATE,ISURF,ICOMP(5),FRAC(5),NPTS, IUNITS
      COMMON/XDATA/ VOLTS(40),AMPS(40),P(40)
      COMMON/XDATA/ TB(2,40),TC(4,40),TE(4,40)
          COMMON/SOLUTE/ PPMBN, PPMLI
C
      READ(J,1)
    1 FORMAT( )
      READ(J,10) IDNUM,IDATE,ISURF,IUNITS
   10 FORMAT(10X,I5,9X,I6,10X,I5,10X,I5)
      READ(J,1)
      READ(J,20) ICOMP(1),ICOMP(2),ICOMP(3),ICOMP(4),ICOMP(5)
   20 FORMAT(5I15)
      READ(J,1)
      READ(J,30) FRAC(1),FRAC(2),FRAC(3),FRAC(4),FRAC(5)
   30 FORMAT(5E15.5)
      READ(J,1)
      READ(J,40) NPTS,PPMBN,PPMLI
   40 FORMAT(10X,I5,5X,F10.1,5X,F10.1)
      READ(J,1)
      DO 50 N=1,NPTS
      IF(IDNUM.GE.1000) GO TO 45
      READ(J,60) VOLTS(N),AMPS(N),TC(1,N),TC(2,N),TC(3,N),TC(4,N),
     &           TB(1,N),TB(2,N),TE(1,N),TE(2,N),TE(3,N),TE(4,N),
     &           P(N)
C       Units input:  IUNITS = 0 if TC temperatures in deg C
C             IUNITS = 1 if TC temperatures in deg F
C    Default is IUNITS = 0.
         IF (IUNITS.EQ.1) THEN
            TC(1,N) = (TC(1,N)-32.)*(5./9.)
            TC(2,N) = (TC(2,N)-32.)*(5./9.)
            TC(3,N) = (TC(3,N)-32.)*(5./9.)
            TC(4,N) = (TC(4,N)-32.)*(5./9.)
          TE(1,N) = (TE(1,N)-32.)*(5./9.)
            TE(2,N) = (TE(2,N)-32.)*(5./9.)
            TE(3,N) = (TE(3,N)-32.)*(5./9.)
            TE(4,N) = (TE(4,N)-32.)*(5./9.)
            TB(1,N) = (TB(1,N)-32.)*(5./9.)
            TB(2,N) = (TB(2,N)-32.)*(5./9.)
         ENDIF
      GO TO 50
   45 CONTINUE
      READ(J,70) VOLTS(N),AMPS(N),TC(1,N),TC(2,N),TC(3,N),TC(4,N),
```

```
     &              TB(1,N),TB(2,N),TE(1,N),TE(2,N),TE(3,N),TE(4,N),
     &              P(N)
  50  CONTINUE
  60  FORMAT(F5.1,1X,F4.2,10F6.1,F5.1)
  70  FORMAT(F5.2,F5.2,10F6.1,F5.1)
C
      RETURN
      END
C ***************************************************************
      SUBROUTINE OUTPUT(J)
      COMMON/XDATA/ IDNUM,IDATE,ISURF,ICOMP(5),FRAC(5),NPTS, IUNITS
      COMMON/XDATA/ VOLTS(40),AMPS(40),P(40)
      COMMON/XDATA/ TB(2,40),TC(4,40),TE(4,40)
      COMMON/XOUTP/ DELT(40),QLOSS(40),ALPHA(40),TWALL(40),FLUX(40)
      COMMON/XOUTP/ TCVAR1(40),TCVAR2(40)
          COMMON/SOLUTE/ PPMBN, PPMLI
C
      WRITE(J,5)
   5  FORMAT(10X,'IDNUM',11X,'DATE',8X,'SURFACE')
      WRITE(J,10) IDNUM,IDATE,ISURF
  10  FORMAT(10X,I5,9X,I6,10X,I5)
      WRITE(J,20)
  20  FORMAT(6X,'COMPONENT',6X,'COMPONENT',6X,'COMPONENT',
     &        6X,'COMPONENT',6X,'COMPONENT')
      WRITE(J,30) ICOMP(1),ICOMP(2),ICOMP(3),ICOMP(4),ICOMP(5)
  30  FORMAT(5I15)
      WRITE(J,40)
  40  FORMAT(7X,'FRACTION',7X,'FRACTION',7X,'FRACTION',
     &        7X,'FRACTION',7X,'FRACTION')
      WRITE(J,50) FRAC(1),FRAC(2),FRAC(3),FRAC(4),FRAC(5)
  50  FORMAT(5E15.5)
      WRITE(J,60)
  60  FORMAT(11X,'NPTS')
      WRITE(J,70) NPTS
  70  FORMAT(10X,I5)
C
      WRITE(J,80)
  80  FORMAT(/,9X,'V',4X,'I',2X,'TC-1',2X,'TC-2',2X,'TC-3',2X,'TC-4',
     &        2X,'TB-1',2X,'TB-2',2X,'TE-1',2X,'TE-2',2X,'TE-3',
     &        2X,'TE-4',4X,'P')
C
      DO 100 N=1,NPTS
      WRITE(J,110) VOLTS(N),AMPS(N),TC(1,N),TC(2,N),TC(3,N),TC(4,N),
     &              TB(1,N),TB(2,N),TE(1,N),TE(2,N),TE(3,N),TE(4,N),
     &              P(N)
```

```
 100  CONTINUE
 110  FORMAT(4X,F6.2,F5.2,10F6.1,F5.1)
      WRITE(J,120)
 120  FORMAT(/,2X,'NO',1X,' SUPERHEAT',2X,'HEAT FLUX',5X,'ALPHA',
     &       5X,'QLOSS',5X,'TWALL',4X,'TCVAR1',4X,'TCVAR2')
C
      DO 130 N=1,NPTS
      WRITE(J,140) N,DELT(N),FLUX(N),ALPHA(N),QLOSS(N),TWALL(N),
     &           TCVAR1(N),TCVAR2(N)
 130  CONTINUE
 140  FORMAT(2X,I2,1X,F10.1,1X,4F10.1,F10.2,F10.1)
C
      IF((PPMBN+PPMLI).LE.0.) GO TO 900
      WRITE(J,150) PPMBN
 150  FORMAT(/,' BORON CONCENTRATION   =',F8.1,' PPM')
          WRITE(J,160) PPMLI
 160  FORMAT(/,' LITHIUM CONCENTRATION =',F8.1,' PPM')
 900  CONTINUE
      RETURN
      END
C ***************************************************************************
      SUBROUTINE SDFOUT(J)
      COMMON/XDATA/ IDNUM,IDATE,ISURF,ICOMP(5),FRAC(5),NPTS, IUNITS
      COMMON/XDATA/ VOLTS(40),AMPS(40),P(40)
      COMMON/XDATA/ TB(2,40),TC(4,40),TE(4,40)
      COMMON/XOUTP/ DELT(40),QLOSS(40),ALPHA(40),TWALL(40),FLUX(40)
      COMMON/XOUTP/ TCVAR1(40),TCVAR2(40)
C
      DO 10 N=1,NPTS
          ZKW = 1000.
      WRITE(J,20) DELT(N),FLUX(N)/ZKW,ALPHA(N)/ZKW,TWALL(N),
     &           TB(1,N),P(N)
  10  CONTINUE
  20  FORMAT(5X,F10.4,5X,F10.1,5X,F10.1,3F10.1)
C
      RETURN
      END
```

Sample input file for PBDATA

```
          IDNUM           DATE        SURFACE
            442         041101             12
      COMPONENT      COMPONENT      COMPONENT      COMPONENT      COMPONENT
              6              0              0              0              0
       FRACTION       FRACTION       FRACTION       FRACTION       FRACTION
    0.10000E+01    0.00000E+00    0.00000E+00    0.00000E+00    0.00000E+00
           NPTS
             14
    V    I  TC-1  TC-2  TC-3  TC-4  TB-1  TB-2  TE-1  TE-2  TE-3  TE-4    P
 20.6 0.71 165.6 166.0 166.0 166.1 158.7 158.4 164.8 164.9   0.0   0.0 14.0
 30.1 1.04 171.3 172.1 171.5 172.2 158.1 157.7 169.5 169.5   0.0   0.0 14.0
 40.4 1.39 180.5 181.3 181.1 181.5 158.9 158.5 177.3 177.7   0.0   0.0 14.0
 50.4 1.72 186.1 186.9 187.1 187.4 159.3 159.0 182.3 182.5   0.0   0.0 14.1
 60.8 2.08 186.8 187.4 187.8 187.8 159.0 158.7 183.4 183.9   0.0   0.0 14.0
 70.4 2.40 187.1 188.2 188.5 188.9 158.3 157.8 184.0 183.9   0.0   0.0 14.0
 80.5 2.74 187.6 189.1 189.1 189.8 158.6 158.5 185.2 184.7   0.0   0.0 14.0
 90.5 3.08 188.2 190.2 189.7 190.5 158.9 158.5 185.7 185.2   0.0   0.0 14.0
100.4 3.41 188.7 191.3 190.7 191.2 158.6 158.7 186.5 185.5   0.0   0.0 14.0
105.0 3.56 189.0 191.9 190.7 192.3 158.4 158.3 186.8 185.9   0.0   0.0 13.9
110.2 3.74 189.5 192.5 191.4 192.8 158.9 158.8 187.2 186.4   0.0   0.0 14.0
114.9 3.88 189.8 193.4 191.8 193.6 158.7 158.0 188.1 185.9   0.0   0.0 14.0
120.1 4.07 190.2 194.1 192.5 194.2 159.2 158.2 188.3 186.9   0.0   0.0 14.0
125.8 4.24 190.6 194.9 193.1 195.2 161.0 159.0 188.9 187.3   0.0   0.0 14.0
```

Sample output file for PBDATA

IDNUM	DATE	SURFACE		
442	41101	12		
COMPONENT	COMPONENT	COMPONENT	COMPONENT	COMPONENT
6	0	0	0	0
FRACTION	FRACTION	FRACTION	FRACTION	FRACTION
0.10000E+01	0.00000E+00	0.00000E+00	0.00000E+00	0.00000E+00
NPTS				
14				

V	I	TC-1	TC-2	TC-3	TC-4	TB-1	TB-2	TE-1	TE-2	TE-3	TE-4	P
20.60	0.71	165.6	166.0	166.0	166.1	158.7	158.4	164.8	164.9	0.0	0.0	14.0
30.10	1.04	171.3	172.1	171.5	172.2	158.1	157.7	169.5	169.5	0.0	0.0	14.0
40.40	1.39	180.5	181.3	181.1	181.5	158.9	158.5	177.3	177.7	0.0	0.0	14.0
50.40	1.72	186.1	186.9	187.1	187.4	159.3	159.0	182.3	182.5	0.0	0.0	14.1
60.80	2.08	186.8	187.4	187.8	187.8	159.0	158.7	183.4	183.9	0.0	0.0	14.0
70.40	2.40	187.1	188.2	188.5	188.9	158.3	157.8	184.0	183.9	0.0	0.0	14.0
80.50	2.74	187.6	189.1	189.1	189.8	158.6	158.5	185.2	184.7	0.0	0.0	14.0
90.50	3.08	188.2	190.2	189.7	190.5	158.9	158.5	185.7	185.2	0.0	0.0	14.0
100.40	3.41	188.7	191.3	190.7	191.2	158.6	158.7	186.5	185.5	0.0	0.0	14.0
105.00	3.56	189.0	191.9	190.7	192.3	158.4	158.3	186.8	185.9	0.0	0.0	13.9
110.20	3.74	189.5	192.5	191.4	192.8	158.9	158.8	187.2	186.4	0.0	0.0	14.0
114.90	3.88	189.8	193.4	191.8	193.6	158.7	158.0	188.1	185.9	0.0	0.0	14.0
120.10	4.07	190.2	194.1	192.5	194.2	159.2	158.2	188.3	186.9	0.0	0.0	14.0
125.80	4.24	190.6	194.9	193.1	195.2	161.0	159.0	188.9	187.3	0.0	0.0	14.0

NO	SUPERHEAT	HEAT FLUX	ALPHA	QLOSS	TWALL	TCVAR1	TCVAR2
1	7.4	2368.2	321.7	51.4	165.9	0.38	5.2
2	13.8	5128.9	370.5	50.9	171.7	0.77	5.5
3	22.3	10323.0	462.1	44.9	181.0	0.75	3.3
4	27.6	18460.2	668.5	36.1	186.8	0.96	3.5
5	28.4	33294.7	1172.5	21.0	187.2	0.82	2.9
6	29.8	46470.1	1557.2	17.5	187.9	1.34	4.4
7	30.0	64316.5	2146.9	12.5	188.5	1.61	5.3
8	30.4	83125.3	2730.4	10.5	189.1	1.77	5.7
9	31.2	103693.9	3324.2	9.1	189.8	2.10	6.6
10	31.9	113823.7	3564.6	8.7	190.3	2.57	7.9
11	31.9	126315.9	3955.9	8.1	190.8	2.59	7.9
12	33.0	136605.4	4143.6	8.1	191.3	3.05	9.0
13	33.1	150938.4	4555.8	7.4	191.8	3.24	9.5
14	32.4	165335.0	5096.1	7.0	192.4	3.66	10.9